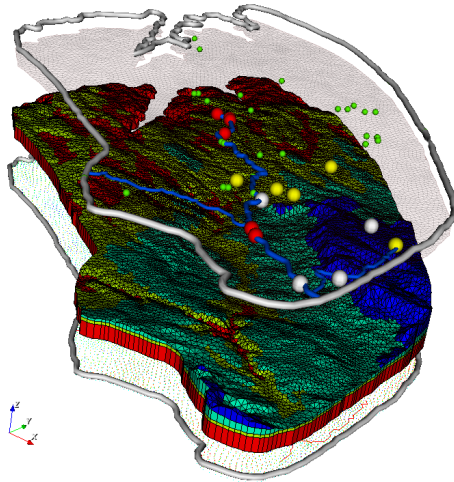


Agnes Sachse, Karsten Rink, Wenkui He and
Olaf Kolditz

OpenGeoSys - Tutorial

Computational Hydrology I: Groundwater Flow Modelling



11th December 2017

Springer

Foreword

This tutorial presents the application of the open-source software *OpenGeoSys* (*OGS*) for computational hydrology. The material is based on the content of a one-week HIGRADE (<http://www.higrade.ufz.de>) (Bissinger and Kolditz, 2008) training course at the Helmholtz Centre for Environmental Research in Leipzig, Germany. The book contains general information regarding hydrological and groundwater flow modelling and the pre-processing and step-by-step model set-up of a case study with *OGS* and related components such as the *OGS Data Explorer*. In addition, it also illustrates the application of pre- and post-processing tools such as *ArcGIS* or *ParaView* for the preparation of input data as well as the optimal presentation of simulation results.

This *OGS* tutorial is the result of a close cooperation of the Helmholtz Centre for Environmental Research (UFZ) with partner universities (Technische Universität Dresden, Christian-Albrechts University Kiel, University of Potsdam, University of Tübingen) in the field of hydrological modelling. The UFZ Departments of Environmental Informatics (ENVINF), Catchment Hydrology (CATHYD) and Computational Hydrosystems (CHS) have been involved in the preparation of this *OpenGeoSys* Tutorial. These voluntary contributions are highly acknowledged.

This book is intended primarily for graduate students and applied scientists, who deal with hydrological system analysis and hydrological modelling. It is also a valuable source of information for professional hydrologists wishing to advance their knowledge in numerical modelling of coupled hydrological-hydrogeological systems. As such, this book will be a valuable aid in training of hydro-system-modelling.

There are various commercial software tools available to solve complex scientific questions in hydrology and hydrogeology. This book will introduce the user to a non-commercial numerical software code for hydrological and hydrogeological modelling which can even be adapted and extended based on the needs of the researcher.

This tutorial is the first in a series that will represent further applications of *OGS* in environmental sciences. The planned tutorials series includes:

- Computational Hydrology I: Groundwater flow modelling, Sachse et al. (2014),
- Computational Hydrology II: Density-dependent flow and transport processes (2015*),
- Reactive Transport Modelling II (2015*),
- Geothermal Energy I: Shallow geothermal systems (2015*),
- Geothermal Energy II: Enhanced geothermal systems (2015*),
- OGS Data Explorer, Rink et al. (2015*),
- Computational Geotechnics (2016*),
- Multiphase Flow (2016*).

(*publication time is approximated)

Book overview

Each chapter guides the user through the process of establishing a hydrological and/or groundwater flow model using the software code *OpenGeoSys*. After a short introduction about the scope of the Book, chapters 1 and 2 give a general overview of hydrology and hydrogeology with the important keywords in those sciences highlighted. Chapter 3 focusses on hydrological and groundwater flow modelling using the *OGS* framework and gives an overview of the graphical user interface, the *OpenGeoSys Data Explorer*. The Theis-benchmark for groundwater flow to a well in a confined aquifer explained in chapter 4 is one of the important benchmarks for hydrological and hydrogeological modelling systems and is the first application of *OGS*. Chapter 5 is concerned with the set-up of a hydrological and hydrogeological model for a catchment study (in this case, the Ammer catchment in Germany). This chapter describes in detail the workflow of modelling hydrological and groundwater flow, starting from GIS data, preparing input files with the *OpenGeoSys Data Explorer*, using the actual groundwater simulator and related post-processing.

The appendix includes information on several special topics in greater detail. Appendix A.1 gives a short overview about the key functionalities of the Geographical Information System *ArcGIS*. A summary of all software which can be coupled with *OGS* is presented in appendix B, namely the hydrological model *JAMS*, the hydrodynamic model *SWMM* and the multi-scale hydrological model *mHM*. The last part of the appendix includes a short installation guide to *OGS* and some links to further literature and websites.

Acknowledgements

We deeply acknowledge the continuous support to the *OpenGeoSys* development activities by following institutions:



We would like to express our sincere thanks to HIGRADE in providing funding the *OpenGeoSys* training course at the Helmholtz Centre for Environmental Research.

We also wish to thank the *OpenGeoSys*-developer group for their technical support.

Contents

Foreword	v
1 Hydrology	1
1.1 Water Resources Situation	1
1.2 Water Cycle and Water Balance.....	2
1.3 Catchment Characteristics.....	5
1.4 Hydrological Parameters	6
1.5 Hydrological Processes	6
2 Hydrogeology	13
2.1 Aquifer Types	13
2.2 Aquifer Characteristics.....	14
2.3 Groundwater Flow Equation.....	16
3 Modelling with <i>OpenGeoSys</i>	19
3.1 Hydrologic Modelling and Simulation	19
3.2 <i>OpenGeoSys</i> Process Simulation.....	20
3.3 Modelling Workflow	22
3.4 <i>OpenGeoSys Data Explorer</i>	24
4 Benchmark: Theis problem	31
4.1 Benchmark Definition.....	31
4.2 <i>OGS</i> Input Files	32
4.3 Theis Method in 1.5D: Radial Symmetry	37
4.4 Theis Problem in 2D	41
4.5 Theis Problem in 2.5D: Axial Symmetry	44
4.6 Theis Problem in 3D	46
4.7 Results	47
4.8 Groundwater Flow and Liquid Flow	49

5	Case Study: Ammer Catchment	51
5.1	Introduction	51
5.2	Catchment Description	51
5.3	Model Set-up	53
5.4	Available data sets	54
5.5	Data Integration	57
5.6	Finite Element Meshing	61
5.7	Assigning Boundary Conditions	67
5.8	Preparations for the Groundwater Flow Simulation	73
5.9	Groundwater Flow Simulation	83
5.10	OGS Simulation Results	85
5.11	Visual Analysis	87
A	Geographical Information Systems	91
A.1	Introduction to <i>ArcGIS</i>	91
A.2	Hydrology Tool in <i>ArcGIS</i>	92
B	Coupled Hydrosystems	95
B.1	OGS#JAMS	95
B.2	OGS#SWMM	97
B.3	OGS#mHM	98
C	OpenGeoSys Installation Guide	101
C.1	OGS Download and Installation	101
C.2	Source Code Availability	102
	References	103

List of Contributors

Lars Bilke, MSc,
Helmholtz Centre for Environmental Research – UFZ, Dept. of Environmental Informatics, e-mail: lars.bilke@ufz.de

Jens-Olaf Delfs, PhD,
Christian-Albrechts-University, Kiel, e-mail: jod@gpi.uni-kiel.de

Thomas Fischer, PhD,
Helmholtz Centre for Environmental Research – UFZ, Dept. of Environmental Informatics, e-mail: thomas.fischer@ufz.de

Wenkui He, MSc,
Helmholtz Centre for Environmental Research – UFZ, Dept. of Environmental Informatics, e-mail: wenkui.he@ufz.de

Leslie Jakobs, MA,
Helmholtz Centre for Environmental Research – UFZ, Dept. of Environmental Informatics, e-mail: leslie.jakobs@ufz.de

Thomas Kalbacher, PhD,
Helmholtz Centre for Environmental Research – UFZ, Dept. of Environmental Informatics, e-mail: thomas.kalbacher@ufz.de

Olaf Kolditz, PhD,
Helmholtz Centre for Environmental Research – UFZ, Dept. of Environmental Informatics, Technische Universität Dresden, Applied Environmental System Analysis, e-mail: olaf.kolditz@ufz.de

Karsten Rink, PhD,
Helmholtz Centre for Environmental Research – UFZ, Dept. of Environmental Informatics, e-mail: karsten.rink@ufz.de

Agnes Sachse, Dipl.-Geogr.,
Helmholtz Centre for Environmental Research – UFZ, Dept. of Environmental Informatics, e-mail: agnes.sachse@ufz.de

Stephan Schulz, MSc,
Helmholtz Centre for Environmental Research – UFZ, Dept. of Catchment
Hydrology, e-mail: stephan.schulz@ufz.de

Benny Selle, PhD,
University of Potsdam, Germany, e-mail: bselle@uni-potsdam.de

Marc Walther, Dipl.-Hydrol.,
Helmholtz Centre for Environmental Research – UFZ, Dept. of Environ-
mental Informatics, e-mail: marc.walther@ufz.de, formerly Technische
Universität Dresden, Institute for Groundwater Management,

Wenqing Wang, PhD,
Helmholtz Centre for Environmental Research – UFZ, Dept. of Environ-
mental Informatics, e-mail: wenqing.wang@ufz.de

Chapter 1

Hydrology

AGNES SACHSE AND LESLIE JAKOBS

Water is one of Earth's most precious resources. Without it, life could not exist. Abundant in some places, elusive in others, and unusable in yet other places, water and access to it is vital for human existence. Its distribution, movement, processes, and properties comprise hydrology, or the study of water. Hydrology investigates the changes water undergoes as well the changes it incurs in the atmosphere, on the earth's surface, and underground.

A subset of hydrology is hydrogeology, which focuses on water found beneath the earth's surface and its movement, properties, and processes. Groundwater flows through and reacts with substances at different rates. It shapes the underground as much as it does the surface, and experiences temperature and pressure changes.

Before explaining the fundamental concepts of hydrology and hydrogeology (Sec. 2) we will start with an overview on the world's water resources situation (Sec. 1.1).

1.1 Water Resources Situation

In order to understand the global water resources situation, it is important to touch on two points: the availability of water (Fig. 1) and access to it in light of a booming human population (Fig. 2). The availability of freshwater differs greatly all around the world. With a projected population of 9 billion by 2050 (UNEP, 2008), what effects will this have on our sources of freshwater? Can engineering solutions sustainably support areas prone to water scarcity? What areas will be most affected and how will they be affected?

As our population grows, our demand for water for food production, industry, sanitary services, and of course drinking increases greatly. The UNEP (United Nations Environment Program (UNEP, 2008)) analysed the world's

water resources in 2008. Findings show that megacities continue to grow, but often not in proximity to freshwater resources, and urban waters often contend with pollution and sanitation problems. Access to water and water rights are a source of conflict, and climate change models predict increasing water scarcity. Hence, there is a sense of urgency to understand and develop creative ways to improve access to freshwater.

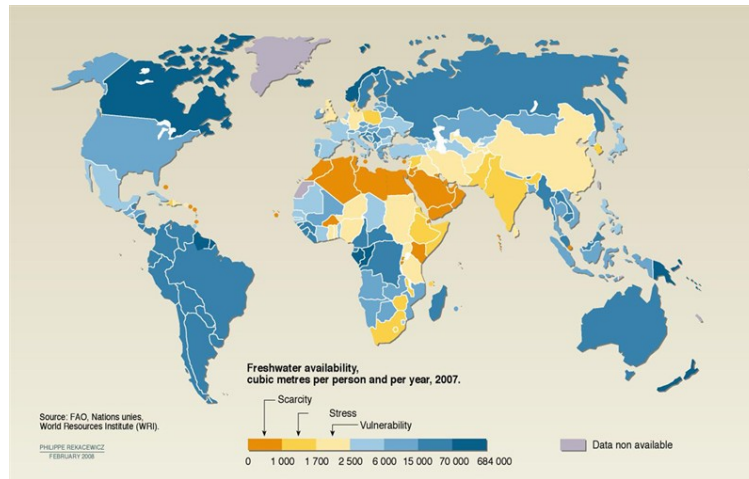


Fig. 1: Global water stress and scarcity. Graphic obtained from UNEP (2008), Vital Water Graphics - An Overview of the State of the World's Fresh and Marine Waters. Sources: FAO, United Nations, World Resource Institute (WRI), Designer: Philippe Rekacewicz (Le Monde diplomatique), February 2006, <http://maps.grida.no/go/graphic/global-waterstress-and-scarcity> (Rekacewicz, 2009)

For more information regarding a detailed analysis of world's water resources the interested reader is referred to "Vital Water Graphics - An Overview of the State of the World's Fresh and Marine Waters - 2nd Edition - 2008" (<http://www.unep.org/dewa/vitalwater/>).

1.2 Water Cycle and Water Balance

The **water cycle**, or hydrologic cycle, (Fig. 3) is the most fundamental principle of hydrology and illustrates the circulation of water from land to the atmosphere to land (Maidment, 1993). Water evaporates from the ocean, surface waters and land in the form of transpiration. In its vapour state, it cools and condenses, and falls back to the earth in the form of precipitation. It

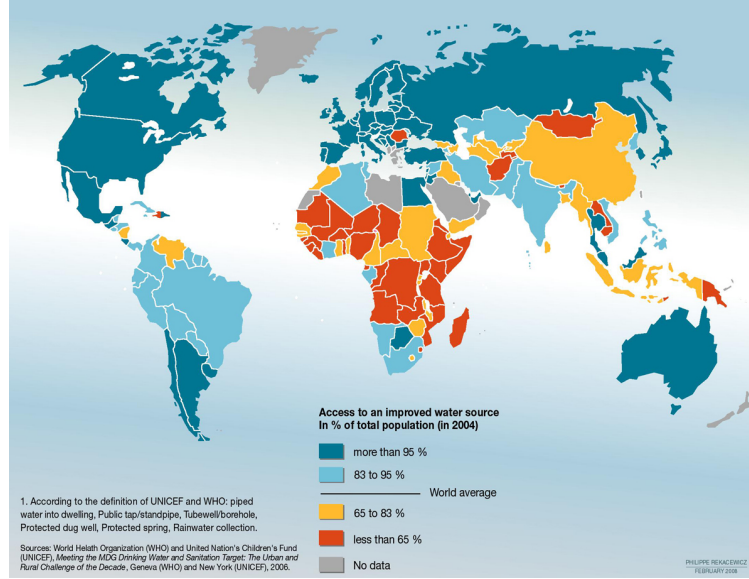


Fig. 2: Proportion of population with improved drinking water supply in 2004. Graphic obtained from UNEP (2008), Vital Water Graphics - An Overview of the State of the World's Fresh and Marine Waters. Sources: FAO, United Nations, World Resource Institute (WRI), Designer: Philippe Rekacewicz (Le Monde diplomatique) (Rekacewicz and Bournay, 2007)

flows by gravity along surficial water courses or into the ground. Water is always in motion. The main categories are (Peixoto and Kettani, 1973):

- marine (oceans contain $1350 \times 10^{15} m^3$ water),
- terrestrial (land: $33.6 \times 10^{15} m^3$),
- as well as atmospheric ($0.013 \times 10^{15} m^3$).¹

Precipitation and evapotranspiration between atmosphere and land surfaces comprise $99 \times 10^{12} m^3$ and $62 \times 10^{12} m^3$ of water, respectively. Precipitation and evapotranspiration between atmosphere and oceans contain $324 \times 10^{12} m^3$ and $361 \times 10^{12} m^3$ of water, respectively. Runoff and groundwater flow from terrestrial to marine water bodies are in the order of $37 \times 10^{12} m^3$.² The **water budget** in a watershed is described by the basic equation in hydrology (Maidment, 1993):

$$P + G_{in} - (Q + ET + G_{out}) = \Delta S \quad (1)$$

¹ 10^{15} is peta

² 10^{12} is tera

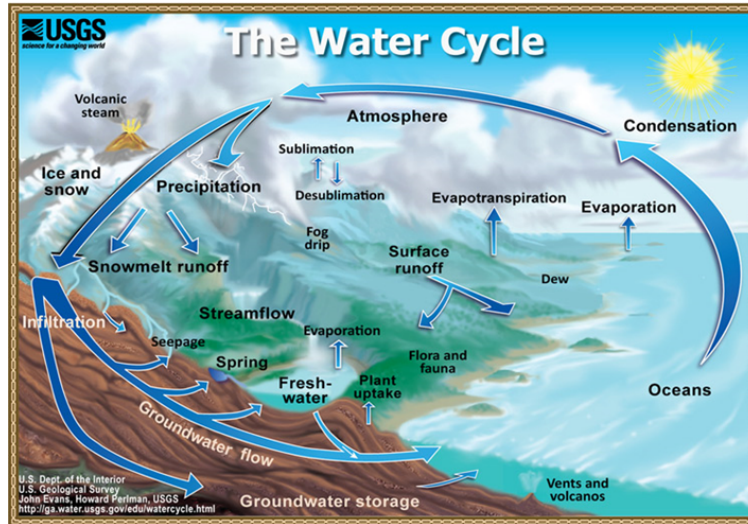


Fig. 3: The water cycle. (Evans and Perlman, 2014)

with: P precipitation, Q stream outflow (runoff), G_{in} groundwater inflow, G_{out} groundwater outflow, ET evapotranspiration, and ΔS change in storage. The link between surface hydrology and subsurface hydrology (hydrogeology) is depicted in Fig. 4. Surface **hydrology** for the most part focuses on surface waters (rivers and lakes), land surface and vegetation, the unsaturated subsurface of soil and roots (vadose zone). **Hydrogeology** deals with the water-saturated zone (phreatic zone) and groundwater topics.

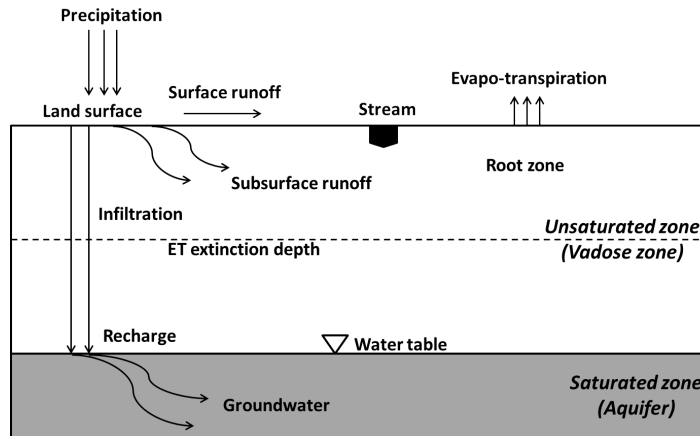


Fig. 4: Terrestrial hydrosystems divided into vadose and phreatic zones.

1.3 Catchment Characteristics

A **catchment**, or watershed, is the area of land that receives precipitation and supplies the outflowing watercourse (Maidment, 1993). It is important to distinguish between **topographical and hydrologic catchments** (Fig. 5). The topographical shape of a catchment is defined based on elevation and covers surface runoff processes. A common tool for delineation of topographical watersheds is *ArcGIS* (see Appendix A). The subsurface structure is important for groundwater excess flow to enter surface waters (interflow and base flow). Major physical characteristics of catchments are:

- geomorphology (surface, shape),
- topography (hypso graphical curve, slope, altitude, aspect),
- hydrography (order of watercourses), and
- agro-pedo-geological factors (soil, vegetation, geology).

The shape of a catchment influences the form of its characteristic hydrograph. There is an order of catchment stream contributors according to Strahler's system of hydrographic network classification (Maidment, 1993).

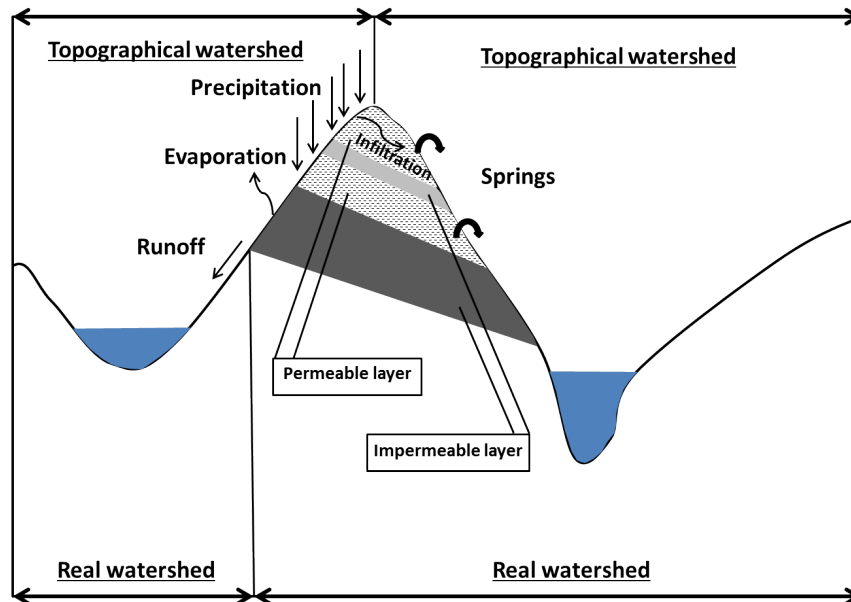


Fig. 5: Difference between topographical and real (hydrological) watershed; modified based on Musy (2001).

1.4 Hydrological Parameters

Precipitation, temperature, humidity and wind are hydrological parameters and they influence the hydrological systems by different process types (e.g. evaporation, runoff, erosion). Due to the content of the tutorial, we will focus mostly on precipitation and its processes. Types of precipitation are: dew, rain, ice, snow, hail and fog. The distribution of rainfall is mainly influenced by geographical conditions (equatorial zones, subtropical zones, arctic areas, monsoon).

1.5 Hydrological Processes

Hydrological parameters are the driving forces of hydrological processes. The most important hydrological processes are briefly presented in this section.

Runoff

The following types of **runoff** are distinguished (Fig. 6:

- Surface runoff (Overland Flow),
- Subsurface Flow (Lateral Flow, Hypodermic Flow, Interflow),
- Baseflow (Stream Flow).

The **runoff hydrograph** is a graph showing the rate of flow (discharge) versus time past a specific point in a river, or other channel or conduit carrying flow (Gupta, 2001). The rate of flow is typically expressed in cubic metres per second (m^3/s).

Infiltration

Infiltration is the flow of water through the soil surface into a porous medium under gravity action and pressure effects. **Hydraulic conductivity** (at saturation k_s) is an essential parameter of infiltration. It represents the limiting value of infiltration if the soil is saturated and homogeneous. **Percolation** is vertical water flow in soils (porous unsaturated environment) on the groundwater layer under the influence of gravity.

One runoff process that contributes to interflow is transmissivity feedback. This occurs when a network of macropores is activated following rapid infiltration. Macropores and natural pipes are void spaces in the soil that provide

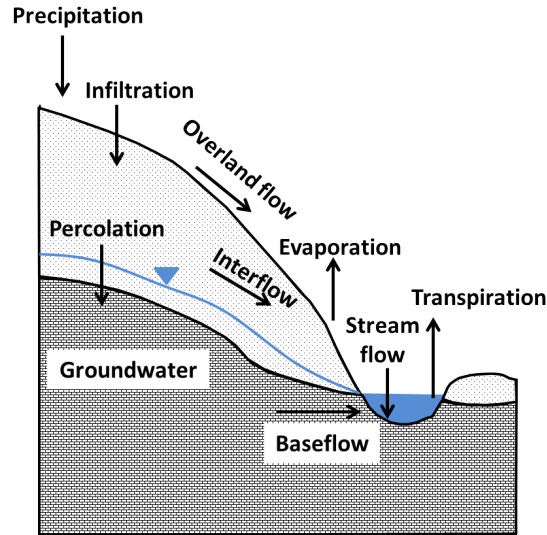


Fig. 6: Basic runoff processes

preferential pathways for water to move downslope. Decayed plant roots, burrowing insects and animals, and chemical reactions between water and soil minerals are a few ways that macropores form. Macropore networks are more likely in deep-soiled areas with considerable organic materials. Thus, humid climates are more likely to have substantial interflow through macropore networks.

Groundwater ridging is a process that occurs in sloped drainage basins where the water table is much closer to the surface near the stream channel than it is further away from the stream. In some cases the groundwater ridge can reach the soil surface and contribute to surface runoff through saturation excess overland flow.

Factors affecting infiltration processes are as follows:

- precipitation (amount, intensity, duration),
- soil compaction due to raindrop impact and other causes,
- initial soil humidity,
- soil type (texture, structure)
- hydrodynamic characteristics (influence capillary forces and adsorption),
- soil and land cover and vegetation (has positive influence on infiltration by increasing the time of water penetration in soil),
- topography and morphology of slopes,
- evaporation.

Infiltration models are used to estimate infiltration rates. The main hypotheses of Green-Ampt model are: the humidity front is perfectly defined; a

transmission zone, where in time and space water storage and hydraulic conductivity are constant; the suction forces of the humidity front are constant.

$$i(t) = K_s \left(1 + \frac{h_0 - h_f}{z_f(t)} \right) \quad (2)$$

with: K_s hydraulic conductivity at saturation, h_0 surface pressure load, h_f pressure load at humidity front, z_f humidity front depths.

Soil Water Flow

Soil water flow under saturated conditions can be described with **Darcy's law** (Eq. 3) which postulates that rate of water flow through a soil mass is proportional to the hydraulic head gradient (Kutilek and Nielsen, 1994). Henry Darcy (1803-1858) was a french hydraulic engineer who designed a vertical experimental tank (Fig. 7) to investigate the water flow. He observed a loss of energy occurs and as a result a head drop across the sand filter when water flowing through porous material.

Darcy's law is also applied for flow through unsaturated soil under the condition of laminar flow. The coefficient of permeability in a unsaturated soil cannot generally assumed to be constant. The Richards Equation combines Darcy's law with the conservation of mass and describes the rate of water flow through a unsaturated soil, which is linearly proportional to the hydraulic head gradient.

$$q = \frac{Q}{A} = -K \frac{\Delta h}{L} \quad (3)$$

with: q specific discharge, Q flow, A total cross-sectional area through which flow occurs, K hydraulic conductivity, Δh head difference, L length.

Hydraulic conductivity is the coefficient of permeability (or hydraulic conductivity) also quantified the permeability of soil or rock, it contains density and viscosity of the fluid which flows through medium. **Permeability** is the property of rocks and soils that is an indication of the ability for gases or fluids to flow through rocks and soils. High permeability will allow fluids and gases to move rapidly through rocks. It depends only on material properties of porous medium.

The validity of Darcy's law depends on the flow regime within the porous media (Fig. 8).

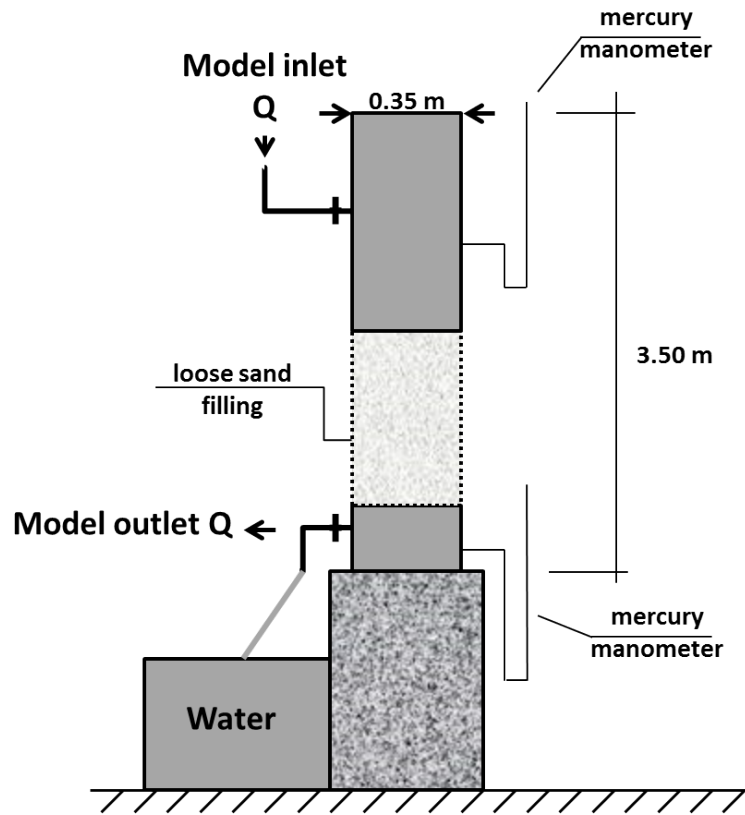


Fig. 7: Darcy's apparatus; modified based on Musy (2001).

Evaporation and Transpiration

Evaporation is a process, in which water from open water surfaces (oceans, seas, lakes and rivers), from uncovered soil and from surfaces covered by snow and glaciers goes into the atmosphere in a vapour state. The meteorological factors influencing evaporation are available water quantity, solar radiation, atmospheric pressure and wind, water and air temperature, humidity. **Transpiration** is a process in which a fraction from the water assimilated by vegetation is set free into the atmosphere in vapour state. **Evapotranspiration** is the sum of evaporation and transpiration. So the evapotranspiration is the total quantity of water, in the shape of vapour, transferred from atmosphere, hydrosphere, biosphere, lithosphere and anthroposphere.

Empirical and semi-empirical as well as formulas with physical base exist for estimation of evaporation. The Penman (1948) formula accounting for aerodynamic influences:

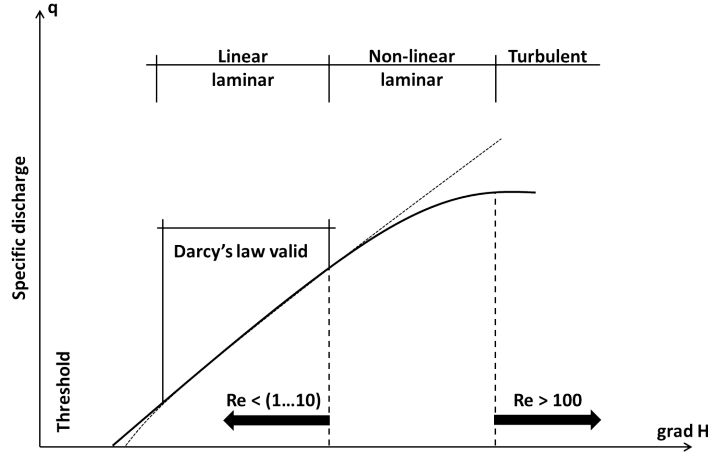


Fig. 8: Range of Darcy's Law depending on Reynolds number (Re); modified based on VICAIRe (2006).

$$ET_0 = \frac{R_n \Delta + \frac{\rho c_p \delta e}{r_a}}{\lambda (\Delta + \lambda)} \quad (4)$$

The calculation requires: daily mean temperature, wind speed, relative humidity and solar radiation. Monteith (1981) has improved the Penman formula by introducing the effect of diffusion resistance of evaporation surface. The Penman-Monteith relation reads:

$$ET_0 = \frac{R_n \Delta + \frac{\rho c_p \delta e}{r_a}}{\lambda \left[\Delta + \lambda \left(1 + \frac{r_s}{r_a} \right) \right]} \quad (5)$$

with:

- R_n – net solar radiation [W/m^2],
- Δ – rate of change of saturation specific humidity with air temperature,
- λ – psychrometric constant (vaporization constant heat at constant pressure, i.e. $2.45 [MJ/kg]$),
- ρ – air volume mass [kg/m^3],
- δe – humidity deficit [kPa],
- c_p – specific heat capacity of air [$J/(kgK)$],
- r_a – aerodynamic resistance [s/m],
- r_s – diffusion resistance of evaporation surface [s/m].

Response analysis

Hydrographs (Fig. 9) provide important information about hydrological processes in watersheds (catchments) (Musy and Highy, 1998; Shaw et al., 2011). What is the hydrological response after rainfall events? How can fast (surface runoff) and delayed (subsurface passage) processes be distinguished?

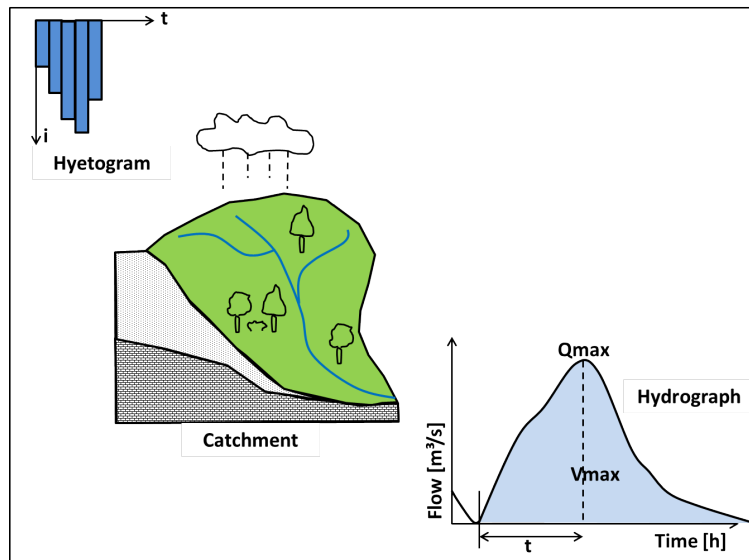


Fig. 9: Hydrological response of a catchment; modified based on Musy (2001).

The **hydrological catchments response** can be influenced by many factors (Musy and Highy, 1998) that are related to:

- climatic conditions of the environment, rain (spatial and temporal distribution, intensity and rain duration),
- catchment morphology (shape, dimension, aspect),
- physical properties of the catchment (soil nature, vegetation coverage),
- structure of the hydrographic network (dimensions, hydraulic properties),
- previous soil humidity.

Chapter 2

Hydrogeology

AGNES SACHSE, LESLIE JAKOBS AND OLAF KOLDITZ

Hydrogeology is the study of water in geologic formations beneath the earth's surface (Hölting, 2013). Groundwater moves in soil and rock (aquifers) and supplies springs, wells, and when near the surface, lakes and streams. The upper limit of the saturated zone is called the water table. Aquifer formations have different geological characterizations:

- **Lithology** is the physical makeup, including the mineral composition, grain size and grain packing of the sediments or rocks that make up the geological systems.
- **Stratigraphy** describes the geometrical and age relations between the various layers, beds and formations in geologic systems of sedimentary origin.
- **Structural features** such as cleavages, fractures, folds and faults are the geometrical properties of the geologic systems produced by deformation after deposition or crystallization.

2.1 Aquifer Types

An **aquifer** is a saturated permeable geologic unit that can transmit significant quantities of water under ordinary hydraulic gradients (Hölting, 2013; Kresic, 2007). The below definitions of aquifer types are from Freeze and Cherry (1979):

- An **aquitard** is a saturated bed in a stratigraphic sequence with such low permeability that it cannot deliver water at a productive rate.
- An **aquiclude** is defined as a saturated geologic unit incapable of transmitting significant quantities of water under ordinary hydraulic gradients and that restricts vertical flow.

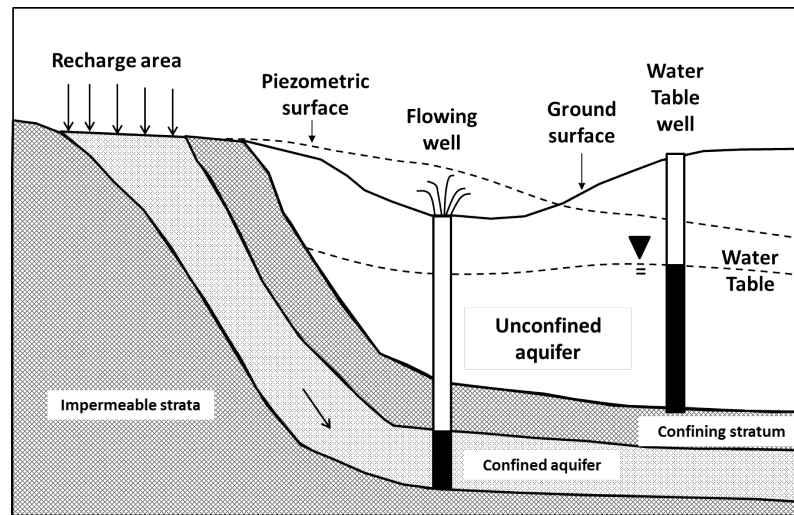


Fig. 1: Schematic cross section illustrating unconfined and confined aquifers.

Figure 10 illustrates unconfined and confined aquifers.

- **Unconfined aquifers** are exposed at surface. These aquifers are bounded by the water table (water level in borehole). The water table can have tendency to mimic the topographic contours of the land surface above.
- A **confined aquifer** is an aquifer, where a low permeability layer (e.g. clay) borders the upper surface of the aquifer, thereby confining the groundwater under pressure. Artesian conditions exist when this impermeable layer is breached, and water rises up above the top of aquifer. A confined aquifer is fully saturated (Kresic, 2007).

Groundwater recharge (GWR) is the inflow of water to a groundwater reservoir from the surface infiltration of precipitation and its movement to the water table.

2.2 Aquifer Characteristics

Aquifers are formed from different rocks, e.g., unconsolidated sediments, sedimentary rocks, igneous and metamorphic rocks, and have corresponding characteristics. Originated rock types are responsible for source (yield), storage, filtering and routing of groundwater. Based on Gupta (2001), aquifers are characterised by the following parameters:

- **Porosity n** of a soil or rock is that fraction of a given volume of material that is occupied by void space, or interstices. Porosity, indicated by the

symbol n , is usually expressed as the ratio of the volume of voids. Most rocks naturally contain a certain percentage of voids that can be occupied by water.

- **Percolation** is the rate at which water moves downward through porous medium.
- **Permeability** k is an expression of movement of water in any direction.
- **Specific yield** is the ratio of the volume of water, that, after saturation, can be drained by gravity (Eq. 6).
- **Storage coefficient** S is the volume of water that an aquifer releases from or takes into storage per unit surface area of aquifer per unit change in head normal to that surface (Eq. 7).
- **Hydraulic conductivity** K is a constant that serves as a measure of the permeability of the porous medium.
- **Transmissivity** T rate at which water is transmitted through a unit width of aquifer under unit hydraulic gradient; $T = Kb$, where b is the saturated thickness of aquifer.

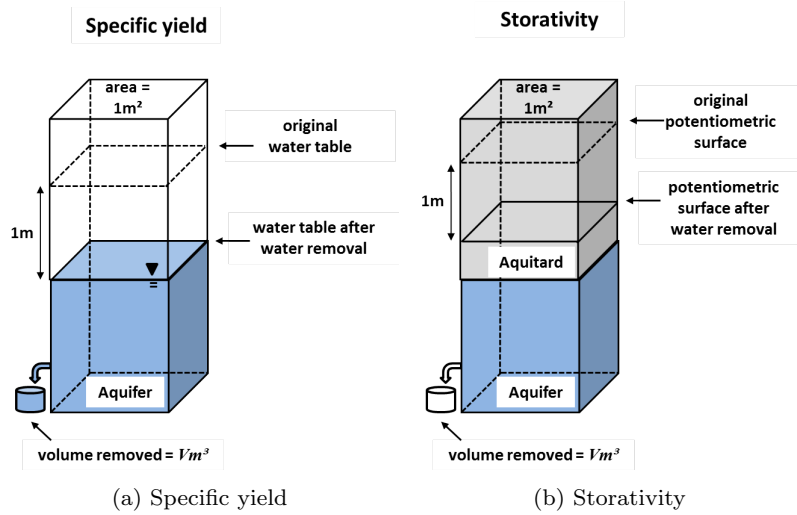


Fig. 2: Specific yield in an unconfined aquifer and storativity of an confined aquifer; modified based on Hornberger et al. (1998).

Storage characteristics are different in unconfined and confined aquifers (Fig. 11).

$$S = \frac{V}{A\Delta h} \quad \text{Specific yield} \quad (1)$$

$$S = S_S b \quad \text{Storativity = Capacity} \quad (2)$$

2.3 Groundwater Flow Equation

In this chapter we briefly describe the derivation of the groundwater flow equation. The groundwater flow equation is derived from the conservation principles of mass and momentum balance. The basic idea is the Eulerian concept of motion in the frame of continuum mechanics.

We start with the equation of fluid mass balance in a static (i.e. non-deformable) porous medium (Eq. 8). In case of a porous medium, the available room for fluid flow is reduced to the pore space. The ratio of pore space to the total volume of a porous medium is given by the porosity n . The porosity can change in case of deformation processes, which is neglected here. All variables and parameters of the equations are given at the end of this section.

$$\frac{\partial n\rho}{\partial t} + \nabla \cdot (n\rho\mathbf{v}) = Q_\rho \quad (3)$$

For an incompressible fluid (such as water) we have

$$\rho \frac{\partial n}{\partial t} + \rho \nabla \cdot (n\mathbf{v}) = Q_\rho \quad (4)$$

Incompressibility means that the density of the fluid is nearly constant in the given range of groundwater pressure values, i.e. $\rho = \rho_0$. Now dividing by the reference density ρ_0 we yield

$$\frac{\partial n}{\partial t} + \nabla \cdot (n\mathbf{v}) = \frac{Q_\rho}{\rho_0} \quad (5)$$

The temporal change of porosity is expressed by the storativity concept in groundwater hydraulics. There is a linear relationship between porosity and groundwater pressure changes. The proportion factor is given by the storativity coefficient S (see Sec. 2.2).

$$\frac{\partial n}{\partial t} = S \frac{\partial h}{\partial t} \quad (6)$$

Now we make use of Darcy's law (see Sec. 1.5).

$$n\mathbf{v} = \mathbf{q} = -\mathbf{K}\nabla h \quad (7)$$

Combining the above balance (Eq. 10) and constitutive equations (Eq. 11- 12) we yield the groundwater flow equation.

$$\begin{aligned} S \frac{\partial h}{\partial t} + \nabla \cdot (n\mathbf{v}) &= Q \\ S \frac{\partial h}{\partial t} - \nabla \cdot (\mathbf{K}\nabla h) &= Q \end{aligned} \quad (8)$$

$$S \frac{\partial h}{\partial t} - \frac{\partial}{\partial x} \left(K_x \frac{\partial h}{\partial x} \right) - \frac{\partial}{\partial y} \left(K_y \frac{\partial h}{\partial y} \right) - \frac{\partial}{\partial z} \left(K_z \frac{\partial h}{\partial z} \right) = Q$$

With following parameters [units]:

- h – hydraulic head or piezometric head [m],
- \mathbf{K} – hydraulic conductivity tensor [m/s],
- K_x, K_y, K_z – hydraulic conductivity values in coordinate directions [m/s],
- n – porosity [m^3/m^3],
- \mathbf{q} – Darcy or percolation velocity [m/s],
- Q_ρ – source-sink term of groundwater [kg/m^3s],
- S – storage coefficient [1/m],
- t – time [s],
- \mathbf{v} – pore velocity vector [m/s],
- ρ – fluid density [kg/m^3].

The theoretical derivation of the groundwater flow equation is the prerequisite for the practical application of the numerical modelling of hydrological processes in *OpenGeoSys*.

Chapter 3

Modelling with *OpenGeoSys*

KARSTEN RINK, AGNES SACHSE AND OLAF KOLDITZ

3.1 Hydrologic Modelling and Simulation

Numerous hydrologic models are available to understand, simulate and predict hydrologic behaviour of and within watersheds based on well-established physically-based equations (Westervelt, 2001). Such models can be roughly divided into the following categories:

- field scale or watershed scale hydrologic and soil erosion models,
- field scale or watershed scale water quality models,
- groundwater flow models.

This tutorial will mainly focus on the application and set-up of numeric groundwater flow models. The basic setup of such a models is detailed in the following workflow presented by Kresic (2007):

1. development of a conceptual model
2. selection of a computer code that can most effectively simulate the conceptual model
3. definition of a model geometry, i.e. the lateral and vertical extent of the model area as well as the domain discretisation
4. input of hydrogeological parameters for each model cell, e.g. hydraulic conductivity, including possible anisotropy, storage properties, effective porosity, etc.
5. definition of boundary condition for the model that influence water fluxes entering or leaving the model domain
6. definition of initial conditions, i.e. the estimated distribution of hydraulic head in the model domain
7. definition of external or internal hydraulic stresses estimated along the model boundaries, such as areal recharge, well pumping, spring discharge, inflow from water from other sources (e.g. adjacent aquifers).

After such a model has been compiled, it can be used to run simulations. A subsequent calibration is performed to match the simulation results with observed data. Examples include the hydraulic head measured in monitoring wells or the flux along model boundaries measured or calculated externally to the model. Calibration is an iterative process where input parameters for the numerical model are adjusted such that simulation results of subsequent model runs are fitting the data measured at observation sites more and more closely.

In this tutorial we will apply the workflow described above with the numerical software framework *OpenGeoSys* (Sec. 3.2). Its practical application is presented in detail based on a benchmark simulating the transient lowering of the water table induced by a pumping well (Chap. 4) and a real-world case study on groundwater recharge in a small river catchment (Chap. 5). An overview of other existing simulation codes is presented in Tab. 1, compiled from two recent review papers concerned with hydrological (Maxwell et al., 2014b) and reactive transport modelling (Steefel et al., 2014).

3.2 *OpenGeoSys* Process Simulation

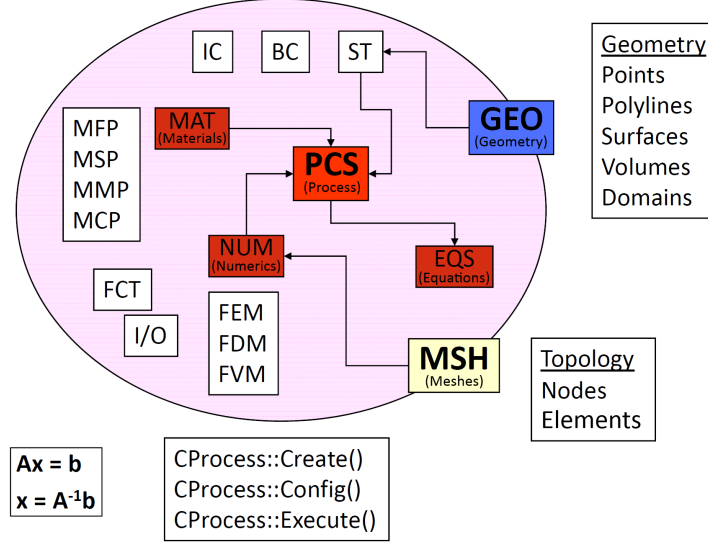
OpenGeoSys (*OGS*) is a professional open-source platform for numerical simulation of thermo-hydro-mechanical/chemical processes in porous media. The basic concept is to provide a flexible numerical framework for solving multi-field problems in porous and fractured media for applications in geoscience and hydrology.

OGS has been successfully used in various environmental disciplines such as groundwater remediation and surface hydrology, water resources management, radioactive waste disposal, geothermic energy resources, CO₂ storage and technical energy storage systems. Numerical simulations are based primarily on an object-oriented implementation of the Finite Element Method (FEM) including a broad spectrum of interfaces for pre- and postprocessing. The structure of *OGS* input files reflect this object-orientated approach for the solution of initial-boundary-value-problems, originally proposed in Kolditz and Bauer (2004). The basic structure is illustrated in Fig. 12, with the process-object (PCS) as the central unit for input configuration. Depending on the selected THMC process, e.g. groundwater flow, input files are constructed in a specific way to include the relevant information required for simulation of this process. Details on the structure of *OGS* input files are found in the practical examples presented in chapters 4 and 5.

The aim of the *OGS*-framework is to provide an open platform to the community, outfitted with professional software-engineering tools such as platform-independent compiling and automated benchmarking. *OGS* has been in development since the mid-eighties. While the current version is *OGS 5*, the development of *OGS 6* is currently in a concept stage with the

Table 1: Overview of numerical simulation codes in alphabetical order

Acronym	Symbol	Reference
CATHY	CATchment HYdrology	(Camporese et al., 2010)
CrunchFlow	Software package for simulating reactive transport	(Steefel and Lasaga, 1994)
DuMuX	DUNE for multi-{phase, component, scale, physics, ...} flow and transport in porous media	(Flemisch et al., 2011)
eSTOMP	Subsurface Transport Over Multiple Phases, parallel version	(Yabusaki et al., 2011)
FEFLOW	Finite element groundwater, mass and heat transport simulator	(Diersch and Kolditz, 1998)
HydroGeoSphere	A Fully Integrated, Physically Based Hydrological Model	(Brunner and Simmons, 2012)
HP1/HPx	Versatile coupled reactive transport code for variably-saturated flow conditions	(Nakhaei and Šimunek, 2014)
HYDROGEO-CHEM	A coupled model of variably saturated flow, thermal transport, and reactive biogeochemical transport	(Yeh et al., 2012)
HYTEC	Reactive transport code	(Windt et al., 2014)
MIN3P	Multicomponent reactive transport code	(Maier et al., 2013)
MODFLOW	Finite difference groundwater simulator	(Hughes et al., 2014)
OpenGeoSys	Open-source, finite element, THMC simulator for porous and fractured media	(Kolditz et al., 2012a)
ORCHESTRA	Modelling platform for equilibrium chemistry with the option of including kinetics and/or transport processes	(Meeussen, 2003)
ParFlow	Parallel Flow; integrated hydrological modeling	(Maxwell, 2013)
PAWS	Process-based Adaptive Watershed Simulator	(Shen et al., 2013)
PIHM	Penn State Integrated Hydrologic Model	(Shen and Phanikumar, 2010)
PFLOTRAN	Open-source, massively parallel multi-scale and multiphysics code for subsurface flow and transport applications	(Hammond et al., 2012)
PHREEQC	Computer program for a large variety of aqueous geochemical calculations	(Appelo et al., 2014)
PHT3D	Multi-component reactive transport code specifically designed for simulating flow and reactive transport processes in saturated porous media	(Appelo and Rolle, 2010)
TOUGHREACT	A simulation program for subsurface reactive chemical transport under non-isothermal multi-phase flow conditions	(Xu et al., 2012)
tRIBS	Triangulated Irregular Network (TIN)-Based Real Time Integrated Basin Simulator	(He et al., 2014)

Fig. 1: Object-orientated structure of *OGS*-projects.

focus on computational efficiency as well as intuitive interfaces for developers and users. Visit the *OpenGeoSys* community webpage (www.opengeosys.org) for more information on new releases, publications, courses and other community efforts.

3.3 Modelling Workflow

A large variety of tools for data processing and environmental modelling is available either as commercial products or as scientific frameworks (Tab. 1). As the functionality of each framework is limited and often focussed on solving a specific type of challenge, linking those tools is a challenging task, but often necessary for processing and integrating data from different sources.

To prevent loss of information and ensure efficient processing of all model-related data, the development of continuous workflows is of vital importance. Fig. 13 shows the different components of a typical data

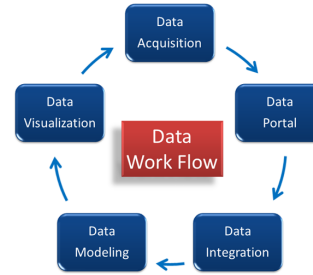


Fig. 2: Modelling workflow concept (Kolditz et al., 2012c)

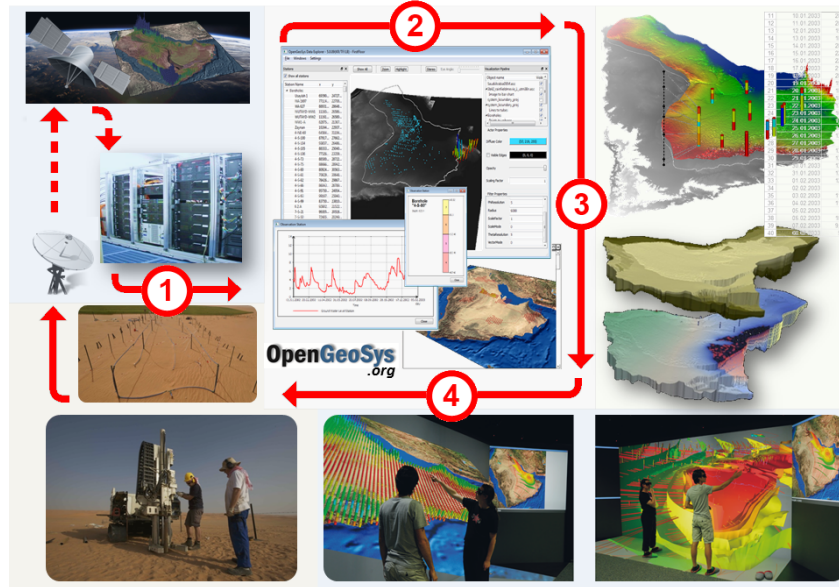


Fig. 3: *OGS* workflow concept for hydrological modelling

workflow, starting with the acquisition of the data, the storage in databases using established data models and meta data standards, the integration of heterogeneous data sets from various sources, the modelling process itself using the processed data sets as well as an integrated scientific visualisation of input-, modelling- and simulated data.

OpenGeoSys provides parts of this workflow concept, including data integration and visualisation (Sec. 3.4) as well as numerical process simulation (Sec. 3.2). Based on a study of groundwater recharge in Saudi Arabia (Rink et al., 2012b), Fig. 14 illustrates such a project workflow consisting of the following four steps:

1. data is acquired from various sources, e.g. remote sensing and ground-truth geophysical measurements
2. all data is integrated via the *OGS Data Explorer* and prepared for numerical simulations of different processes
3. data and simulation results are analysed and validated
4. high-performance visualisation techniques are employed to discuss scenarios or improve monitoring concepts.

Other examples where *OGS* has been employed for the simulation of hydrological processes include case studies in China (Sun et al., 2012), Israel/Palestine (Gräbe et al., 2013), the Oman (Walther et al., 2014) as well as multiple regions in Germany (Rink et al., 2011; Selle et al., 2013a).

Benchmarking

Benchmarking is an acknowledged and approved scientific methodology to test and to improve knowledge about complex systems behaviour. There are different benchmarking techniques, such as:

- process analysis with increasing complexity: have we addressed all important phenomena?
- model comparison: have we selected an appropriate conceptual model?
- code comparison: have we implemented the underlying conceptual model correctly?
- etc.

There have been several benchmarking projects and initiatives in geosciences in the past, e.g., HYDROCOIN, INTRAVALEX, DECOVALEX (Jing et al., 1995; Tsang et al., 2009; Wang et al., 2011), CO2BENCH (Kolditz et al., 2012a). Most of them are related to research of nuclear waste deposition as for this purpose longterm calculations are necessary for safety assessment issues. New and more comprehensive benchmarking initiatives recently came up in hydrology (Kalbacher et al., 2012; Maxwell et al., 2014a) and geosciences (SSBENCH (Steeffel et al., 2014)), showing the popularity and necessity of those activities to the scientific community.

A comprehensive book has been published recently, containing a large assembly of benchmarks and examples for porous media mechanics collected over the last twenty years (Kolditz et al., 2012b). Analysis of thermo-hydro-mechanical-chemical (THMC) processes is essential to many applications in environmental engineering, such as geological waste deposition, geothermal energy utilisation, carbon capture and storage, water resources management, hydrology, or even climate change. The benchmark book is part of the *OpenGeoSys* initiative – an open source project to share knowledge and experience in environmental analysis and scientific computation.

For this tutorial the classic “Theis” example has been selected for getting started using *OGS*. The benchmark describes the transient lowering of the water table caused by a pumping well. Chapt. 4 contains an extensive explanation on all steps for the set up the *OGS* configuration files and running the benchmark.

3.4 OpenGeoSys Data Explorer

As described in the previous sections, the *OpenGeoSys* software framework contains multiple algorithms for the simulation of (coupled) thermal, hydrological, mechanical and chemical processes using a large amount of FEM-related functionality and various numerical solvers. However, it does not provide functionality to actually set up a model. As a command line tool, it also does

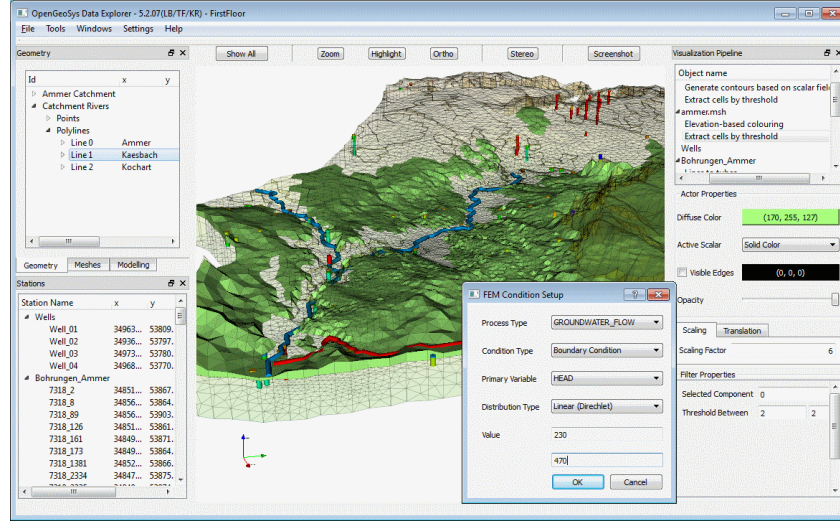


Fig. 4: The graphical user interface of the *Data Explorer* shows a number of data sets from a groundwater recharge study.

not support data visualisation or modification; and even simulation results cannot be directly verified without the help of other software.

To address these issues, the *OpenGeoSys Data Explorer* has been developed as a graphical user interface for *OpenGeoSys* (Fig. 15). This framework allows to visualise and assess input data as well as simulation results in a 3D space. Additional non-spatial information, such as time series data or borehole stratigraphies attached to 3D data sets, may be viewed in separate 2D windows. As with the *OpenGeoSys* simulation software itself, the *Data Explorer* is platform independent and employs the same basic data structures and file formats as the command line tool. In addition, it does also provide a large number of interfaces for the import of files created by established geoscientific software products such as the geographic information system *ArcGIS*, the groundwater modelling software *GMS* (<http://www.aquaveo.com/gms>) and, to a certain degree, complex software solutions used in the mining or petroleum industry such as *Petrel* (<http://www.software.slb.com>) or *Gocad* (<http://www.gocad.org>). For an overview of the currently supported file formats see Tab. 2. Furthermore, all data sets can be exported to established graphics formats, allowing the use of specialised software such as *ParaView* (Ahrens et al., 2005) or *Unity* (Goldstone, 2011) to create visualisation projects for presenting complex environmental data and simulations in an easy-to-understand manner.

The *Data Explorer* supports users in the preparation of simulation models by allowing them to see how various data sets complement or interact with

Table 2: Overview of existing interfaces.

Data type	Formats / Programmes
Raster data	GeoTIFF, Esri ASCII Raster, NetCDF, JPEG, etc.
Features	Esri Shapes, Petrel borehole data, GMS borehole data
Meshes	FEFLOW, GMS, GMSH, TetGen, VTK, etc.
Time series data	CSV, WaterML
Graphic formats	VTK, OpenSG, Unity, VRML

each other. When heterogeneous data sets from different sources are integrated into a model, inconsistencies between those data sets are a frequently encountered problem. Typical examples in the scope of hydrological data include the course of rivers not quite matching the underlying terrain model, subsurface layers penetrating each other or boreholes not starting at ground level but instead above or below the surface. The reasons for such inconsistencies are manifold and can be attributed to different data acquisition methods (such as remote sensing data scanned from orbit via satellites, borehole logs created manually using core samples, etc.), data conversion problems, artefacts in the data (e.g. due to cloud cover or water reflection in satellite data or extreme weather events at observation sites) or human errors when transferring data. However, if models for the simulation of processes such as groundwater recharge are based on faulty or conflicting information, they might produce erroneous or deceptive results.

The option to visualise the data in an interactive 3D scene allows researchers to at least roughly assess the quality of the data and detect inconsistencies, artefacts or missing information by visual inspection. The *Data Explorer* provides a number of visualisation options to support users in this assessment process by allowing the adjustment of a number of parameters for each data set. Generic parameters such as super elevation factors, transparency, or the colour lookup table used for depicting data sets can be easily defined. More advanced algorithms include the selection of specific materials or stratigraphic layers while concealing the rest of the data set, highlighting certain features for better visibility, and the calculation of iso-surfaces from volumetric data (Rink et al., 2014). In addition, the framework shows the underlying data of visualised objects (such as point coordinates, mesh element information, etc.) in tabular form in a separate menu for verifying information based on exact numbers. The *Data Explorer* offers several options for modifying data sets to a certain degree. For example, geometric surfaces can be triangulated, polylines can be connected in a user-defined sequence and data might be converted or mapped to other data sets using a number of different algorithms. In addition, the material groups of existing models can be changed, mesh elements can be removed based on a number of cri-

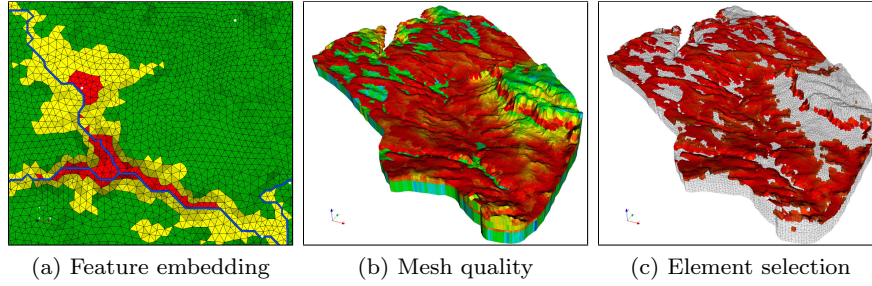


Fig. 5: Mesh quality validation: (a) Embedding geometric information representing rivers (blue) and wells (white) into the mesh structure. (b) Element quality based on edge ratio. Red/orange signifies large differences in edge length, green/blue signifies roughly equilateral elements. (c) Further analysis reveals that elements with a large edge ratio are the result of a thin surface layer.

teria and subsets of existing domains can be extracted based on triangulated surfaces (Rink et al., 2013).

Geometry data can be used to create discretise the domain into a finite element mesh. Optionally, digital elevation models can be applied to assign elevation values to mesh nodes in the domain. (Fig. 18a). Parameters such as the density of mesh elements and the degree of adaptive refinement towards selected features can be defined by the user. For detailed simulations, it is preferable to integrate additional data into the mesh that will be relevant for the model later on. Examples include polylines that represent the courses of rivers as well as a number of boreholes and wells or point data to designate the location of observation sites such as production wells (Fig. 16a). Boundary conditions will be later applied to these objects (Fig. 17) and integrating them into the mesh at the beginning of the model setup will ensure a less error-prone configuration of the model later on. 3D meshes can be either imported from other software or created in the *Data Explorer* by extruding the 2D mesh into one or more subsurface layers (Fig. 18c). These new layers may either have a constant thickness (although the thickness of different layers may vary) or they can be based on elevation maps of subsurface layer boundaries in raster format (i.e. DEMs of layer boundaries, usually interpolated from borehole data). Depending on the type of mesh to be created, different approaches are employed for the domain discretisation, including the use of different external FEM mesh generators such as *GMSH* (Geuzaine and Remacle, 2009) or *TetGen* (Si, 2013).

Once a mesh has been created or imported into the framework, the quality of all mesh elements can be verified with respect to well-establish criteria (Fig. 16). Implemented metrics include the ratio of the longest to shortest

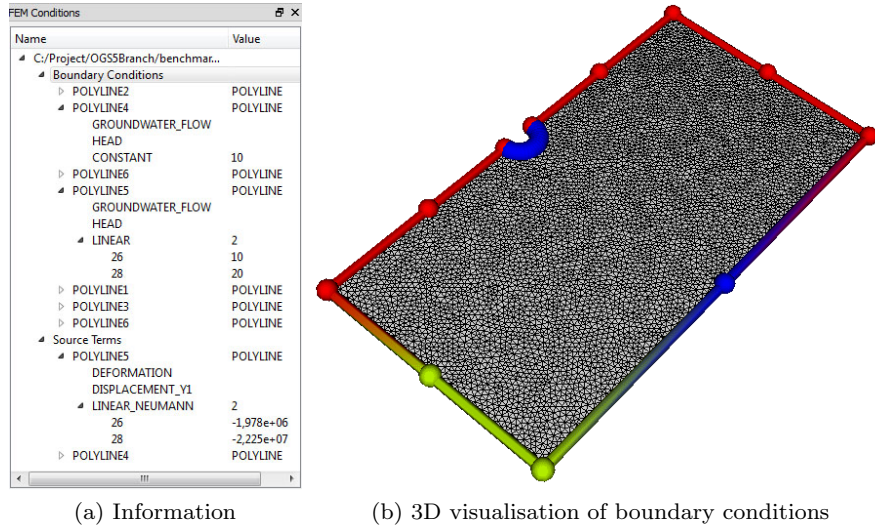


Fig. 6: Example for visualisation of FEM related data. Depicted are a number of boundary conditions for a FEM Mesh along with detailed information about their properties.

element edge, the equiangular skew (i.e. deviation from the optimal inner angle of an element), or the ratio between shortest edge and radius of the circumsphere (a metric used in Delaunay tetrahedralisation (Aurenhammer, 1991)). Results of such an analysis are mapped onto the mesh (Fig. 16) and can be further refined using a number of visualisation techniques, incorporating other data sets when required. In addition, a set of automated tests can be applied to meshes to detect some obvious potential problems, including zero-volume-elements, non-convex elements, non-planar surfaces or nodes with a dangerously small distance between each other. It is worth noting that not all of these issues will cause problems during the simulation of all processes. For instance, the simulation of groundwater recharge presented in Chap. 5 consists mainly of layered flows. Large differences between the horizontal and vertical extent of mesh elements will most likely have no effect on a correct result, whereas mass transport processes explicitly require a high resolution in vertical direction to ensure a stable solution.

Once simulation results are available, they can be visualised concurrently with input and model data in the *Data Explorer* (Fig. 18d). Such an integrated visualisation is helpful for verifying the plausibility of simulation results or presenting the case study an outside audience. Correlations to input data sets might become visible and a comparison between observed and simulated

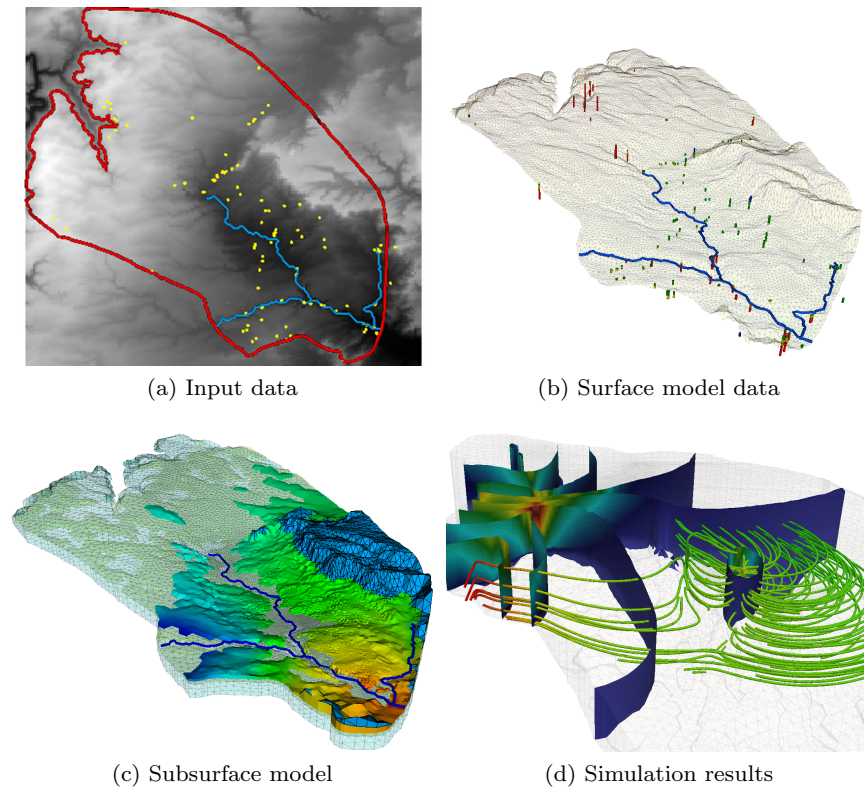


Fig. 7: Visualisation of data sets at various stages of the modelling process. (a) Input data from geographic information systems (GIS). (b) 3D surface model based on GIS data. (c) Subsurface model with layers interpolated based on borehole data. Different information is displayed for each geological layer. (d) Representation of simulation results using established visualisation techniques such as isosurface and stream tracers.

parameters is easily accomplished. An overview over the data visualisation at various stages of the modelling process is given in Fig. 18.

This section outlined a number of features of the *Data Explorer*-framework in general. A more detailed insight into working with the programme is given in chapter 5. Starting with a number of hydrogeological input data sets, a 3D subsurface mesh representing a river catchment will be created based on a number of input data sets. This mesh is then used to assign boundary conditions and run a groundwater flow simulation based on the finite element method.

For more information about the *OGS Data Explorer*, the interested reader is referred to articles on visualisation (Rink et al., 2014) and model creation (Rink et al., 2013) using this framework. A comprehensive specification of the functionality of the programme can also be found in the *OpenGeoSys Data Explorer User Manual* (Rink, 2013) available from <http://www.opengeosys.org> together with the simulation software and the *Data Explorer* software itself.

Download and installation instructions for the command line and graphical user interface can be found in Appendix C. *OpenGeoSys* is an open-source software available under BSD license. The source code for the framework as well as the user manual may be found on GitHub at <https://github.com/ufz/ogs>.

Chapter 4

Benchmark: Theis problem

WENKUI HE, MARC WALTHER AND OLAF KOLDITZ

4.1 Benchmark Definition

The Theis problem describes a transient lowering of the water table caused by a pumping well (see Fig. 19). In order to show the basic steps to set up simple numerical models with different dimensions in *OGS*, we consider a homogeneous, isotropic, confined aquifer in setups with different dimensions (2D, 3D, radial symmetric 1.5D and 2.5D, see also Tab. 4). For the different setups, we evaluate the plausibility of the processes `GROUNDWATER_FLOW` and `LIQUID_FLOW` to model confined groundwater flow in porous media under a stress condition. The governing equation for groundwater flow process in a confined aquifer is given in Eq. 14 with the primary variable hydraulic head. For the liquid flow process, Eq. 15 with pressure as its primary variable governs the flow. In Sec. 2.3, the derivation as well as physical meanings of groundwater flow equations are explained in great detail.

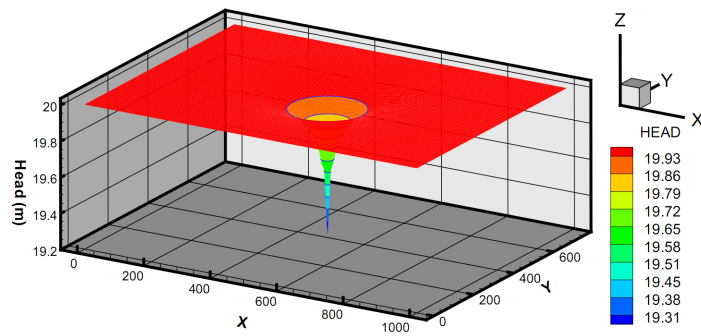


Fig. 1: Cone of depression caused by pumping (Kolditz et al., 2012b)

- GROUNDWATER_FLOW:

$$S_s \frac{\partial h}{\partial t} = \nabla(K \cdot \nabla h) + q \quad (1)$$

- LIQUID_FLOW:





$$\frac{S_s}{\rho g} \frac{\partial p}{\partial t} = \nabla \left(\frac{k}{\mu} (\nabla p + \rho g \nabla z) \right) + q \quad (2)$$

The parameters for aquifer & fluid properties, and well operations are given in Tab. 3.

Table 1: Parameters and their values applied for Theis problem

Parameter	Symbol	Value	Unit
Pumping rate	Q	1.4158E-2	m ³ /s
Hydraulic conductivity	K	9.2903E-4	m/s
Intrinsic permeability	κ	1.2391E-10	m ²
Specific Storage	S_s	1E-3	1/m
Well radius	r_w	0.3048	m
Study area length	r_b	1000	m
Density of water (10 °C)	ρ	999.7026	kg · m ⁻³
Viscosity of water (10 °C)	μ	1.308E-03	Pa · s

Table 2: Summary of the model concepts for Theis' problem

Dimension	1.5D	2D	2.5D	3D
Geometry				
Concept	Radial symmetry	—	Axisymmetry	—
Key Word	\$AXISYMMETRY	—	\$AXISYMMETRY	—

4.2 OGS Input Files

Tab. 5 gives the directory structure for the Theis' problem, which contains benchmarks with different geometry and model approaches. The numerical simulation with *OGS* relies on file based model setups, which means each model needs different input files that contain information on specific aspects of the model. All the input files share the same base name but have a unique

file ending, with which the general information of the file can already be seen. For example, a file with ending `.pcs` provides the information of the process involved in the simulation such as groundwater flow or Richards flow; whereas in a file with ending `.ic` the initial condition of the model can be defined. Tab. 6 gives an overview and short explanations of the *OGS* input files needed for one of the benchmarks.

Table 3: *OGS* directory structure for the Theis problem

Model approach	Directory name
GROUNDWATER_FLOW	GWF_Theis_1.5D
	GWF_Theis_2.5D
	GWF_Theis_2D
	GWF_Theis_3D
LIQUID_FLOW	LF_Theis_1.5D
	LF_Theis_2.5D
	LF_Theis_2D
	LF_Theis_3D

Table 4: *OGS* input files for the Theis problem (groundwater flow)

Object	File	Explanation
GEO	GWF_Theis.gli	system geometry
MSH	GWF_Theis.msh	finite element mesh
PCS	GWF_Theis.pcs	process definition
NUM	GWF_Theis.num	numerical properties
TIM	GWF_Theis.tim	time discretization
IC	GWF_Theis.ic	initial conditions
BC	GWF_Theis.bc	boundary conditions
ST	GWF_Theis.st	source/sink terms
MFP	GWF_Theis.mfp	fluid properties
MMP	GWF_Theis.mmp	medium properties
OUT	GWF_Theis.out	output configuration

The basic structure and concept of an input file is illustrated in the example below (Listing 4.1). As we can see, an input file begins with main keywords which contain sub keywords with corresponding parameter values. When an input file ends with the keyword `#STOP`, everything written after file input terminator `#STOP` is unaccounted for input. Please also refer to the *OGS* input file description in the keyword description to the *OGS* webpage (<http://www.opengeosys.org/help/documentation>)

Listing 4.1: Example for input file

```
#MAIN_KEYWORD1
$SUB_KEYWORD1
value value value
$SUB_KEYWORD2
value value
#MAIN_KEYWORD2
$SUB_KEYWORD1
value value
[...]
```

We consider different geometric set-ups for the simulation of the Theis problem for which we need to specify the corresponding geometry definitions and finite element meshes (see Tab. 4). According to the different formulations of the Theis problem in terms of hydraulic head h (Eq. 14) and liquid pressure p (Eq. 15), the general input files are as follows.

- PCS - process definition: we distinguish between groundwater and liquid flow

Listing 4.2: Example process file for GROUNDWATER_FLOW: GWF_Theis.pcs

```
#PROCESS
$PCS_TYPE
GROUNDWATER_FLOW ; for equation ()
$PRIMARY_VARIABLE
HEAD
#STOP
```

Listing 4.3: Example process file for LIQUID_FLOW: LF_Theis.pcs

```
#PROCESS
$PCS_TYPE
LIQUID_FLOW ; for equation ()
$PRIMARY_VARIABLE
PRESSURE1
#STOP
```

- IC/BC/ST: initial and boundary conditions are process-specific (PCS_TYPE) and related to geometries (GEO_TYPE)
 - PCS_TYPE : related process, primary variables
 - GEO_TYPE : related geometry such as domain, point, polyline or surface
 - DIS_TYPE : values corresponding to a specific distribution

Listing 4.4: Example initial condition file: GWF_Theis.ic

```
#INITIAL_CONDITION
$PCS_TYPE
GROUNDWATER_FLOW
$PRIMARY_VARIABLE
```

```

HEAD
$GEO_TYPE
DOMAIN
$DIS_TYPE
CONSTANT 0.0
#STOP

```

Listing 4.5: Example boundary condition file: GWF_Theis.bc

```

#BOUNDARY_CONDITION
$PCS_TYPE
GROUNDWATER_FLOW
$PRIMARY_VARIABLE
HEAD
$GEO_TYPE
POINT INIFINIT
$DIS_TYPE
CONSTANT 0.0
#STOP

```

Listing 4.6: Example process file: GWF_Theis.st

```

#SOURCE_TERM
$PCS_TYPE
GROUNDWATER_FLOW
$PRIMARY_VARIABLE
HEAD
$GEO_TYPE
POINT WELL
$DIS_TYPE
CONSTANT_NEUMANN -194.69
#STOP

```

- NUM: numerical properties are process-specific (PCS_TYPE)
 - PCS_TYPE : related process
 - LINEAR_SOLVER : method and relevant parameters such as error tolerance for linear solver

Listing 4.7: Example numerical file: GWF_Theis.num

```

#NUMERICS
$PCS_TYPE
GROUNDWATER_FLOW
$LINEAR_SOLVER
; method error_tolerance max_iterations theta precond storage
2 5 1.e-014 1000 1.0 100 4
#STOP

```

- TIM: time stepping are process-specific (PCS_TYPE)
 - PCS_TYPE : related process
 - TIME_STEPS : time step and time step size

- TIME_END : total simulation time
- TIME_START : starting time for simulation
- TIME_UNIT : unit of time (by default is second)

Listing 4.8: Example time stepping file: GWF_Theis.tim

```
#TIME_STEPPING
$PCS_TYPE
GROUNDWATER_FLOW
$TIME_STEPS
10 0.864
10 7.776
10 77.76
10 777.6
10 7776
10 77760
$TIME_END
864000
$TIME_START
0.0
#STOP
```

- OUT: output control are process-specific (PCS_TYPE)
 - PCS_TYPE : related process
 - NODE_VALUES : node-based output for defined variable
 - GEO_TYPE : related geometry such as domain, point, polyline or surface
 - DAT_TYPE : output file format
 - TIM_TYPE : output frequency or output for selected time series

Listing 4.9: Example output file: GWF_Theis.out

```
#OUTPUT
$PCS_TYPE
GROUNDWATER_FLOW
$NOD_VALUES
HEAD
$GEO_TYPE
DOMAIN
$DAT_TYPE
TECPLOT
$TIM_TYPE
STEPS 1
#STOP
```

- MFP/MMP: Material properties are defined in the following two files for fluid and porous medium properties.
 - MFP : fluid properties
 - MMP : properties of the porous medium

Listing 4.10: Example fluid property file: GWF_Theis.mfp

```
#FLUID_PROPERTIES
$FLUID_TYPE
LIQUID
$DENSITY
1 999.7026
$VISCOSITY
1 1.308E-03
#STOP
```

Listing 4.11: Example medium property file: GWF_Theis.mmp

```
#MEDIUM_PROPERTIES
$GEOMETRY_DIMENSION
1
$GEOMETRY_AREA
1
$STORAGE
1 1.0e-3
$PERMEABILITY_SATURATION
1 1.0
$PERMEABILITY_TENSOR
ISOTROPIC 9.29036e-4
#STOP
```

The above described *OGS* files can be used for arbitrary geometric set-ups (the keyword `GEOMETRY_DIMENSION` in the *MMP* file should adapt to the *GLI* and *MSH* file explained below), which is one of the advantages of the object-oriented *OGS* file concept.

The geometries of a model domain as well as its finite element discretization are defined in *GLI* and *MSH* file, respectively. The main functions of the two files are listed below. The *OpenGeoSys Data Explorer* is one of the tools to prepare and create the *GLI* and *MSH* file. For more details please refer to Chap. 5.

- *GLI*: geometries for model domain, boundary conditions, source terms, output and initial condition descriptions.
- *MSH*: finite element mesh containing grid nodes and element sequences.

4.3 Theis Method in 1.5D: Radial Symmetry

For the simulation of Theis problem in 1.5D (illustrated in Fig. 20) and 2.5D (see Sec. 4.5), axisymmetric coordinate systems are applied. A summary of the model concepts, implemented geometries and their related key words in *OGS* are listed in Tab. 4. For the radial-symmetric problem, a one dimensional line mesh is applied. The governing equations for the Theis well problem are

$$S_s \frac{\partial h}{\partial t} = \frac{1}{r} \frac{\partial}{\partial r} \left(K_r r \frac{\partial h}{\partial r} \right) + \frac{\partial}{\partial z} \left(K_z \frac{\partial h}{\partial z} \right) + q \quad (3)$$



Fig. 2: Theis problem in 1.5D: Radial symmetry

with initial and boundary conditions

$$\begin{aligned} h(t=0, r) &= h_0 \\ \lim_{r \rightarrow 0} \left(r \frac{\partial h}{\partial r} \right) &= \frac{Q}{2\pi T} \\ \lim_{r \rightarrow \infty} h(t, r) &= h_0 \end{aligned} \quad (4)$$

where h_0 is the constant initial hydraulic head $[L]$, Q is the constant discharge rate $[L^3T^{-1}]$, T is the aquifer transmissivity $[L^2T^{-1}]$, t is time $[T]$ and r is the radial distance at any point $[L]$.

For the Theis well problem, an analytical solution exists.

$$h(t, r) = h_0 - \frac{Q}{4\pi T} W(u) \quad (5)$$

with the well function

$$\begin{aligned} W(u) &= -Ei(-u) = \int_u^\infty \frac{\exp(-\xi)}{\xi} d\xi \\ W(u) &= -0.5772 - \ln(u) + \sum_{i=1}^{\infty} (-1)^{i-1} \frac{u^i}{i \times i!} \\ \text{with } u &= \frac{S}{4T} \frac{r^2}{t} \end{aligned} \quad (6)$$

where $W(u)$ is the well function defined by an infinite series for a confined aquifer and S is the aquifer storage $[-]$.

The distribution of the hydraulic head at the end of the simulation time is demonstrated in Fig. 21. Some of the input files for the simulation are presented in Sec. 4.2. Here we would explain more input files which need to be specified based on different geometry of problems.

- Initial condition: A hydraulic head of 0 m is given for the whole domain as the initial condition for the numerical simulations (the input file is already given in Sec. 4.2).
- Boundary condition: Since the aquifer should be infinite in radial extent in order to fulfill the assumption required by the Theis' solutions, a relatively huge study area length of 1000 m is applied. The hydraulic head at the end

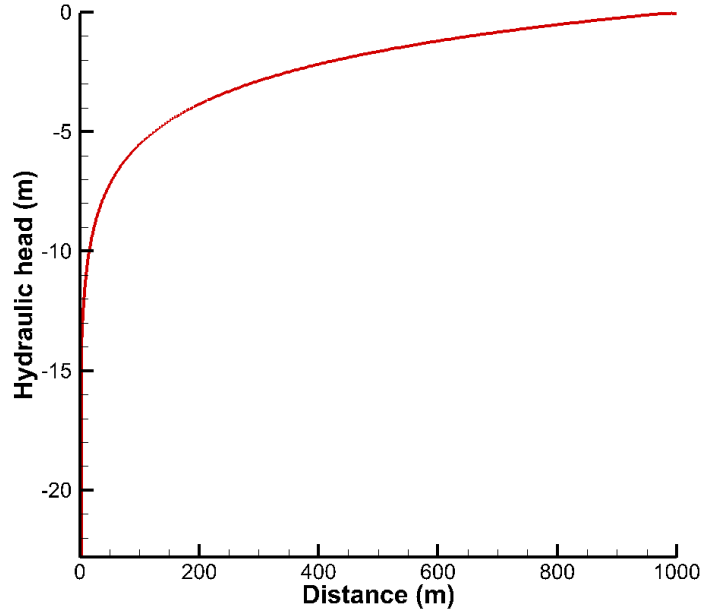


Fig. 3: Distribution of the hydraulic head at the end of simulation time (Theis 1.5D)

of radial extent (at POINT INFINIT) is set as 0 m as the boundary condition (the input file is already given in Sec. 4.2).

- Source/sink terms: Pumping well

In the case of Theis' 1.5D, the whole well is abstractly represented by a single point, hence both the radius and the depth of the well are regarded as 1 m. The discharge rate is thereby calculated by:

$$q = \frac{Q}{2\pi \cdot 1 \cdot 1} = -2.253E-3 \text{ (m} \cdot \text{s}^{-1}\text{)} \quad (7)$$

Listing 4.12: Source term file for Theis 1.5D: GWF_Theis.st

```
#SOURCE_TERM
$PCS_TYPE
  GROUNDWATER_FLOW
$GEO_TYPE
  POINT WELL
$DIS_TYPE
  CONSTANT_NEUMANN -2.253E-3
#STOP
```

- Material conditions: Hydraulic conductivity and specific storage

In the model approach `GROUNDWATER_FLOW`, the value implemented for the keyword `PERMEABILITY_TENSOR` should be the value of hydraulic conductivity, i.e. $K = 9.2903 \times 10^{-4} (m \cdot s^{-1})$ whereas the value implemented for the key word `STORAGE` should be the specific storage, i.e. $S_s = 10^{-3} (m^{-1})$. It is worth to mention that in the model approach `LIQUID_FLOW` the calculation of the material properties is different from that of the `GROUNDWATER_FLOW`. These differences will be explained in the end of this chapter.

Listing 4.13: Medium property file for Theis 1.5D: `GWF_Theis.mmp`

```
#MEDIUM_PROPERTIES
$GEOMETRY_DIMENSION
1
$GEOMETRY_AREA
1
$STORAGE
1 1.0e-3
$PERMEABILITY_SATURATION
1 1.0
$PERMEABILITY_TENSOR
ISOTROPIC 9.29036e-4
#STOP
```

- GLI: geometries for model domain and boundary descriptions,
 - POINTS:
 - 0 – well position
 - 1 – a point used to define the two polylines below
 - 2 – outer boundary
 - 3 – observation point
 - POLYLINE:
 - LEFT: left part of the domain, which has been assigned a finer mesh size
 - RIGHT: right part of the domain, which has a been assigned coarser mesh size

Listing 4.14: Geometry file for Theis 1.5D: `GWF_Theis.gli`

```
#POINTS
0 0 0 0 $NAME WELL
1 300 0 0
2 1000 0 0 $NAME INIFINIT
3 9.639 0 0 $NAME OBS
#POLYLINE
$NAME
LEFT
$POINTS
0
1
#POLYLINE
$NAME
RIGHT
```

```
$POINTS
1
2
#STOP
```

- MSH: finite element mesh containing grid nodes and element sequences.
 - PCS_TYPE : meshes can be associated with processes (not necessary here)
 - AXISYMMETRY : radial symmetry or axis symmetry is applied
 - NODES : grid nodes
 - number of grid nodes
 - grid node number and x, y, z coordinates
 - ELEMENTS : elements
 - number of elements
 - element number with associated material group, geometric element type (triangle or quadrilateral), element grid nodes (number depends on geometric element type)

Listing 4.15: Example mesh file for Theis 1.5D: GWF_Theis.msh

```
#FEM_MSH
$AXISYMMETRY
$NODES
401
0 0 0 0
1 .57 0 0

[.]

399 996.5 0 0
400 1000 0 0
$ELEMENTS
400
0 0 line 0 1
1 0 line 1 2

[.]

398 0 line 398 399
399 0 line 399 400
#STOP
```

4.4 Theis Problem in 2D

We consider the two-dimensional extension of the Theis problem: single well in a horizontal aquifer. The triangle domain used for the simulation is illustrated in Fig. 22, where the red point represents the pumping well. The governing equation system for groundwater flow process in 2D is

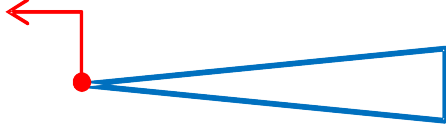


Fig. 4: Theis problem in 2D: Horizontal aquifer

$$S \frac{\partial h}{\partial t} = T \left(\frac{\partial^2 h}{\partial x^2} + \frac{\partial^2 h}{\partial y^2} \right) + q \quad (8)$$

or

$$S_s \frac{\partial h}{\partial t} = K \left(\frac{\partial^2 h}{\partial x^2} + \frac{\partial^2 h}{\partial y^2} \right) + q \quad (9)$$

In order to compare the simulation results of 2D approach with other approaches, the same parameter values, initial conditions and boundary conditions are applied. The triangle geometry and corresponding mesh are shown in Fig. 23b, in which the pumping well is set at the left vertex of the triangle. Since the angle of the left vertex is set as 10° , the source term is calculated as follows:

$$Q_1 = \frac{10}{360} Q = 3.9329 \times 10^{-4} (m^3 \cdot s^{-1}) \quad (10)$$

Listing 4.16: Source term file for Theis 2D: GWF_Theis.st

```
#SOURCE_TERM
$PCS_TYPE
  GROUNDWATER_FLOW
$PRIMARY_VARIABLE
  HEAD
$GEO_TYPE
  POINT_WELL
$DIS_TYPE
  CONSTANT_NEUMANN -3.933E-4
```

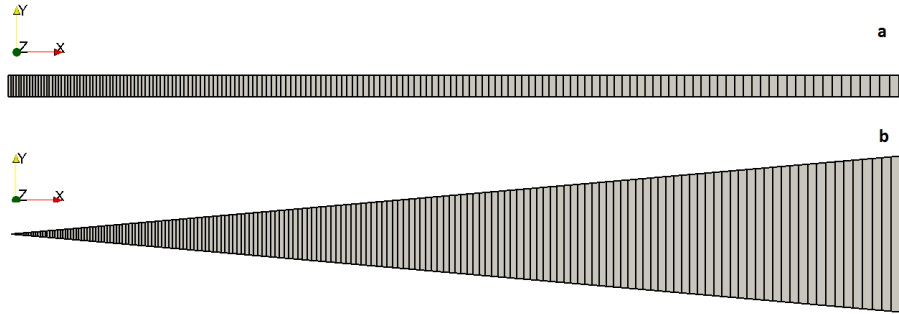


Fig. 5: The implemented mesh: (a) for Theis 2.5D, (b) for Theis 2D

Listing 4.17: Medium property file for Theis 2D: GWF_Theis.mmp

```
#MEDIUM_PROPERTIES
$GEOMETRY_DIMENSION
2
$GEOMETRY_AREA
1.000000e+000
$STORAGE
1 1e-3
$PERMEABILITY_SATURATION
1 1.0
$PERMEABILITY_TENSOR
ISOTROPIC 9.2903e-4
#STOP
```

Listing 4.18: Geometry file for Theis 2D: GWF_Theis.gli

```
#POINTS
0 0 0 0 $NAME WELL
1 1000 87.49 0
2 1000 -87.49 0
3 9.639 0 0 $NAME OBS
#POLYLINE
$NAME
AROUND
$POINTS
0
1
2
0
#POLYLINE
$NAME
r_bc
$POINTS
1
2
#STOP
```

Listing 4.19: Example mesh file for Theis 2D: GWF_Theis.msh

```
#FEM_MSH
$NODES
801
0 0 0 0
1 0.57 0.0498693 0
[.]
799 996.5 -87.183785 0
800 1000 -87.49 0
$ELEMENTS
400
0 0 tri 0 1 401
1 0 quad 1 2 402 401
[.]
398 0 quad 398 399 799 798
399 0 quad 399 400 800 799
#STOP
```

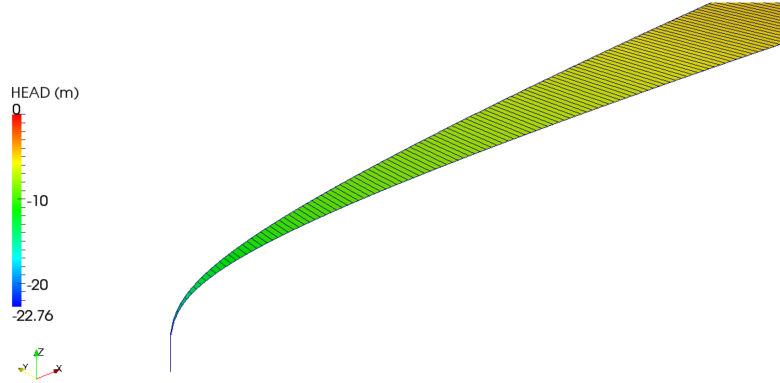



Fig. 6: Distribution of the hydraulic head at the end of simulation time (Theis 2D)

4.5 Theis Problem in 2.5D: Axial Symmetry

For 2.5D (illustrated in Fig. 25), a two dimensional mesh with a width of 1 m is applied (see Fig. 23a, a vertical exaggeration of 5 times is applied). Again, for the radial case, the two dimensional groundwater flow process, Eq. 14, is transformed into Eq. 16. Since discharge is evenly distributed around the



Fig. 7: Theis problem in 2.5D: Axial symmetry

whole surface area of the well (which can be seen as a cylinder), the source term (with the distribution type `CONSTANT_NEUMANN`) applied for Theis' 2.5D is calculated as follows ('1' in the formula represents the length of the 2D mesh in y-direction, i.e. 1 m):

$$q = \frac{Q}{2\pi r_w \cdot 1} = -7.393E - 3 (m \cdot s^{-1}) \quad (11)$$

Listing 4.20: Source term file for Theis 2.5D: `GWF_Theis.st`

```
#SOURCE_TERM
$PCS_TYPE
GROUNDWATER_FLOW
```

```

$GEO_TYPE
POLYLINE WELL
$DIS_TYPE
CONSTANT_NEUMANN -7.393E-3
#STOP

```

Listing 4.21: Example geometry file for Theis 2.5D: GWF_Theis.gli

```

#POINTS
0 0.3048 0 0
1 0.3048 1 0
2 300 1 0
3 1000 1 0
4 1000 0 0
5 300 0 0
6 9.639 1 0 $NAME OBS
#POLYLINE
$NAME
WELL
$POINTS
0
1

[.]

#POLYLINE
$NAME
INIFINIT
$POINTS
3
4
#STOP

```

Listing 4.22: Example mesh file for Theis 2.5D: GWF_Theis.msh

```

#FEM_MSH
$AXISYMMETRY
$NODES
802
0 .3048 0 0
1 .3048 1 0

[.]

800 1000 1 0
801 1000 0 0
$ELEMENTS
400
$ELEMENTS
400
0 0 quad 0 1 2 3
1 0 quad 3 2 4 5

[.]

398 0 quad 797 796 798 799
399 0 quad 799 798 800 801
#STOP

```

4.6 Theis Problem in 3D

The geometry of the Theis problem in 3D is illustrated in Fig. 26. Based on the 2D mesh shown in Fig. 23b, a 3D mesh is generated by extruding the mesh elements into 3D. The 3D mesh consists of one layer with a thickness of 1 m. Similarly, the parameters used in Theis' 2D are applied for Theis' 3D.

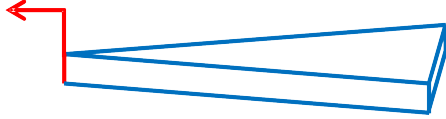


Fig. 8: Theis problem in 3D: Spatial aquifer

Listing 4.23: Source term file for Theis 3D: `GWF_Theis.st`

```
#SOURCE_TERM
$PCS_TYPE
  GROUNDWATER_FLOW
$PRIMARY_VARIABLE
  HEAD
$GEO_TYPE
  POLYLINE WELL
$DIS_TYPE
  CONSTANT_NEUMANN -3.933E-4
#STOP
```

Listing 4.24: Example geometry file for Theis 3D: `GWF_Theis.gli`

```
#POINTS
0 0 0 0
1 1000 87.49 0
2 1000 -87.49 0
3 0 0 -1
4 1000 87.49 -1
5 1000 -87.49 -1
6 9.639 0 0 $NAME OBS
#POLYLINE
$NAME
  WELL
$POINTS
  0
  3
[.]
#POLYLINE
$NAME
  POLYGON_R
$POINTS
  3
  0
  2
```

```

5
3
#SURFACE
$NAME
  INFINIT
$POLYLINES
POLYGON_B
$TYPE
  0

[.]

#SURFACE
$NAME
  S_R
$POLYLINES
POLYGON_R
$TYPE
  0
#STOP

```

Listing 4.25: Example mesh file for Theis 3D: GWF_Theis.msh

```

#FEM_MSH
$NODES
  1602
0 0 0 0
1 0.57 0.0498693 0

[.]

1600 996.5 -87.183785 -1
1601 1000 -87.49 -1
$ELEMENTS
  400
0 0 pris 401 1 0 1202 802 801
1 0 hex 401 402 2 1 1202 1203 803 802

[.]

398 0 hex 798 799 399 398 1599 1600 1200 1199
399 0 hex 799 800 400 399 1600 1601 1201 1200
#STOP

```

4.7 Results

All the simulations are performed for a duration of 10 days with varying time step lengths ranging from 10^{-5} d to 0.9 d. The time series of the hydraulic head drawdown at a distance of 9.639 m from the well are extracted from the simulation results of all the eight cases, and are shown in Fig. 27 together with the analytical solutions. The calculation of the analytical solutions can be found in Srivastava and Guzman-Guzman (1998). 'GF' in the graphic represents the simulations with model approach **GROUNDWATER_FLOW**, whereas 'LF' represents **LIQUID_FLOW**. We can find that all the numerical results obtained with different model approaches are coincident with each other and

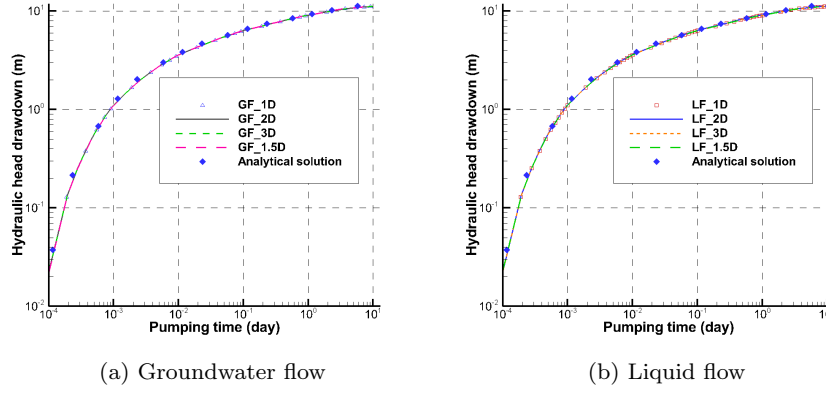


Fig. 9: Calculated drawdowns at a distance of 9.639 m from the well

agree well with the analytical solutions. Comparing the time series of hydraulic drawdowns at positions with different distances from the pumping well (such as 20 m, 40 m), good agreements are also achieved by using different model approaches (not shown here). Additionally, the distribution of the hydraulic head at the end of the simulation time for the 1D as well as the distribution of hydraulic drawdown at the end of the simulation time of 3D mesh are demonstrated in Fig. 21 and Fig. 28, respectively. In order to show the 3D mesh in Fig. 28 clearly, a vertical exaggeration of 5 times is applied.

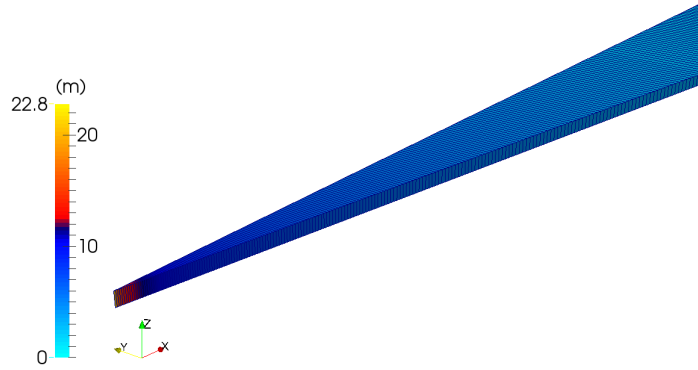


Fig. 10: Distribution of the hydraulic drawdown at the end of the simulation time (Theis 3D)

4.8 Groundwater Flow and Liquid Flow

As mentioned above, we would explain the difference between the model approach `GROUNDWATER_FLOW` and `LIQUID_FLOW` in this section.

First of all, the primary variable of `GROUNDWATER_FLOW` is hydraulic head, whereas that of `LIQUID_FLOW` is water pressure. The process and its primary variable can be defined in the PCS file. Secondly, in the MMP file under the keyword `PERMEABILITY_TENSOR` and `STORAGE` the value of hydraulic conductivity and specific storage should be given. However, in the model approach `LIQUID_FLOW`, the value used for the key word `PERMEABILITY_TENSOR` is the intrinsic permeability, which is calculated as follows by using the value of hydraulic conductivity as well as the density and dynamic viscosity of water (see Tab. 3).

$$k = \frac{K\mu}{\rho g} = 1.2391 \times 10^{-10} (m^2) \quad (12)$$

whereas the value implemented for the keyword `STORAGE` should be the whole parameter term on the left hand side of Eq. 15, i.e.

$$\frac{S_s}{\rho g} = 1.02 \times 10^{-7} (Pa^{-1}) \quad (13)$$

Besides pressure gradient, gravity is also considered as the driven force for groundwater flow in the model approach `LIQUID_FLOW`. In the benchmark Theis' 3D for model approach `LIQUID_FLOW` the gravity effect is included.

Although it could be more difficult to set up a model with the approach `LIQUID_FLOW` considering the unit conversions, it has all the functionalities of `GROUNDWATER_FLOW`. Moreover, it can be used to simulate density dependent flow processes such as seawater intrusion.

Chapter 5

Case Study: Ammer Catchment

AGNES SACHSE, BENNY SELLE AND KARSTEN RINK

5.1 Introduction

This chapter explains the step by step development of a steady state groundwater flow model with the help of the geographical information system *Arc-GIS* and the numerical modelling tool *OpenGeoSys*. This groundwater flow model of a catchment in southwestern Germany was developed in the context of the Water Earth System Science (WESS) competence cluster. Details on the project may be found in an article by Grathwohl et al. (2013) or at www.wess.info. This case study focusses on the identification of flow paths and travel times of groundwater with respect to a number of production well sites. To this end, the best possible representation of the groundwater flow system was implemented as an *OpenGeoSys* simulation model. For more details on the development of a conceptual model of groundwater flow for the study area and the practical context of this work the interested reader is referred to articles by Pavlovskiy and Selle (2014) and Selle et al. (2013a).

5.2 Catchment Description

The Ammer catchment in southwestern Germany (Fig. 29) has an extent of approximately 180 km² (Selle et al., 2013a). The river Ammer has an average discharge of circa 1 m³/s which mainly originates from groundwater. The geology of the catchment comprises a sequence of Triassic strata forming a landscape characterised by escarpments. The topography of the catchment is hilly with altitudes ranging from 312 and 600 m a.s.l. The study area has humid climate conditions with an annual average precipitation between 700

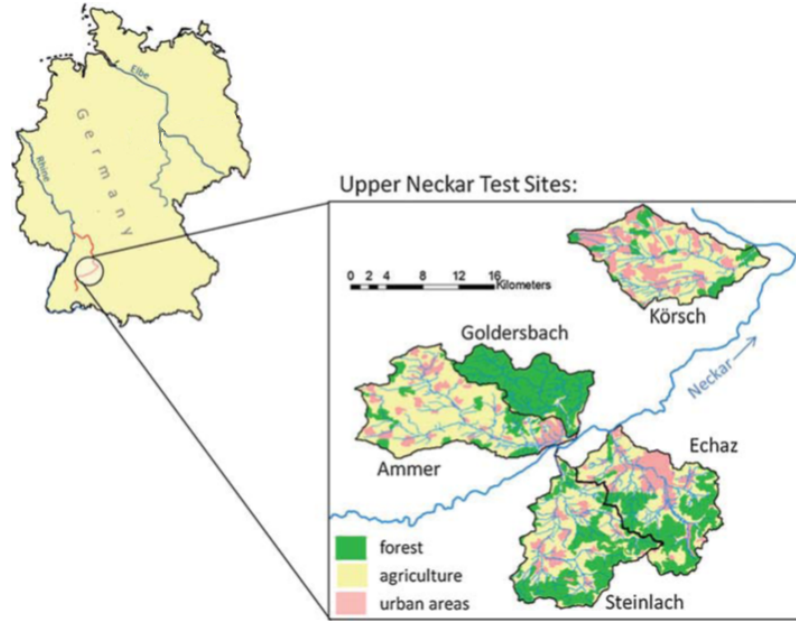


Fig. 1: Locations of Upper River Neckar catchments. The Ammer is part of the Upper Neckar River basin. Figure was modified and based on Schwientek et al. (2013).

and 800 mm. The mean annual air temperature is about 8°C . The majority (70%) of the catchment is used for agriculture and 17% are urban areas.

The hydrogeological setting (Fig. 30) of the Ammer catchment (Pavlovskiy and Selle, 2014; Villinger, 1982) is dominated by the Upper Muschelkalk (*mo*) which forms the main aquifer. It has an average thickness of 85 m, is partly karstified and mainly consists of dolomitic, micritic and bioclastic limestone. The main aquifer slightly dips towards the southeast and is unconfined in the northwest of the catchment. It becomes confined towards the southeast where it is increasingly overlaid by Keuper layers (Villinger, 1982). These layers are the

- Gipskeuper (*km1*): up to 100 m
- Lettenkeuper (*ku*): 20 m
- Schilfsandstein (*km2*): 20 m
- Bunte Mergel (*km3*): 25 m
- Stubensandstein (*km4*): 30 m

The primary discharge of the aquifer system in the study area is groundwater discharge to the river Ammer and its tributaries (Harress, 1973; Plümacher, 1999; Villinger, 1982), which mainly comes from the Upper Muschelkalk (*mo*) aquifer and also from the Gipskeuper (*km1*) aquifer. There is also ground-

water abstraction from four well sites of the Upper Muschelkalk with an average production of approximately 140 l/s of drinking water. Groundwater recharge from streams may be locally important, e.g. for the Kochart Creek. Additional information on the Ammer catchment can be found in Grathwohl et al. (2013) and Selle et al. (2013b).

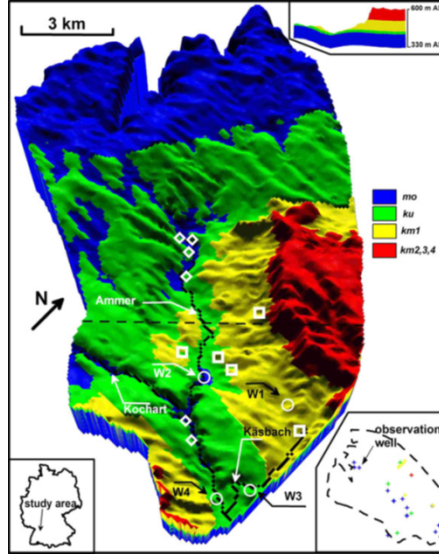


Fig. 2: 3D view of the Ammer catchment with the river Ammer and two tributaries, the Kochart and the Käsbaach Creek. Gipskeuper springs are marked by squares, Upper Muschelkalk springs by diamonds and drinking water production well sites by circles W1, W2, W3, W4 (Selle et al., 2013a).

5.3 Model Set-up

The numerical model is based on the conceptual model of groundwater flow presented by Pavlovskiy and Selle (2014). It represents the best characterisation of the groundwater recharge and discharge processes for the aquifer system of the Ammer catchment. In order to simulate the groundwater flow processes within the Ammer catchment, a large number of input data sets from different sources are required. By employing the *OpenGeoSys Data Explorer* we are able to integrate hydrological, geological and geographic input data from different sources to set-up the model. The framework of the *Data Explorer* also supports the creation of finite element meshes and boundary- and initial conditions to complex, unstructured geometries (Rink et al., 2013).

For this case study, a step by step description of the complete model setup will be provided in the following, including remarks on the simulation and post processing of the three-dimensional flow-model. The model set-up will be performed using the *Data Explorer* Interface and covers the following working steps:

1. import of *ArcGIS* data
2. definition of model geometry
3. generation of surface and subsurface meshes
4. setup of steady state model, including initial conditions, boundary conditions and material properties
5. simulation
6. visualisation of results and post processing

For additional information regarding the general use of *OpenGeoSys Data Explorer*, the user is referred to Sec. 3.4 or a detailed explanation in the *OpenGeoSys Data Explorer Manual* (Rink, 2013).

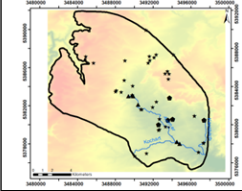

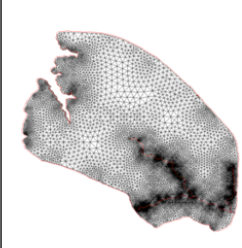
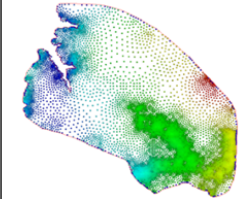

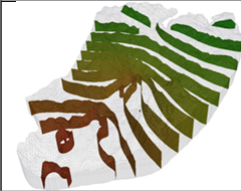
The set-up of the Ammer catchment model is established according to the work flow illustrated in Tab. 7.

5.4 Available data sets

All available topographical, geological and hydrological data of the Ammer catchment (Tab. 8) were organised and digitalised in the geographic information system *ArcGIS* (for further information the user is referred to appendix A). The input data for the model setup (Fig. 31) contains:

- digital elevation model of the Ammer catchment with 100 m resolution (*AmmerDEM.asc*)
- boundary of the study area, which is the subsurface catchment of the study area (*boundary_polygon.shp*)
- river network consisting of the Ammer river itself as well as its tributaries Käsba and Kochart (*Ammer_River_Polyline.shp*, *Kaeschbach_River_polyline.shp* and *Kochart_River_polyline.shp*)
- four groundwater production well sites including their abstraction rates (*wells.shp*)
- observation wells including measured water levels (*observation_wells.shp*)
- raster data of hydrogeologic subsurface layers: Schilfsandstein / Bunte Mergel / Stubensandstein: (*1_km2_4-up.asc*); Gipskeuper: (*2_km1-up.asc*); Lettenkeuper: (*3_ku-up.asc*); top of Upper Muschelkalk: (*4_mo-up.asc*); bottom of Upper Muschelkalk: (*5_mo-down.asc*)
- spatial distributed groundwater recharge with a 500 m resolution from the Atlas “Wasser- und Bodenatlas Baden-Württemberg” (Heinrich and Leibundgut, 2000) (*AmmerGWR.asc*)

Table 1: Workflow for model setup.

	ArcGIS output: *.shp, *.asc	Data base: Geographic data related to topography, DEM, river network, borehole position are prepared in an <i>ArcGIS</i> project (Sec. 5.4)
	OGS DE output: *.gli, *.gml	Data integration: Data from <i>ArcGIS</i> can be directly imported to <i>OGS</i> and visualised by using the <i>OGS Data Explorer</i> (Sec. 5.5)
	GMSH / OGS DE output: *.msh, *.mmp	Domain meshing: For numerical analysis the model domain needs to be discretised into a finite element mesh. For this purpose, several meshing tools (<i>GMSH</i> , <i>TetGen</i>) are available via the <i>Data Explorer</i> . Assignment of material groups is also integrated into the meshing procedure (Sec. 5.6)
	OGS DE output: *.bc, *.st, *.ic	Initial and boundary conditions as well as source/sink terms for computing groundwater flow. (Sec. 5.7)
	OGS output: *.pcs, *.num, *.tim, *.out	Simulation: Finally, the groundwater model is ready for simulation. Additional <i>OGS</i> files have to be completed for model runs (Sec. 5.9)
	OGS DE output: *.vtk, *.tec	Visualisation: The <i>OGS Data Explorer</i> provides a large variety of tools for combined analysis of data and simulation results including 3D visualisation (Sec. 5.11)

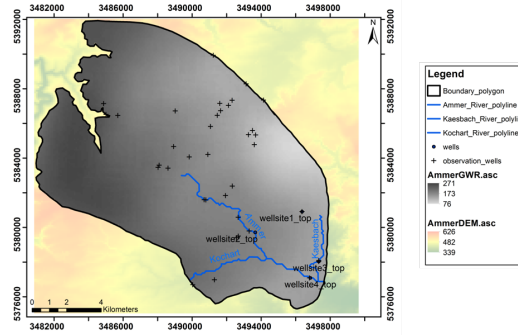


Fig. 3: Input data for the hydrological modelling, visualised in *ArcGIS*.

Table 2: Configuration files for the Ammer case study.

File	Description
boundary_polygon.shp	Catchment boundary
Ammer_River_Polyline.shp	Ammer River
Kaesbach_River_Polyline.shp	Kaesbach River
Kochart_River_Polyline.shp	Kochart River
wells.shp	pumping well sites
observation_wells.shp	observation wells
springs-Upper-Muschelkalk.shp	springs of Upper Muschelkalk aquifer
springs-Gipskeuper.shp	springs of Gipskeuper aquifer
1_km2_4_up.asc	Raster data of the upper boundary of Schilfsandstein/Bunte Mergel/Stubensandstein
2_km1_up.asc	Raster data the upper boundary of of Gipskeuper
3_ku_up.asc	Raster data the upper boundary of Lettenkeuper
4_mo_up.asc	Raster of upper boundary of Upper Muschelkalk
5_mo_down.asc	Raster of lower boundary of Upper Muschelkalk
AmmerDEM.asc	Digital Elevation Model
AmmerGWR.asc	Raster data of groundwater recharge

The digital elevation model with a resolution of 100 m covers the whole Ammer catchment. This DEM is used later in Sec. 5.6 for meshing of the surface domain. The different raster files of the hydrogeological layers have the same spatial resolution as the DEM. The subsurface boundary of the Ammer catchment was obtained from the study by Villinger (1982) and represents the extension of the Ammer case study. It differs in spatial extension from the topography of the river Ammer. The river network consisting of the Ammer with its tributaries Käsba and Kochart, drains the catchment and the mesh is refined along the polylines representing the streams to better represent the

topography of the catchment. The raster files for each hydrogeological layer have been calculated based on a map of the geological layering (Reuther, 1973). Four groundwater production well sites (Selle et al., 2013a) can be found in the Ammer catchment. These abstraction rates will be implemented via source terms to the groundwater flow model. The observation wells (unpublished data; Landesanstalt für Umwelt, Messungen und Naturschutz Baden-Württemberg) are used for the comparison with simulated hydraulic heads. The replenishment of the aquifer system was digitised from the Atlas “Wasser- und Bodenatlas Baden Württemberg” (Heinrich and Leibundgut, 2000). The calculation of the groundwater recharge is based on dominant catchment characteristics such as land use, soils and geology. The springs represent the outflow of the Upper Muschelkalk and Gipskeuper aquifer systems and the discharge elevation of the springs is used as a boundary condition for the numerical model.

5.5 Data Integration

Setting up a new model usually starts with the import of a number of geographic and hydrogeological datasets. When the *OpenGeoSys Data Explorer* (`ogs-gui.exe`) is started, it opens with an empty project by default. To create a new model project we click on **File** → **Import files** and **Shape Files** to use already existing information regarding the model geometry. These data sets were previously organised in a geographical information system (GIS) such as *ArcGIS* (see Appendix A). The GIS data for the Ammer catchment contains several vector data sets which can be easily imported into the *Data Explorer*. These vector data sets from *Esri* shape files can be represented both as polygons or polylines (Fig. 32). Point data from *Esri* shape files can be imported both as geometric points or as observation sites (stations). The import as stations is useful for borehole records.

Download and import all the following geometry files from the *OpenGeoSys*-Homepage (<http://www.opengeosys.org/resources/downloads>):

- Boundary-polygon.shp (as polyline/surface)
- Ammer-River-polyline.shp (as polyline)
- Kaesbach-River-polyline.shp (as polyline)
- Kochart-River-polyline.shp (as polyline)
- springs-Upper-Muschelkalk.shp (as Geometry-Points)
- springs-Gipskeuper.shp (as Geometry-Points)
- observation-wells.shp (as Geometry-Points)
- wells.shp (as Geometry-Points)

Make sure, that all listed files are loaded successfully in the **Geometry Data View**. If you double click on “Boundary_polygon” in the **Geometry Data View**

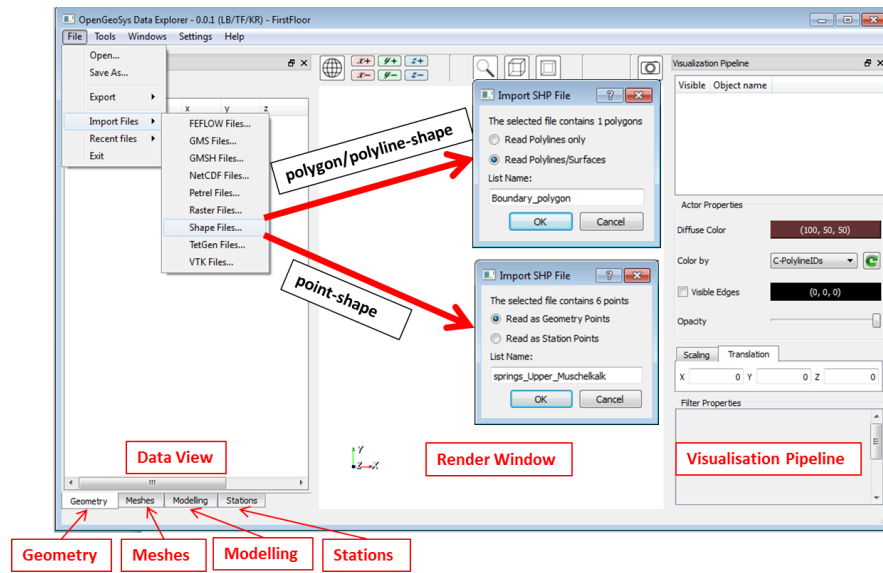
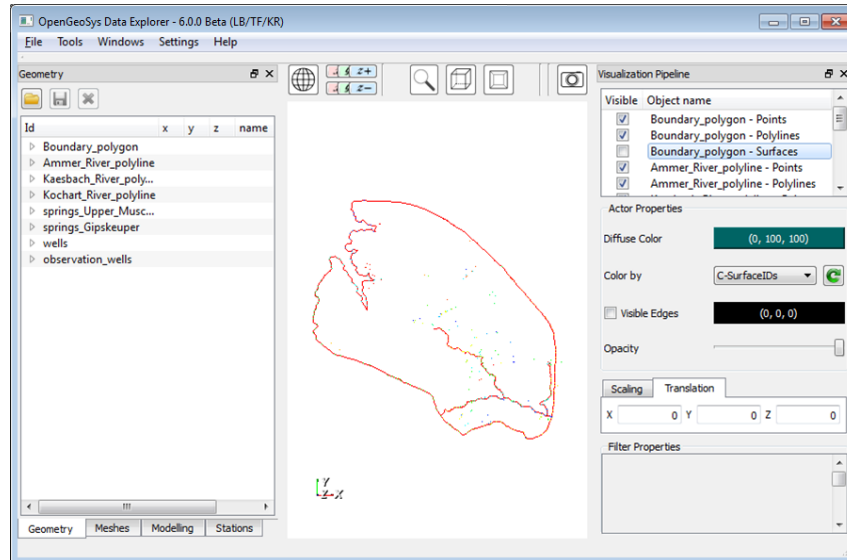
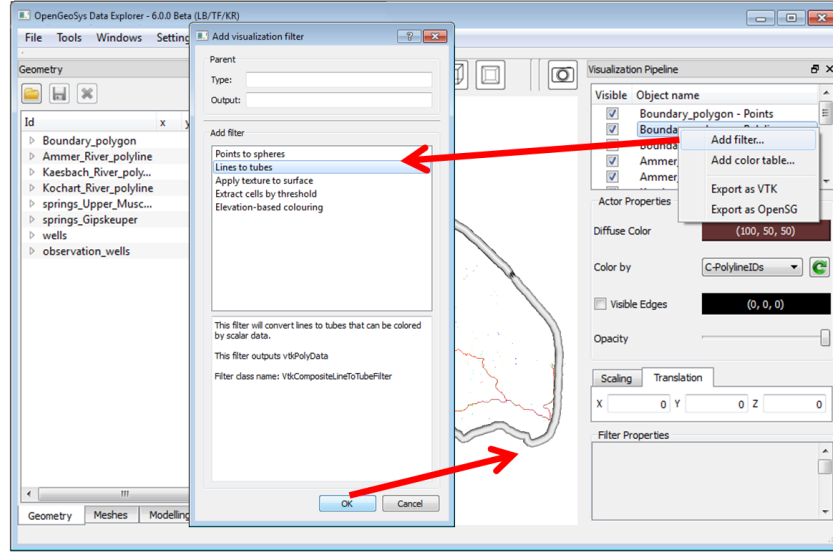
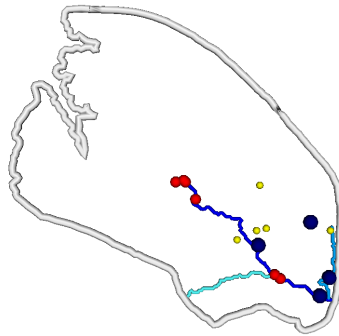
Fig. 4: Importing data into the *OpenGeoSys Data Explorer*.

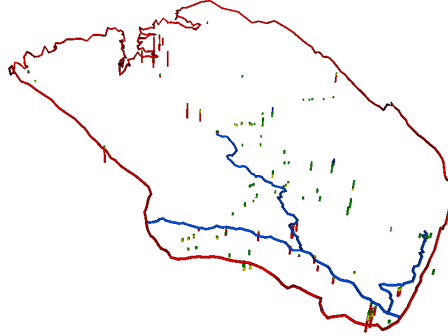
Fig. 5: Overview of all imported geometry files.



(a) Workflow to visualise the geometry



(b) Final visualisation



(c) Isometric view

Fig. 6: Visualisation of geometry data in the *OpenGeosys Data Explorer*.

you can see that the dataset contains points, polylines and surface data. Switch off the boundary_polygon-Surfaces in the Visualisation Pipeline to get an clear overview about all imported geometry files (Fig. 33).

To emphasise some geometric elements, you can right-click, for example on boundary_polyline-Polyline to add the filter “Lines to tubes” for line elements. Point elements can be accentuated by the “Points to spheres”-filter (Fig. 34). The Actor Properties in the Visualisation Pipeline, especially the Diffuse Color-property enable a coloured design of the emphasised points or line elements.

Table 3: Assigning names to geometry points.

File	Point	Name
wells	0	wellsite1_top
wells	1	wellsite1_bottom
wells	2	wellsite2_top
wells	3	wellsite2_bottom
wells	4	wellsite3_top
wells	5	wellsite3_bottom
wells	6	wellsite4_top
wells	7	wellsite4_bottom
springs_Upper_Muschelkalk	0	mo_0
springs_Upper_Muschelkalk	1	mo_1
springs_Upper_Muschelkalk	2	mo_2
springs_Upper_Muschelkalk	3	mo_3
springs_Upper_Muschelkalk	4	mo_4
springs_Upper_Muschelkalk	5	mo_5
springs_Gipskeuper	0	km1_0
springs_Gipskeuper	1	km1_1
springs_Gipskeuper	2	km1_2
springs_Gipskeuper	3	km1_3
springs_Gipskeuper	4	km1_4
observation_wells	0	obs_well1
observation_wells	1	obs_well2
observation_wells
observation_wells	35	obs_well36

The points within the geometries of *wells*, *spring_Upper_Muschelkalk*, *spring_Gipskeuper* and *observation_wells* need some modification: for better differentiation we have to set the names given in Tab. 9 to the geometric points of those geometries. To change the point-name, double click on the “wells-file” in the **Geometry Data View** and select **Point 0**. By right-clicking on this point you can choose the option **Set name...** You can save each geometry file when clicking on the floppy disk symbol on the top of the **Geometry Data View**. To save the whole project, click **Files** → **Save data as OpenGeoSys project (*.gsp)**. This saves automatically all geometry and mesh files as a sequence of gml- and vtu-files. Those geometric elements (such as the catchment boundary, the river network,...) are the prerequisite of the finite element meshing.

5.6 Finite Element Meshing

The mesh creation process via the *OpenGeoSys Data Explorer* requires the selection of geometric data sets and parametrisation of those elements by the graphical user interface of *OpenGeoSys Data Explorer*. The mesh generation should be done with great care, since it influences both the quality and time of the solution of the equation system. Some general considerations for the mesh generation:

- i The mesh should approximate the domain sufficiently well: The model domain can only be a rough approximation of the real terrain and sub-surface structure. However, this approximation should be close enough to the real-world region of interest that artefacts or simplifications in the overall structure are not resulting in a (fundamentally) different behaviour of the investigated phenomenon.
- ii The mesh density should be sufficiently high: In FEM meshes, properties (e.g. porosity, permeability, etc.) are assigned to elements. These properties can change across elements to model the changing conditions in the subsurface. If in the region of interest changes occur within small distances, element sizes of the model have to be small enough to represent these gradients adequately.
- iii The number of mesh elements should be sufficiently small: The runtime of the simulation is (among other things) dependent on the number of mesh elements. An increase in the number of elements will typically result in a polynomial rise of the runtime of several parts of simulation process. Obviously, there is a conflict between criteria (ii) and (iii) and a suitable trade-off has to be found for a specific model application.

Based on the geometric input data of the subsurface boundary of the study area, the Ammer river network, springs, observation wells and groundwater abstraction wells, a 2D surface mesh can be constructed (Fig. 35). Note that the river network is used for mesh generation but no boundary conditions will be imposed, as groundwater discharge will be represented to happen via springs.

5.6.1 Surface Meshing

Before we can create the 2D mesh make sure that you downloaded the actual *GMSH* version (Geuzaine and Remacle, 2009). Implement the mesh generator software in *OGS* by clicking on **Settings** → **Data Explorer Settings** → **Path to GMSH**. To generate the surface mesh for the Ammer catchment we have to click on **Tools** → **Mesh Generation** (Fig. 36). The *Data Explorer* will generate a 2D mesh by employing the finite element mesh generator *GMSH*. Click on **Tools** in the main menu of the *Data Explorer* and select **Mesh Gen-**

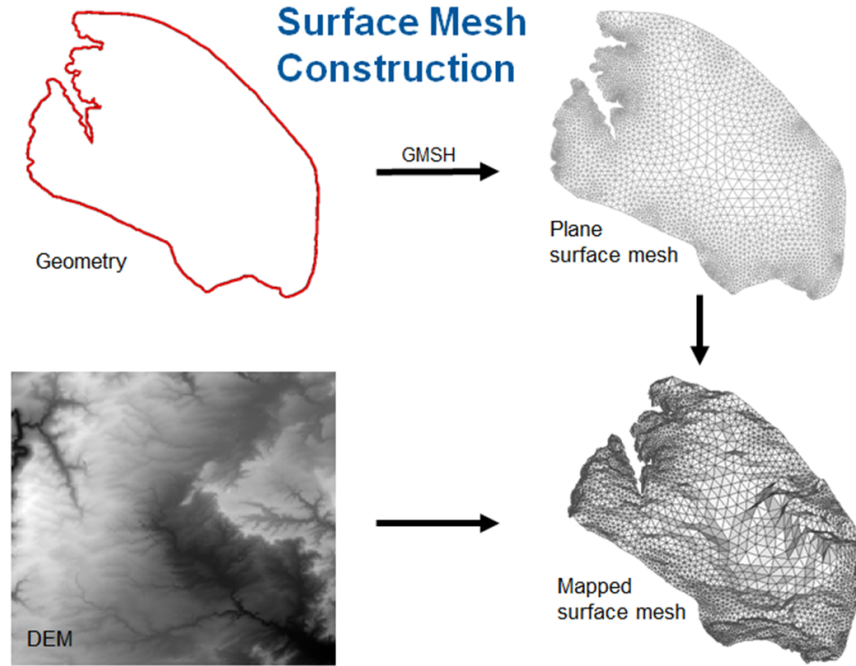


Fig. 7: Surface mesh generation in the *OpenGeoSys Data Explorer*.

eration.... In the appearing dialogue window choose all shape files listed in Tab. 8. This will result in an integration of the points of the geometric data set to be included in the finite element model as mesh nodes. Likewise, the polyline features will be integrated as mesh element edges (Fig. 37). The second tab of the dialogue, labelled **Advanced**, allows the user to modify the default meshing options. Most importantly, it allows to select whether **Adaptive meshing** (i.e. refinement towards interesting features) or **Homogeneous meshing** (i.e. mesh elements of roughly the same size) will be performed for creating the surface mesh. For this case study, we will choose the **Homogeneous meshing** with an **Element Size** of 200. This will result in mesh elements with an edge length of roughly 200 metres, which matches the cell size of the DEM raster used for mapping the 2D mesh afterwards. A shorter edge length will not result in a better representation of the surface given this particular DEM, and a longer edge length will result in missing features. The mesh generation process can take several seconds depending on the selected options before the triangulated 2D mesh “tmp_gmsh” appears in the **Meshes Data View**. Save the **tmp_gmsh-mesh** file as “ammer_2Dmesh.msh” using the disk symbol right above the Meshes Data View.

The 2D mesh file in our example (Listing 5.1) contains 11943 nodes and 24147 triangles, although these numbers may vary slightly in your case. This

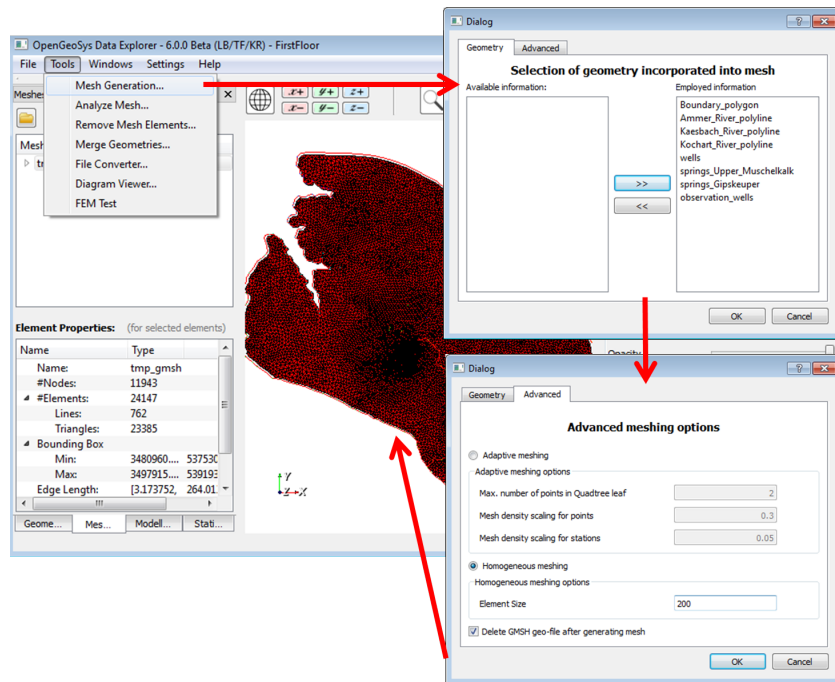


Fig. 8: Generating the mesh for the Ammer catchment.

mesh is the prerequisite for the structural 3D mesh containing the geological layers of the Ammer catchment.

Listing 5.1: Example for 2D mesh file.

```
#FEM_MSH
$PCS_TYPE
NO_PCS
$NODES
11943
0 3484965.87555 5391892.50684999 0
1 3485588.09311999 5391873.06197 0

[..]

$ELEMENTS
24147
0 0 line 0 563
1 0 line 563 564
2 0 line 564 565

[..]

24144 0 tri 1790 1793 465
24145 0 tri 383 382 1443
24146 0 tri 382 11934 1443
#STOP
```

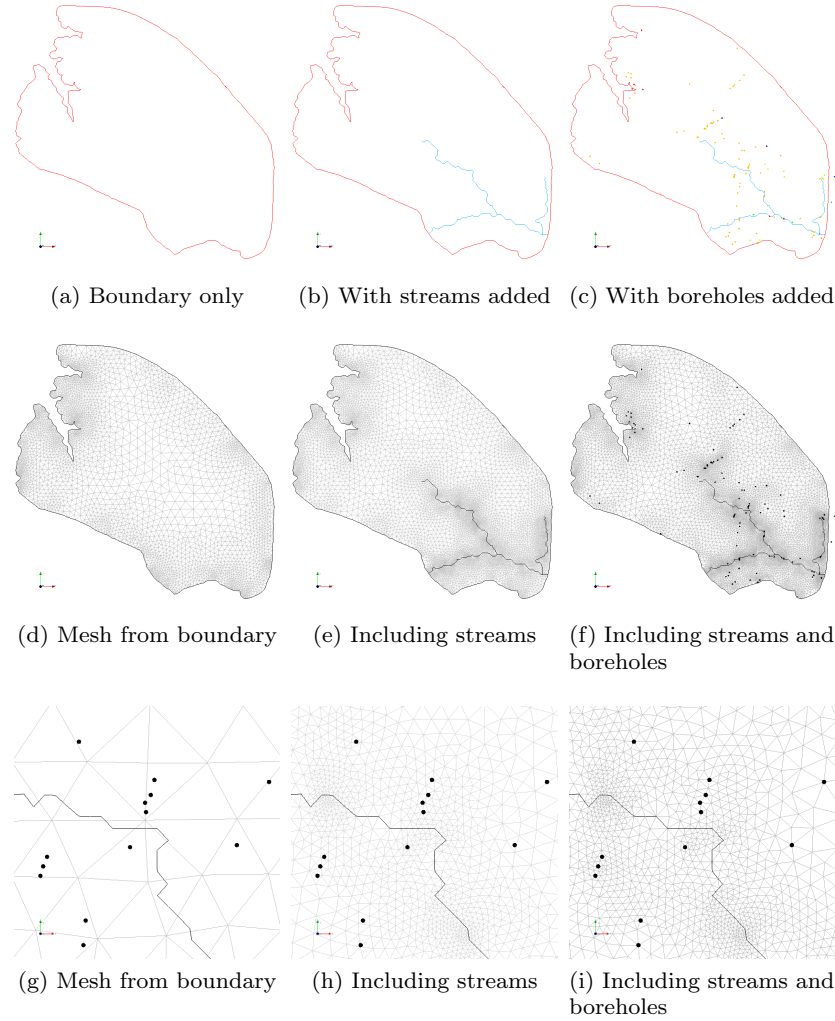


Fig. 9: Effect of adding information to the meshing process. The upper row shows geometric input data, with one data set added in each column. The resulting meshes are depicted in the second row. The meshes in figures 37e and 37f have a similar refinement but in one mesh boreholes are located directly on mesh nodes and in the other mesh they are not. The bottom row gives a close-up of this effect to visualise how geometric information matches mesh nodes and edges if it has been integrated into the meshing process.

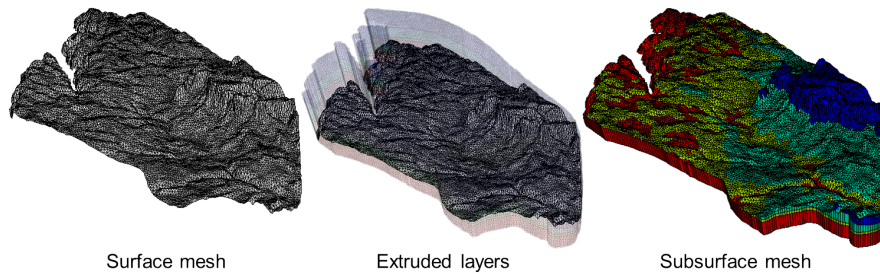


Fig. 10: 2D meshes can be extruded to generate 3D meshes.

5.6.2 Volume Meshing

To generate a 3D mesh, the previously constructed 2D mesh has to be extruded (Fig. 38). The result is a 3D subsurface mesh representing the geological layers of the Ammer catchment. Four layers have to be added to the surface mesh using (mainly) prism elements. The interfaces between those layers are mapped based on the asc-raster files listed in Tab. 8. From top to bottom, these are the upper boundaries of Stubensandstein / Bunte Mergel / Schilfsandstein (*1_km2_4-up.asc*), Gipskeuper (*2_km1-up.asc*), Lettenkeuper (*3_ku-up.asc*), Upper Muschelkalk (*4_mo-up.asc*) plus the bottom interface of Upper Muschelkalk (*5_mo-down.asc*).

To extrude the mesh, follow these instructions (Fig. 39):

- Right-click on the 2D mesh in the **Mesh Data View**
- Click on **Edit mesh**
- Specify in the appearing dialogue the number of mesh layers, which should be attached to the 2D mesh. Due to the geology of the Ammer catchment we have to add four layers and press **Next**.
- Activate **Add layers based on raster files** and click **OK**
- Load the layer of the surface (this is the DEM) and all subsequent geological layers including the bottom edge of the structural model
- Choose **Prisms** element as 3D mesh elements and click **OK**

As the interfaces between subsurface layers have been interpolated based on borehole data, some of the resulting mesh elements might be (partly) located above the interface specified by the DEM. In an automatic post-processing step all parts of the 3D mesh located above surface level will be “cut” away, resulting in outcropping layers in the final 3D mesh. The resulting data set is automatically called **SubsurfaceMesh** and can again be found in the **Mesh Data View**. Four coloured material groups represent the four subsurface layers. When you activate the 3D mesh in the Data View, the following details will be displayed (the exact numbers may slightly vary again):

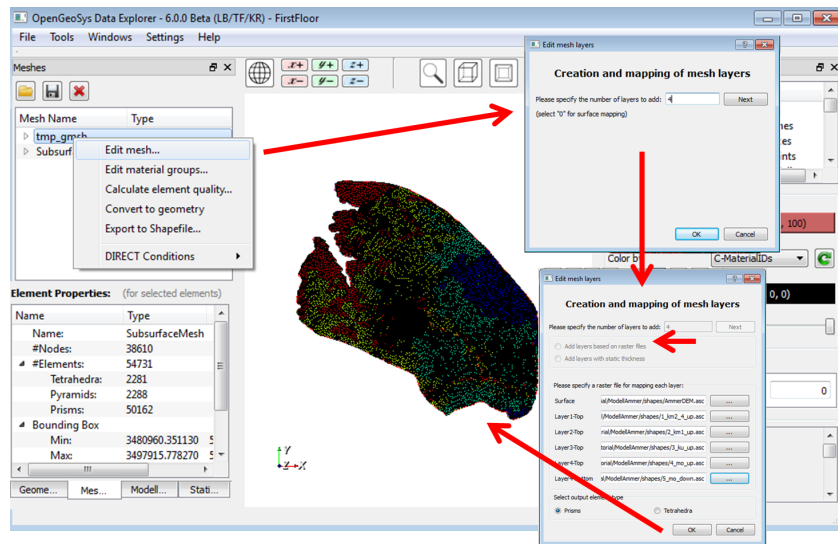


Fig. 11: Construct the 3D mesh by mesh layer mapping.

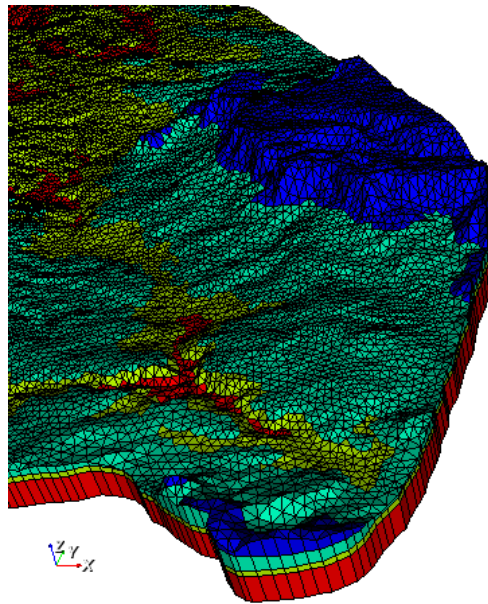


Fig. 12: Final 3D mesh of the catchment with outcropping geological layers.

- amount of mesh nodes: 38610
- element number: 54731
- element types: Tetrahedra, Pyramids and Prisms

Save the 3D mesh as Subsurface.vtu using the disk symbol at the top of the **Data View**. To be able to better discern details in the 3D mesh, you can upscale (super-elevate) the data set in the **Visualisation Pipeline** by setting the **Scaling Factor** to 5 in the **Scaling** mask (Fig. 40).

5.7 Assigning Boundary Conditions

Boundary conditions will be applied to mesh nodes during simulation, *OpenGeoSys* also allows to define them on geometric objects and the subsequent transfer of values onto mesh nodes is nothing the user needs to worry about. Tab. 10 gives an overview of all boundary condition files for the Ammer catchment simulation, which can also be created in the *OpenGeosys Data Explorer*.

Table 4: Boundary condition files for the Ammer case study.

File	Description
ammer.ic	Initial conditions
ammer.bc	Boundary conditions
ammer.st	Source terms

5.7.1 Initial Conditions

Initial conditions of a groundwater flow describe the initial water level of the whole model domain. For simplicity, we use a constant hydraulic head condition of 400 m. The initial conditions can be set by right-clicking on **SubsurfaceMesh** → **DIRECT Conditions** → **Add...** Select in the appearing dialogue **GROUNDWATER_FLOW** as **Process Type**; **Initial condition** as **Condition Type**; **HEAD** as **Primary Variable** and **Domain** as **Distribution Type**. In the text field insert the value “400” for a hydraulic head of 400 m. Click **OK** to set the initial condition on all nodes of the SubsurfaceMesh (Fig. 41).

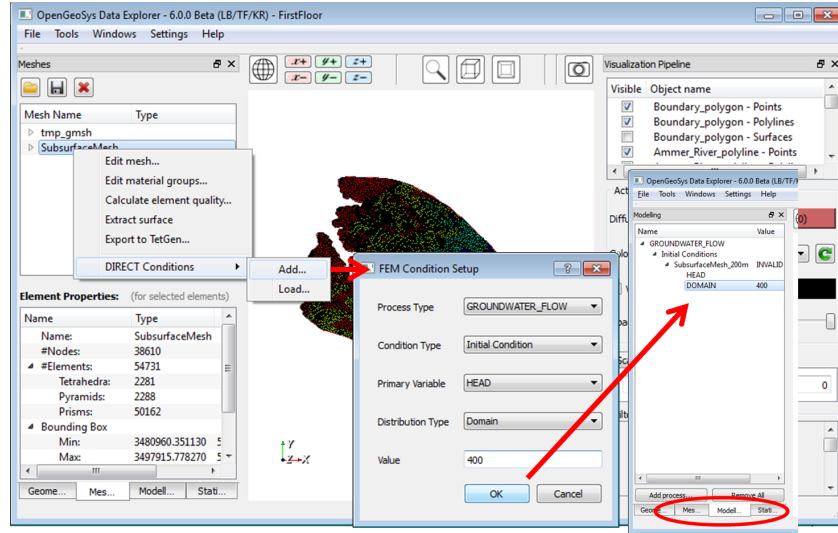


Fig. 13: Set initial conditions on mesh nodes of SubsurfaceMesh.

5.7.2 Source Terms

The groundwater recharge is one of the drivers of groundwater flow and has to be implemented as a source term for the simulation. Since the recharge enters the model domain at the surface, the source terms have to be applied on the top mesh nodes of the subsurface mesh. By right-clicking on **SubsurfaceMesh** in the **Mesh Data View** and selecting **DIRECT conditions**, the same dialogue as described in Sec. 5.7.1 will open. Again, specify **GROUNDWATER_FLOW** as the process, but select **Source Terms** as **Condition Type** now. For the **Primary Variable** select **HEAD** and the **Distribution Type** is **DIRECT**, as we want to apply specific values *directly* on mesh nodes (Fig. 42). Upon clicking **Calculate Values** a new dialogue will open, that allows you to specify the raster file containing the groundwater recharge values of the Ammer catchment. Select the raster file “AmmerGWR.asc” from your working directory. The Raster-file AmmerGWR.asc contains the annual sum of groundwater recharge in millimetre per year (mm/a). To account for the surface area of mesh elements, the calculation method needs to be changed to **Integrate over mesh elements** with a **scaling-factor** of 31536000000.0, which is the conversion of the groundwater recharge from mm/a to m^3/s for each mesh element at the mesh surface.

The pumping rate of the wells is defined as a fixed flux condition (i.e. a *Neumann* boundary conditions) and is part of the source term input file (Fig. 43). Therefore right click on the first point of the wells-file in the **Geometry Data View**. Choose **Set FEM Condition** → **On object...** and enter

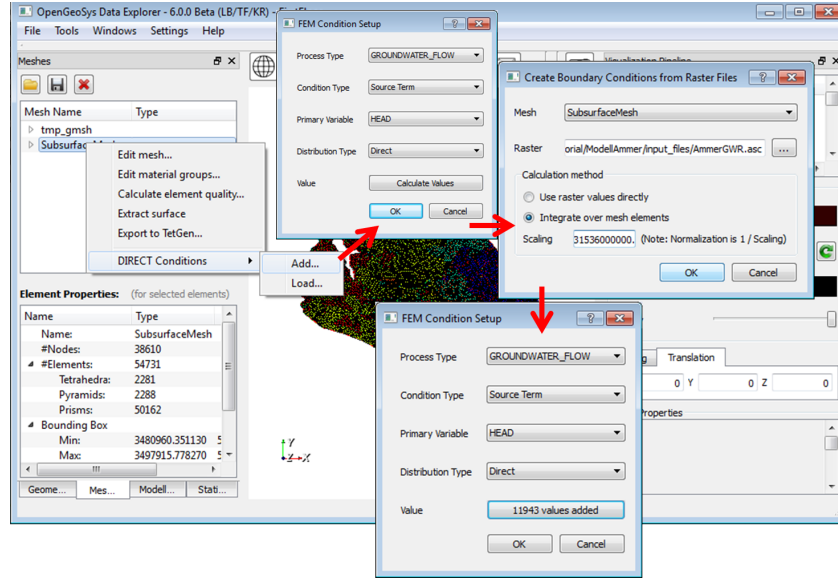


Fig. 14: Groundwater recharge as source term condition.

Table 5: Pumping rates of well sites

Well Points (Geometry)	Point name	pumping rate
0	wellsite1_top	$-0.017m^3/s$
1	wellsite1_bottom	$-0.017m^3/s$
2	wellsite2_top	$-0.017m^3/s$
3	wellsite2_bottom	$-0.017m^3/s$
4	wellsite3_top	$-0.017m^3/s$
5	wellsite3_bottom	$-0.017m^3/s$
6	wellsite4_top	$-0.017m^3/s$
7	wellsite4_bottom	$-0.017m^3/s$

the name (as it is defined in Tab. 11). As soon as you click OK, a new dialog appears where you have to set the source term. Select **GROUNDWATER_FLOW** as Process Type, choose **Source Term** and set the Primary Variable to **HEAD** and automatically the Distribution Type is set to **Constant (Neumann)**. Enter the pumping rate of $-0.017m^3/s$ (Selle et al., 2013a) at the top and the bottom of the well.

The pumping rate of the wells is defined as a fixed flux condition (i.e. a *Neumann* boundary conditions) and is part of the source term input file (Fig. 43). Therefore right-click on the first point of the wells-file in the **Geometry Data View**. Choose **Set FEM Condition → On object...** and enter

the name (as it is defined in Tab. 11). As soon as you click OK, a new dialog appears where you have to set the source term. Select **GROUNDWATER_FLOW** as Process Type, choose **Source Term** and set the Primary Variable to **HEAD** and automatically the Distribution Type is set to **Constant (Neumann)**. Enter the pumping rate of $-0.017\text{m}^3/\text{s}$ (Selle et al., 2013a) at each top or bottom of the well.

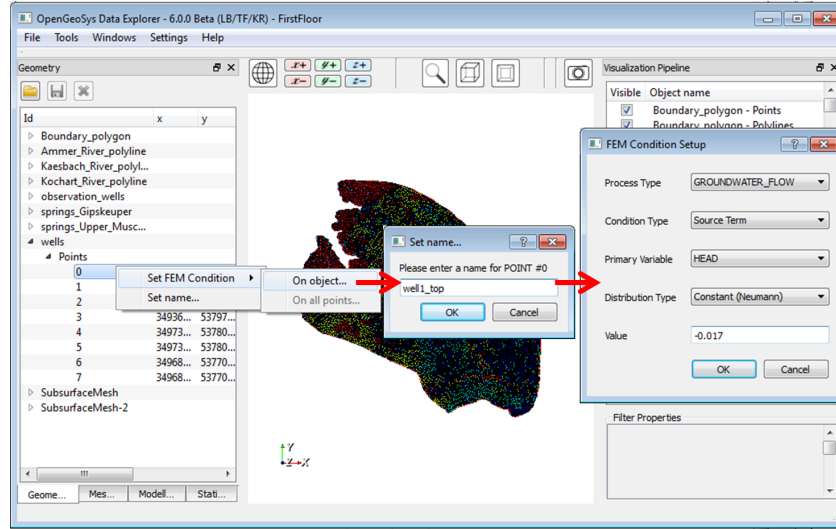


Fig. 15: Set pumping rates on wells as source terms.

5.7.3 Boundary Conditions

The springs of both the Upper Muschelkalk and the Gipskeuper have their discharge close to the surface. We will use this property to implement the ten springs in the model domain as boundary conditions (Fig. 44). The water level of those springs is assumed to be identical with the elevation in the DEM at their respective location. Right-click the first point of the **springs_Upper_Muschelkalk** in the *Geometry Data View*, which is already named as “mo_0” (see Tab. 9). The condition dialogue will open yet again. Again, select **GROUNDWATER_FLOW** as the Process Type, **Boundary Condition** as the Condition Type, set the Primary variable to **HEAD** and the Distribution Type to the fixed hydraulic head which is here represented by **Constant (Dirichlet)**. The value for the Dirichlet boundary conditions for all spring points are listed in Tab. 12. Repeat these instructions for the fixed hydraulic heads of the Gipskeuper springs.

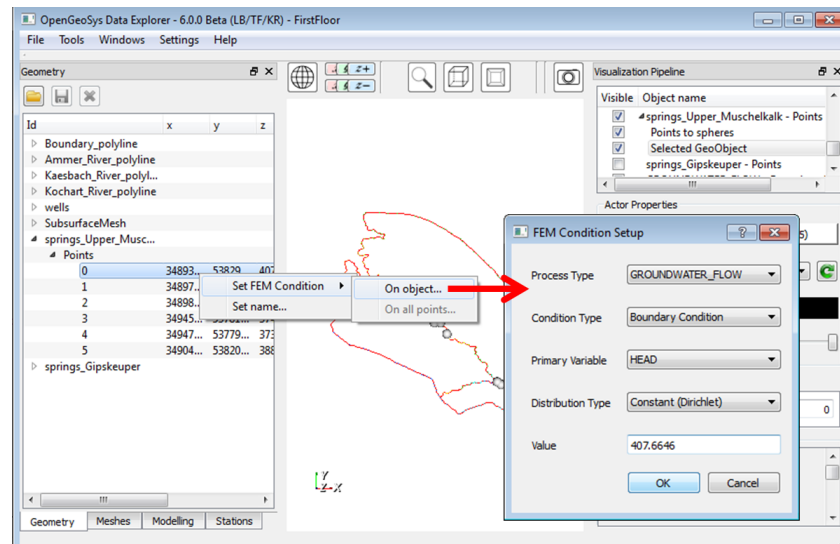


Fig. 16: Set boundary conditions on points.

Table 6: Details for boundary conditions on wells.

Spring	Point Name	HEAD
Upper Muschelkalk	mo_0	407.6646 m
Upper Muschelkalk	mo_1	397.9081 m
Upper Muschelkalk	mo_2	396.2654 m
Upper Muschelkalk	mo_3	374.4069 m
Upper Muschelkalk	mo_4	373.0731 m
Upper Muschelkalk	mo_5	388.9056 m
Gipskeuper	km1_0	387.2844 m
Gipskeuper	km1_1	391.7844 m
Gipskeuper	km1_2	386.8427 m
Gipskeuper	km1_3	384.8551 m
Gipskeuper	km1_4	428.3423 m

The newly generated Dirichlet boundary condition for the springs appears in the **Modelling Data View** and can be emphasised with the “Points to spheres” Filter in the cmdVisualization Pipeline (Fig. 45). See Sec. 5.5 for instructions on how to do this.

Now, all the required condition files have been generated successfully. Save all condition files by right-click on **GROUNDWATER_FLOW** in the **Modelling Data View**. Select in the dialog **Save conditions on all geometries** and **All Types of Conditions** and finally save it as “ammer.cnd”(Fig. 46). Now, all the required condition files have been generated successfully. Save all condi-

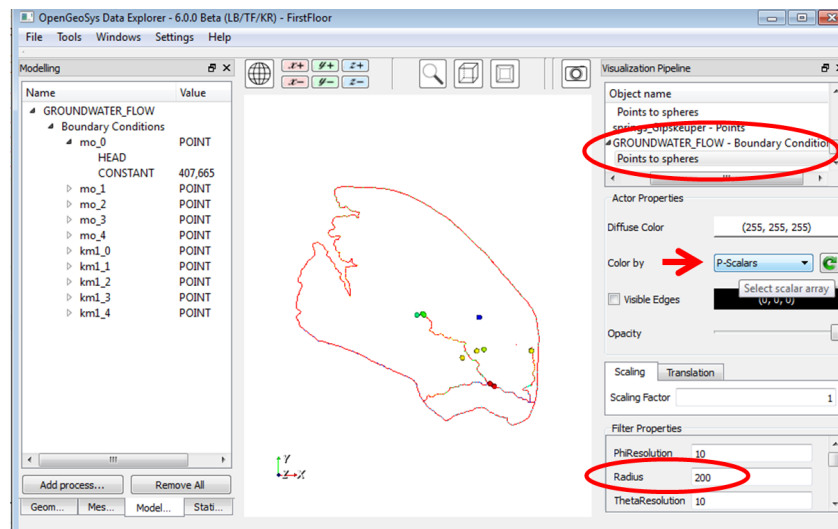


Fig. 17: Visualisation of the Dirichlet boundary conditions of both the Upper Muschelkalk and the Gipskeuper springs. Note that the colouring of the boundary conditions depends on its hydraulic head, when P-Scalar is selected as the data source for colours in the Visualization Pipeline.

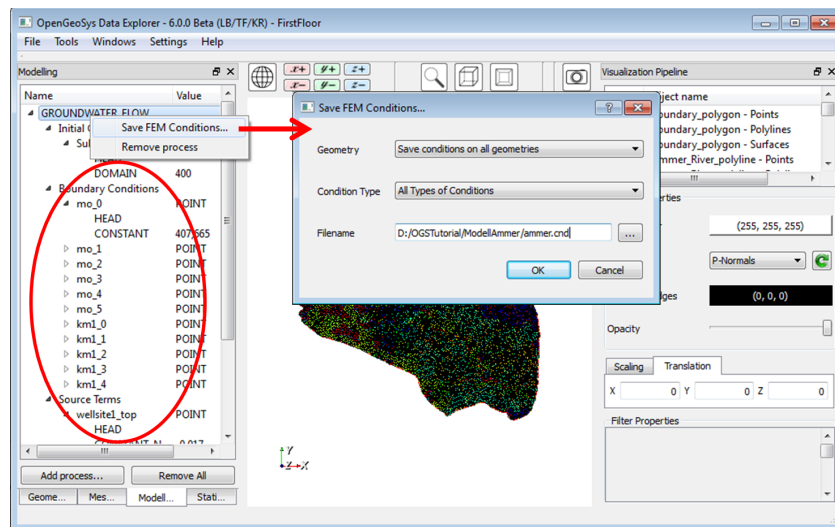


Fig. 18: Save all condition files from the Modelling Data View.

tions file by right-click on `GROUNDWATER_FLOW` in the **Modelling Data View**. Select in the dialog **Save conditions on all geometries** and **All Types of Conditions** and finally save it as “ammer.cnd”(Fig. 46).

5.8 Preparations for the Groundwater Flow Simulation

Before we can start the simulation of the groundwater flow in the Ammer catchment, we have to merge and convert some of our previously generated files due to *OGS* version conflicts. The reason for this is that the *Data Explorer* is a Beta-version already available for the next version of *OpenGeoSys*, where file formats will change. However, *OpenGeoSys* provides a file converter for changing between different file formats (see Sec. 5.8.2). Also, we will need to generate some input files that are not yet implemented in the *Data Explorer* using a text editor. It is recommended to use an external editor tool such as *Notepad++*, *Sublime Text*, *TextPad*, etc.

5.8.1 Merging Geometries

During the simulation we require one file to contain all geometric information. Therefore, we have to merge all geometries imported and saved as gml-Files. Make sure that “Boundary_Polygon”, “Ammer_River_polyline”, “Kaesbach_River_polyline”, “Kochart_River_polyline”, “wells”, “springs_Upper_Muschelkalk” and “springs_Gipskeuper” are all available in the programme and then choose from the main menu **Tools**→**Merge Geometries...** Select all available geometries and save these to **ammer** (Fig. 47).

5.8.2 File Converter

The previously generated files of chapters 5.5–5.7 were created using the *Data Explorer* graphical user interface from *OGS6*. For simulation, we still need to use the executable file of *OGS5*. This means that the files previously generated with the *Data Explorer* need to be converted into *OGS5*-format. We will use the *OGS File Converter* for doing that (Fig. 48). Click on **Tools**→**File Converter** or run `OGSFileConverter.exe` from your *OGS*-directory.

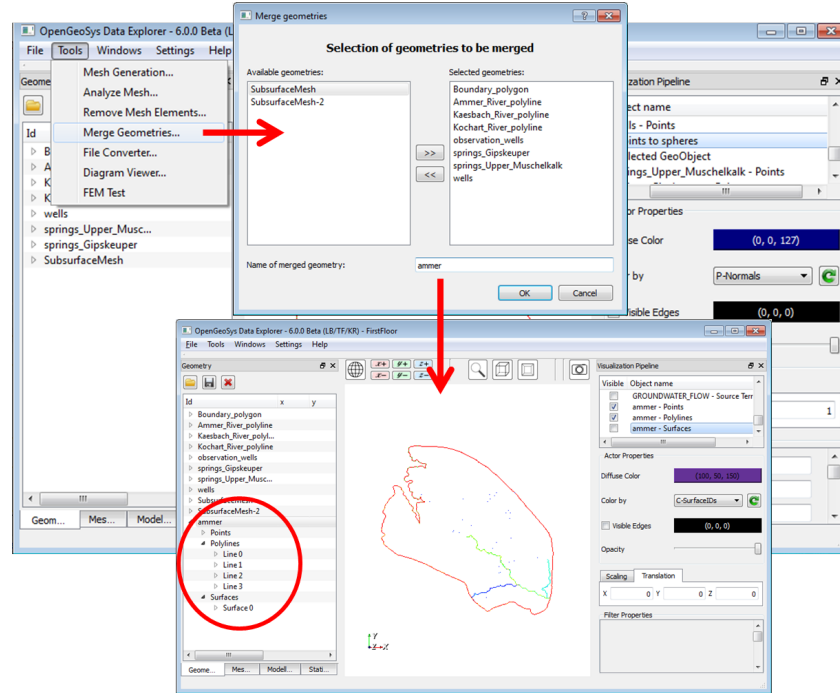


Fig. 19: Merging all geometric files into one gml-file.

Note, that *OGS5*-files are always denoted as ASCII-files while *OGS6*-files are denoted as XML-files. The following file types can be converted:

- Use XML Geometry to ASCII to convert gml-files to *.gli-file
- Use XML meshes to ASCII to convert vtu-files to *.msh-file
- Use XML conditions to ASCII to convert cnd-files to *.bc/*.ic/*.st-files.

Table 7: File conversion overview.

<i>OGS</i> -6 File name	convert to <i>OGS</i> - 5 file	data file
ammer.gml	ammer.gli	geometry file
ammer.cnd	*.bc, *.ic, *.st	boundary condition, initial condition, source term
SubsurfaceMesh.vtu	SubsurfaceMesh.msh	mesh file

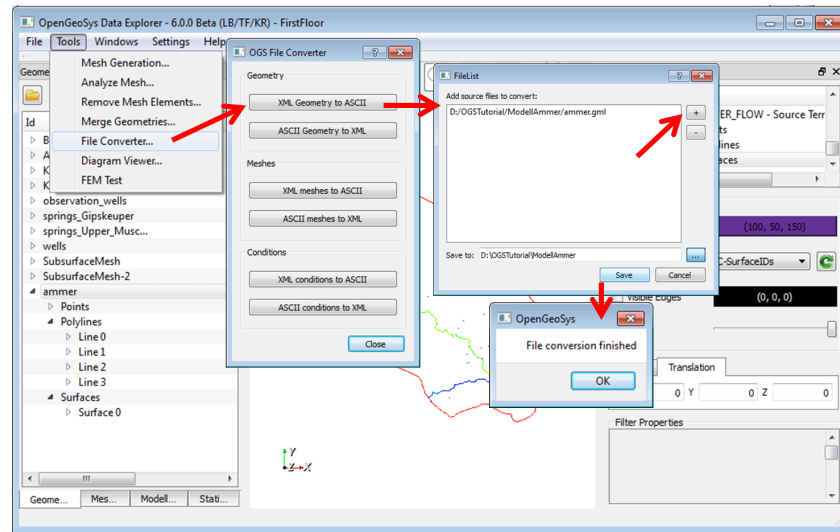


Fig. 20: The File Converter converts files from *OGS-6* to *OGS-5* format

Add in the next dialogue by the plus-function the dataset (e.g. “ammer.gml”, which contains all geometric elements of the Ammer catchment). Repeat this instruction to all files listed in Tab. 13:

Note, that the conversion of the file “ammer.cnd” automatically produces 1) boundary conditions (ammer.bc), (2) initial conditions (ammer.ic) and (3) source term files (ammer.st).

Conversion of ammer.gml to ammer.gli

The converted geometry file **ammer.gli** should contain all geometric information for the Ammer catchment. This file includes 616 POINTS with x-, y-, z- coordinates plus a number of point names that you assigned previously, 4 POLYLINES and 1 SURFACE.

Listing 5.2: Example geometry file: ammer.gli

```
#POINTS
0 3484965.87555 5391892.5068499995 593.15999999999997
1 3485588.0931199999 5391873.0619700002 560.78999999999996
2 3486365.8666300001 5391853.6201999998 559.41999999999996
3 3487085.3054999998 5391795.2855500001 509.88999999999999

[...]

614 3497340 5378030 315 $NAME wellsite3_bottom
615 3496850 5377085 335 $NAME wellsite4_top
616 3496850 5377085 300 $NAME wellsite4_bottom
#POLYLINE
$NAME
```



```

$POINTS
0
1

[...]

561
562
400
#SURFACE
$NAME
0
$TYPE
0
$POLYLINES
0
#STOP

```

Conversion of `ammer.cnd` to `ammer.bc`, `ammer.ic` and `ammer.st`

While the `cnd`-file contains all types of initial and boundary conditions required for the model, the file conversion will output three separate files containing only boundary conditions (Listing 5.3), initial conditions (Listing 5.4) and source/sink terms (Listing 5.5), respectively.

Boundary conditions reference geometrical objects by name. For example, the first boundary condition in the list below refers to a point with the name “mo_0”. See Listing 5.2 on how names are assigned to geometric objects.

Listing 5.3: Example boundary condition file: `ammer.bc`

```

#BOUNDARY_CONDITION
$PCS_TYPE
GROUNDWATER_FLOW
$PRIMARY_VARIABLE
HEAD
$GEO_TYPE
POINT mo_0
$DIS_TYPE
CONSTANT 4.076650000000e+002
#BOUNDARY_CONDITION
$PCS_TYPE
GROUNDWATER_FLOW
$PRIMARY_VARIABLE
HEAD
$GEO_TYPE
POINT mo_1
$DIS_TYPE
CONSTANT 3.979080000000e+002

[...]

#BOUNDARY_CONDITION
$PCS_TYPE
GROUNDWATER_FLOW
$PRIMARY_VARIABLE
HEAD

```

```

$GEO_TYPE
POINT km1_4
$DIS_TYPE
CONSTANT 4.283420000000e+002
#STOP

```

Listing 5.4: Example initial condition file: ammer.ic

```

#INITIAL_CONDITION
$PCS_TYPE
GROUNDWATER_FLOW
$PRIMARY_VARIABLE
HEAD
$GEO_TYPE
DOMAIN
$DIS_TYPE
CONSTANT 4.000000000000e+002
#STOP

```

Listing 5.5: Example source term file: ammer.st

```

#SOURCE_TERM
$PCS_TYPE
GROUNDWATER_FLOW
$PRIMARY_VARIABLE
HEAD
$DIS_TYPE
DIRECT D:\OGSTutorial\ModellAmmer\direct_values0.txt
#SOURCE_TERM
$PCS_TYPE
GROUNDWATER_FLOW
$PRIMARY_VARIABLE
HEAD
$GEO_TYPE
POINT wellsite1_top
$DIS_TYPE
CONSTANT_NEUMANN -1.700000000000e-002

[.]

#SOURCE_TERM
$PCS_TYPE
GROUNDWATER_FLOW
$PRIMARY_VARIABLE
HEAD
$GEO_TYPE
POINT wellsite4_bottom
$DIS_TYPE
CONSTANT_NEUMANN -1.700000000000e-002
#STOP

```

Conversion of SubsurfaceMesh.vtu to ammer.msh

The converted mesh file contains all 38610 nodes of the 3D mesh as well as all the prism-, pyramid- and tetrahedral mesh elements contained in the vtu-

Table 8: Mesh material groups.

Mesh Material_group	geological layer
0	Upper Muschelkalk
1	Lettenkeuper
2	Gipskeuper
3	Schilfsandstein, Stubensandstein, Bunte Mergel

file. The mesh file is similar to the 2D mesh file given in Listing 5.1, giving element IDs, identifiers of the material groups of the four geological layers 0–3 (Tab. 14) as well as the element type and an array of nodes.

Conversion of SubsurfaceMesh.vtu to ammer.msh

The converted mesh file contains all 38610 nodes of the 3D mesh as well as all the prism-, pyramid- and tetrahedral mesh elements contained in the vtu-file. The mesh file is similar to the 2D mesh file given in Listing 5.1, giving elements IDs, identifiers of the material groups of the four geological layers 0–3 (Tab. 14) as well as the element type and an array of nodes.

Listing 5.6: Example for 3D mesh file: ammer.msh

```
#FEM_MSH
$PCS_TYPE
  NO_PCS
$NODES
  38610
0 3494493.58165 5386875.87966999 512.634247246868
1 3494785.24555 5386506.43623 535.5634554289
2 3494649.1376 5386700.87882999 543.367748626366

[.]

$ELEMENTS
  54731
0 3 pris 1231 1087 1089 48 1 3
1 3 pris 1231 1230 1087 48 47 1
2 3 pris 1088 1230 1231 2 47 48

[.]

2243 2 pris 5907 5906 5768 1177 1176 1132
2244 2 pris 5907 5767 5906 1177 1131 1176
2245 2 pris 5910 5911 5912 1180 1181 1182

[.]

12089 1 pris 15199 14897 15198 5907 5767 5906
12090 1 pris 15260 15194 15195 5968 5902 5903
12091 1 pris 15274 15275 15273 5970 5971 5969
```

```
[...]  
54728 0 pris 28457 28460 27132 16517 16520 15224  
54729 0 pris 27050 27049 28110 15142 15141 16172  
54730 0 pris 27049 38601 28110 15141 26658 16172  
#STOP
```

5.8.3 File Editing

Some of the simulation files need to be generated with the help of a text editor programme (Tab. 15). Examples in this book have been created with *Notepad++* (<http://notepad-plus-plus.org/>) but other text editors will be fine, too. *OpenGeoSys* input files allow the use of a wide range of keywords of which only a small subset will be used in the following. A detailed description of OGS input files including many keywords and the required parameters are available at <http://www.opengeosys.org/help/documentation>.

Table 9: List of files which have to be edited for running the Ammer case study.

Object	File	Explanation
PCS	<code>ammer.pcs</code>	process definition: groundwater flow
NUM	<code>ammer.num</code>	numerical properties
TIM	<code>ammer.tim</code>	time discretisation
MMP	<code>ammer.mmp</code>	medium properties of geological layers
OUT	<code>ammer.out</code>	output configuration

PCS – process definition:

We will use the “Groundwater Flow” process in *OGS* to describe infiltration of groundwater recharge to the local aquifer system of the Ammer catchment. Using the designated keyword `GROUNDWATER_FLOW`, Darcy’s equation is selected for solving the problem:

$$S_s \frac{\partial h}{\partial t} = \nabla(K \cdot \nabla h) + q \quad (1)$$

Table 10: Parameters of the governing equation for groundwater flow in confined aquifers.

Parameter	Symbol	Unit
Discharge	Q	m^3/s
Hydraulic conductivity	K	m/s
Specific Storage	S_s	$1/\text{m}$
Density of water (10°C)	ρ	$\text{kg} \cdot \text{m}^{-3}$
Viscosity of water (10°C)	μ	$\text{Pa} \cdot \text{s}$

Listing 5.7: Example process file: ammer.pcs

```
#PROCESS
$PCS_TYPE
GROUNDWATER_FLOW ; for equation ()
#STOP
```

NUM – numerical properties:

The NUM file parameterises the numerics of the linear solver of Eq. 27.

Listing 5.8: Example numeric parameters file: ammer.num

```
#NUMERICS
$PCS_TYPE
GROUNDWATER_FLOW
$LINEAR_SOLVER
; method .... error\_tolerance max\_iterations theta precondition storage
2 0 1.0000000000000000e-10 2000 1.0 100 4
#STOP
```

TIM – time stepping properties of the process:

The temporal resolution and number of time steps of the simulation of the groundwater recharge process is provided by the TIM file.

Listing 5.9: Example time discretisation file: ammer.tim

```
#TIME_STEPPING
$PCS_TYPE
GROUNDWATER_FLOW
$TIME_START
0
```

```

$TIME_STEPS
1 1
$TIME_END
100
#STOP

```

MMP – properties of the porous medium

The material properties, such as the hydraulic conductivity of the hydrogeological layers of the Ammer catchment (see Sec. 5.2) are characterised in the MMP file. Note, that the material properties are ordered from bottom to top (Fig. 49).

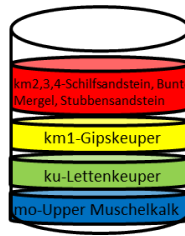


Fig. 21: Scheme of Geology of the Ammer catchment. As noted in Sec. 5.4, the layers *km2*, *km3* and *km4* are merged into one layer.

Listing 5.10: Example medium properties file: ammer.mmp

```

#MEDIUM_PROPERTIES
$NAME
mo
$GEOMETRY_DIMENSION
3
$GEOMETRY_AREA
1.000000000000e+000
$POROSITY
1 0.1
$PERMEABILITY_TENSOR
ISOTROPIC 4.4394111E-05
#MEDIUM_PROPERTIES
$NAME
ku
$GEOMETRY_DIMENSION
3
$GEOMETRY_AREA
1.000000000000e+000
$POROSITY
1 0.1
$PERMEABILITY_TENSOR
ISOTROPIC 1.0000000E-04
#MEDIUM_PROPERTIES

```

```

$NAME
km1
$GEOMETRY_DIMENSION
3
$GEOMETRY_AREA
1.000000000000e+000
$POROSITY
1      0.1
$PERMEABILITY_TENSOR
ISOTROPIC      1.5000454E-05
#MEDIUM_PROPERTIES
$NAME
km2
$GEOMETRY_DIMENSION
3
$GEOMETRY_AREA
1.000000000000e+000
$POROSITY
1      0.1
$PERMEABILITY_TENSOR
ISOTROPIC      3.9741665E-09
#STOP

```

Insert for each geological layer the hydraulic conductivity, as it is defined in Tab. 17.

Table 11: Hydraulic conductivities of each geological layer of the Ammer catchment

Mesh	Mater- ial_Group	Geological Layer	Hydraulic Conductivity
0		<i>mo</i> – Upper Muschelkalk	$4.4394111E-05 \text{ m/s}$
1		<i>ku</i> – Lettenkeuper	$1.0000000E-04 \text{ m/s}$
2		<i>km1</i> – Gipskeuper	$1.5000454E-05 \text{ m/s}$
3		<i>km2</i> , <i>km3</i> , <i>km4</i> – Schilfsandstein, Bunte Mergel, Stubensandstein	$3.9741665E-09 \text{ m/s}$

OUT – define the simulation output

The output file defines which information from the simulation results should be written to the model outputs. For the Ammer study, we will write the groundwater velocity field (**VELOCITY_X1**; **VELOCITY_Y1**; **VELOCITY_Z1**) of the whole domain in *VTK* format. Furthermore, we are interested in hydraulic heads for all observation wells, e.g. a well (**POINT obs_well11**), which will be written in *TecPlot* format.

Listing 5.11: Example output parameterisation file: ammer.out

```

#OUTPUT
$PCS_TYPE

```

```

GROUNDWATER_FLOW
$NOD_VALUES
HEAD
VELOCITY_X1
VELOCITY_Y1
VELOCITY_Z1
$GEO_TYPE
DOMAIN
$DAT_TYPE
VTX
$TIM_TYPE
STEPS 1

#OUTPUT
$PCS_TYPE
GROUNDWATER_FLOW
$NOD_VALUES
HEAD
$GEO_TYPE
POINT obs_well1
$DAT_TYPE
TECPLOT
$TIM_TYPE
STEPS 1
$COMBINE_POINTS

[.]

#OUTPUT
$PCS_TYPE
GROUNDWATER_FLOW
$NOD_VALUES
HEAD
$GEO_TYPE
POINT obs_well135
$DAT_TYPE
TECPLOT
$TIM_TYPE
STEPS 1
$COMBINE_POINTS

#STOP

```

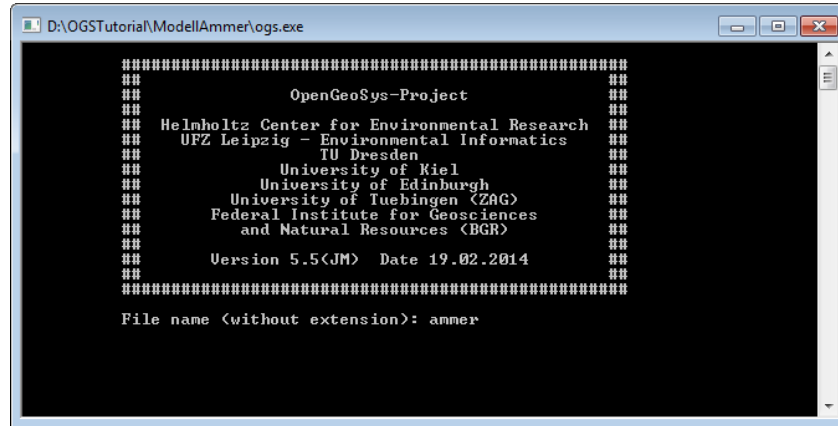
5.9 Groundwater Flow Simulation

Most of the required simulation input files (Tab. 18) for the Ammer catchment were generated with the graphical user interface of *OpenGeoSys* and some input files had to be created manually using a text editor. Now, we will use all of the created input files to simulate with the command line interface of *OpenGeoSys 5* groundwater flow for the Ammer catchment. For this, it is of vital importance that all files have the same base name, i.e. the names of all files without their respective extensions needs to be “ammer” for this case study. A file with a different base name will not be found by the software and will result in either a termination of the programme or false simulation results.

Table 12: Input files for groundwater simulation.

Object	File	Explanation
GEO	ammer.gli	system geometry of Ammer catchment
MSH	ammer.msh	3D finite element mesh
PCS	ammer.pcs	process definition: groundwater flow
NUM	ammer.num	numerical properties
TIM	ammer.tim	time discretisation
IC	ammer.ic	initial conditions
BC	ammer.bc	boundary conditions, e.g. groundwater recharge
ST	ammer.st	source/sink terms
MMP	ammer.mmp	medium properties of geological layers
OUT	ammer.out	output configuration
GWR	direct_values0.txt	groundwater recharge

Collect all these files in one folder and also add the current executable of *OpenGeoSys* (`ogs.exe`) to the folder. At the time of writing, the current *OGS* version is 5.5.4. To start the simulation, start `ogs.exe` and write “ammer” into the console (Fig. 50).

Fig. 22: *OGS* command line interface.

Press `ENTER` and the simulation starts. You can follow the simulation process by the messages output in the console window. Once the simulation has finished, the console window will close automatically.

5.10 OGS Simulation Results

Some new files are generated while the simulation was running:

- ammer_GROUNDWATER_FLOW0000.vtk
- ammer_GROUNDWATER_FLOW0001.vtk
- ammer_time_obs_well1_GROUNDWATER_FLOW.tec
- ammer.txt (only in case you start *OGS* simulation via command line:
ogs.exe ammer > ammer.txt)

The txt-file contains a log of the messages output during the simulation in the command line interface. It includes information which input files have been loaded as well as details of each time step.

Listing 5.12: *OpenGeoSys* runtime output messages for Ammer case study.

```
#####
##                                     ##
##               OpenGeoSys-Project   ##
##                                     ##
##   Helmholtz Center for Environmental Research ##
##   UFZ Leipzig - Environmental Informatics  ##
##                       TU Dresden          ##
##               University of Kiel          ##
##               University of Edinburgh     ##
##               University of Tuebingen (ZAG) ##
##               Federal Institute for Geosciences ##
##               and Natural Resources (BGR)   ##
##                                     ##
##               Version 5.5(JM)   Date 19.02.2014 ##
##                                     ##
#####

File name (without extension): ammer

-----
Data input:
Warning in Surface::Read, polyline not found: 0
GEOLIB::readGLIFile open stream from file ammer.gli ... done
read points from stream ... ok, 617 points read
read polylines from stream ... ok, 4 polylines read
read surfaces from stream ... ok, 0 surfaces read
PCSRead ... done, read 1 processes
BCRead ... done, read 11 boundary conditions
STRead ... done, read 8 source terms
ICRead
OUTRead
TIMRead
MMPRead ... done, read 4 medium properties
NUMRead
MSHRead: ASCII file
Executing ConstructGrid() ... done.
DOMRead: no DDC file

[..]

#####
Time step: 1| Time: 1| Time step size: 1

=====
->Process 0: GROUNDWATER_FLOW
```

```

=====
PCS non-linear iteration: 0/1
Assembling equation system...
Calling linear solver...
  SpBICGSTAB iteration: 207/2000
-->LINEAR solution complete.
  PCS error DOF[0]: 32.3133
->Calculate velocity

This step is accepted.
ArrayName: VELOCITY_X1
Data output: Breakthrough curves - obs_well1

[.]

^O^: Your simulation is terminated normally ^O^
Simulation time: 27s

```

The two *VTK*-files represent the simulation results of the groundwater flow processes (i.e. the distribution of the hydraulic head) for the first two time steps. Specifically, the first time step represents the initial condition and the second time step represents results of groundwater flow simulated with the steady state model.

Listing 5.13: VTK output file from Ammer case study

```

# VTK DataFile Version 3.0
Unstructured Grid from OpenGeoSys
ASCII
DATASET UNSTRUCTURED_GRID
FIELD TimesAndCycles 2
TIME 1 1 double
1.0000000000000e+000
CYLCE 1 1 long
1
POINTS 38610 double
3.494493581650e+006 5.386875879670e+006 5.126342472469e+002
3.494785245550e+006 5.386506436230e+006 5.355634554289e+002
3.494649137600e+006 5.386700878830e+006 5.433677486264e+002
3.494882466850e+006 5.386448104700e+006 5.356029712285e+002

[.]

```

The *TecPlot*-files for each of the observation wells contain the hydraulic heads of this particular observation well for each time step. While this file is meant to be analysed using the plotting programme *TecPlot*, it can also very easily be exported to *Microsoft Excel* to compare measurement data with the newly simulated data. For this particular study, the comparison of simulated water levels with field data showed a good representation of the natural behaviour of the Ammer catchment (see Fig. 51a). Compared to modelling results obtained by (Selle et al., 2013a), slight differences could occur due to recent improvements in the meshing procedures.

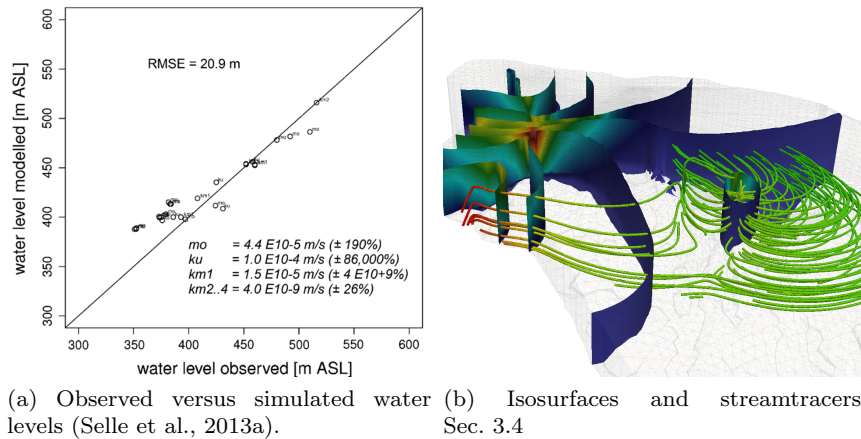


Fig. 23: Some examples of the Ammer catchment model results

Listing 5.14: *TecPlot* output file from Ammer case study.

```
TITLE = "Time curves in points"
VARIABLES = "TIME " "HEAD"
ZONE T="POINT=POINTobs_well1"
0.000000000000e+000 4.000000000000e+002
1.000000000000e+000 3.921171170670e+002
```

For more details regarding the Ammer catchment model results and its interpretation, the interested reader is referred to Selle et al. (2013a).

5.11 Visual Analysis

The *OGS Data Explorer* allows to concurrently visualise model input and output data. Easily adjustable parameters for the visualisation include:

- Scaling, Translation, Tessellation
- Opacity, user defined colours, Scalar arrays
- Thresholding, Isosurfaces

To visualise the simulation results, you can import the *VTK* files via **File** → **Import Files** → **VTK Files** into the **Visualization Pipeline** of the *Data Explorer*. Currently only visualisation of single time steps are possible. Once loaded, all visualisation options are available for manipulation of the result:

- Apply texture to surface
- Extract cells by threshold

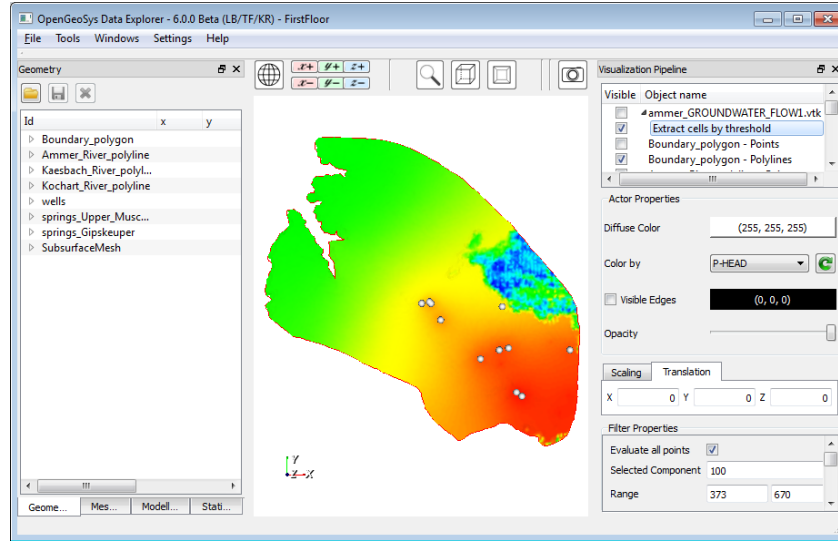


Fig. 24: Visualisation of simulation results by using the filter “Extract cells by threshold”.

- Elevation-based colouring
- Generate contours based on scalar fields
- Surface filter

For more details on each of these filters, the interested reader is referred to the *OpenGeoSys Data Explorer Manual* (Rink, 2013) or articles on this topic (Rink et al., 2013, 2014). As an example, the filter “Extract cells by threshold” can be employed to visualise only specific parts of the hydraulic head in the simulation results (Fig. 52). You can choose the range of the threshold in-between the minimum and maximum of simulated hydraulic heads. If you load the time step 0 of the Ammer model simulation you will see the constant head boundary condition of 400 m for the whole domain. For the second time step, the maxima of the steady state model will be automatically added to the dialogue.

The filter “Generate contours based on scalar fields” enables the illustration of the simulation results as a simplified user-specified contour plot.

More details regarding the visualisation of input data and simulation results of the Ammer catchment can be found in Rink et al. (2013). The output-files of the groundwater flow simulation are saved in *VTK* format, a format of the widely used open-source programming library *Visualization Toolkit* (Schroeder et al., 2006). It is interesting to note that there also exists a freely available graphical user interface for this library, called *ParaView* (Ahrens et al., 2005), which can be employed for the interactive data exploration and visual analysis of simulation results. The *ParaView* frame-

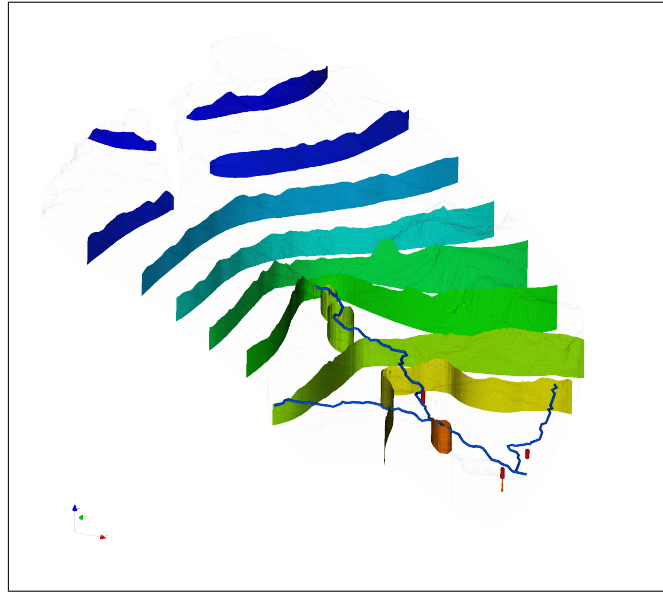


Fig. 25: Visualisation of simulation results by using the filter “Generate contours based on scalar fields”

work implements a large number of well-established visualisation algorithms and techniques for the visualisation and analysis of complex scientific data sets (Fig. 54). *OpenGeoSys* output files are in VTK-format and thus are directly supported by *ParaView*. Note, that *all* data loaded into the *Data Explorer* can also be exported in VTK-format by right-clicking the data set in the **Visualization Pipeline** and selecting **Export to VTK...**

For simulation results, interesting algorithms include:

- contour filter: visualisation of isolines or -surfaces of any variable in the data set
- stream tracer: visualisation of vector data such as flow-paths
- slice filter: extracting of arbitrary cutting planes from a dense data set
- threshold filter: extracting interesting value ranges of variables in the data set
- definition of colour look-up tables and transfer functions: selective dyeing of values/value ranges of interest into easily distinguishable colours
- affine transformations: re-scaling or moving of parts of a data set for better visibility of regions of interest.

More information can be found at www.paraview.org, including an extensive documentation in the *ParaView*-Wiki as well as a number of video tutorials.

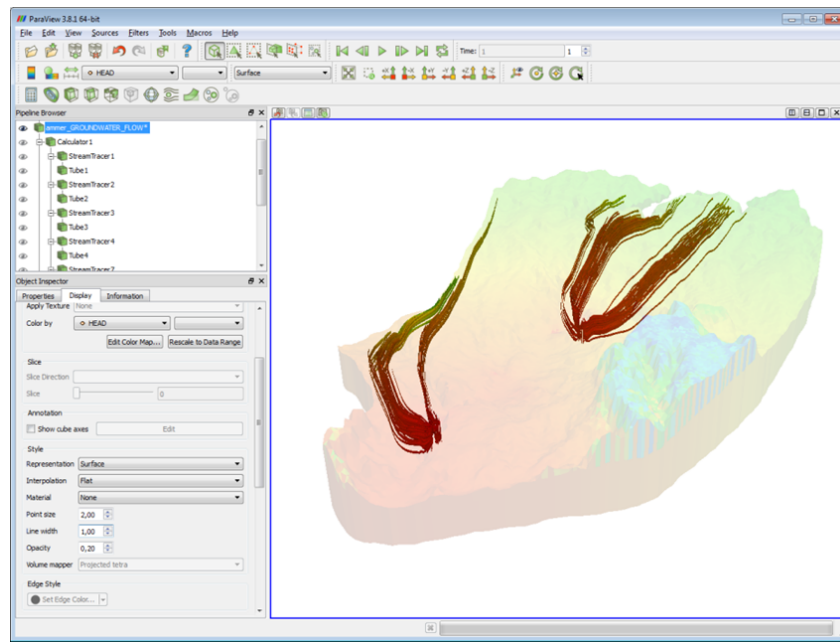


Fig. 26: Using a stream tracer in *ParaView* for the analysis of groundwater flow paths.

Appendix A

Geographical Information Systems

AGNES SACHSE

A.1 Introduction to *ArcGIS*

Pre-formatted data from geographic information systems (GIS) is often required in the process of creating a hydrological model. Geographic information system software is specifically designed for the management, modification and analysis of geographic data and was first introduced in the 1960s (Westervelt, 2001). Modern GIS software also incorporates interfaces for the import of freely available data via web interfaces, scripting support for user-defined extension of existing functionality and semi-automatic packages for user support during complex tasks such as catchment analysis. The commercial geographic information system *ArcGIS* is developed by *Esri*. It is well suited for creating and using maps, compiling geographic data, analysing mapped information, discovering and sharing data, and managing geographic information in databases (Law and Collins, 2013). As such, this software is very useful when organising and analysing data of real case studies and is also an important prerequisite for the modelling of natural systems. Non-commercial software such as *QGis* (<http://www.qgis.org>) or *GRASS* (Neteler and Mitasova, 2008) is already widely used and offers similar features as *ArcGIS*.

ArcGIS provides an infrastructure for generating maps and geographic information available for scientific project partners. Key features include

- **spatial analysis:** extracting subsets of data (e.g. clipping, selecting, splitting), performing statistical analyses, creating overlays or proximity buffers
- **data management:** support of 70 data formats; recording, managing and viewing meta data; creating and managing geo-databases
- **mapping and visualisation:** generating maps for presentations and publications

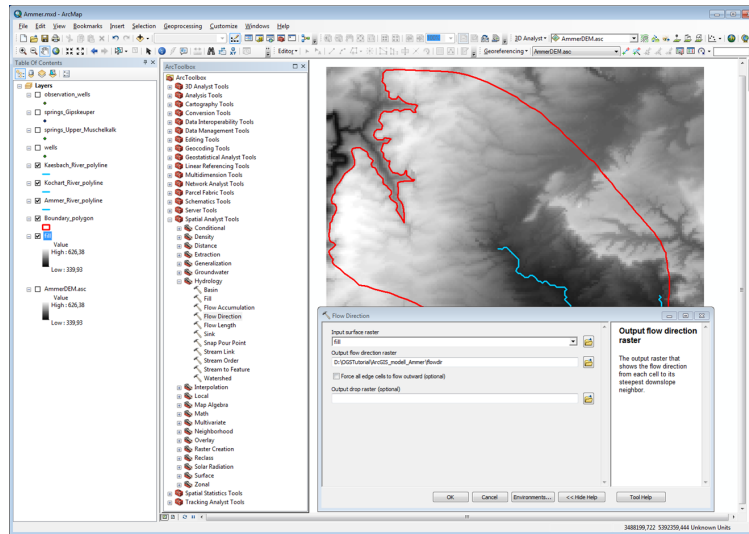


Fig. A.1: Workflow of delineating the *Flow direction* from the depressionsless DEM of the Ammer catchment.

There are two basic classes of data supported by *ArcGIS*: **Feature data** (e.g. shape files) represents data using geometric objects (points, polyline or polygons) and can be optionally linked with attributes. **Raster data** representing an area of interest that are subdivided into rectangular cells or pixels of constant size (e.g. image data such as digital elevation models). More information on *ArcGIS* can be found in the extensive book by Law and Collins (2013) and on the *Esri*-Homepage at <http://www.esri.com/software/arcgis>.

A.2 Hydrology Tool in *ArcGIS*

ArcGIS is a valuable tool when organising data for catchment analysis and hydrological modelling. Possible sources include data from agencies and authorities (e.g. hydrological data bases), digitally-collected data (e.g. satellite data and aerial surveys) or digitised data from physical maps.

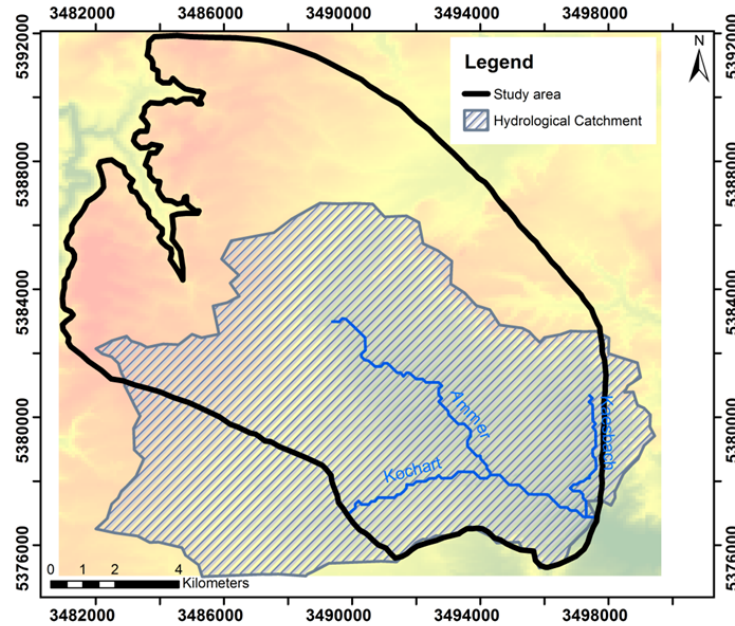


Fig. A.2: The hydrological catchment of the Ammer catchment (blue cross hatching) as a result of watershed delineation process.

Such data collections have to be registered to a common projected coordinate system, such as the well-established UTM system. A catchment analysis can be easily performed in *ArcGIS* by using the hydrologic analysis tools of the *ArcToolbox* after enabling the “Spatial Analyst” extension. For example, a watershed delineation is performed by employing the following algorithms:

- creating a depressionless DEM
- calculating flow direction (Fig. A.1)
- calculating flow accumulation
- finding watershed outlet points
- delineating watersheds

Extensive information on each aspect of this workflow can be found at <http://resources.arcgis.com/en/communities/desktop/> by searching for “Hydrology tools”.

Appendix B

Coupled Hydrosystems

STEPHAN SCHULZ, JENS-OLAF DELFS, THOMAS KALBACHER,
MARC WALTHER AND WENQING WANG

This chapter gives an short overview about methods and models of coupled hydrosystems, especially software, which are coupled with *OpenGeoSys*.

B.1 OGS#JAMS

In the context of groundwater flow modelling hydrological models like *J2000* mostly serve the purpose of providing the groundwater recharge as a second order (Neumann) boundary condition. For this specific task a one-way coupling is sufficient. One-way coupling means that a hydrological model is independently set up and run. Then, modelling results are implemented as input files into the groundwater flow model. For this purpose, *OpenGeoSys* provides interfaces to use output files of the hydrological model *J2000*. In case of more complex interactions between surface water and groundwater more sophisticated types of coupling are needed (e.g. joined coupling, tools coupling).

J2000 is a fully distributed, process-based hydrological model, which is implemented in the modular oriented Java framework *Jena Adaptable Modelling System (JAMS)* (Krause and Kralisch, 2005)). Due to the modular model design, it is possible to set up *J2000* for specific needs, i.e. existing modules can be switched on/off or even new modules can be designed. A commonly applied setting of *J2000* is shown in Fig. B.3. Krause (2001) presents detailed descriptions of these modules. The distribution of the model is realized by the hydrological response units (HRU's) concept. HRU's are spatial entities, which show the same hydrologic response. Usually they are derived from intersecting relevant spatial information like land use, soil type, geology,

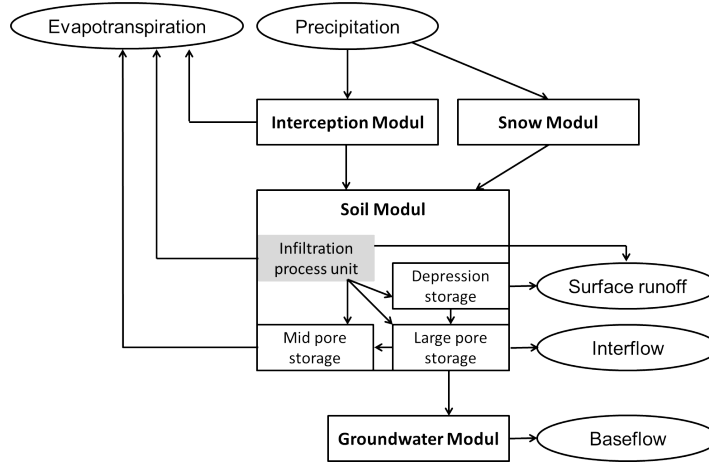


Fig. B.1: Flow chart of the *J2000* model concept for the runoff generation of each HRU (Schulz et al., 2013)

slope etc. Schulz et al. (2013) introduced another solution – they based the derivation of HRU’s on a topological approach. Another important characteristic of *J2000* is routing, i. e. runoff components (surface runoff, interflow and base flow) are transferred within a flow cascade into the corresponding storages of the next HRU or river segment (Krause, 2001).

Usually, the hydrological model *J2000* is calibrated by fitting the simulated runoff to the observed one. Here, the base flow is of particular importance as it represents the previous groundwater recharge in the model (Fig. B.3) – an assumption, which is only valid for effluent conditions.

The set up of a *J2000* model requires several pre-processing steps:

- i the catchment area has to be extracted (see appendix A);
- ii relevant spatial data (land use, soil, geology, elevation, aspect and, slope) has to be prepared and parameterized;
- iii temporal data (precipitation, sunshine hours, wind speed, temperature, relative humidity, absolute humidity, and stream discharge) has to be prepared;
- iv the catchment area has to be subdivided into HRU’s;
- v spatial data has to be projected on the HRU’s; and
- vi model input files with information about HRU’s and routing have to be created.

The last two steps are time consuming and have to be redone, if the subdivision into HRU’s is changed. To simplify the processing of steps (v) and (vi) we developed a toolbox with a GUI (Fig. B.4). The *J2000* pre-processing toolbox comes with a user’s guide, in which the processing steps are described

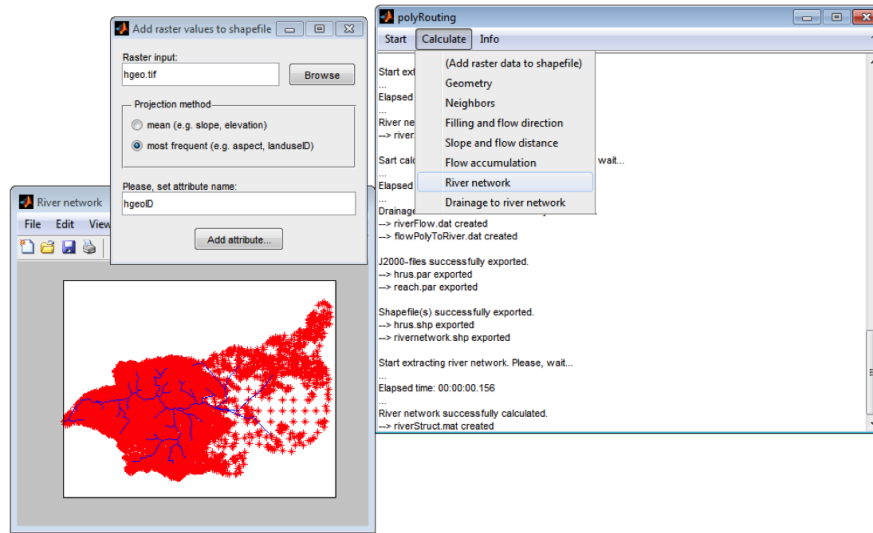


Fig. B.2: Screenshot of the application of the *J2000* pre-processing toolbox

in detail. Prerequisite for the application the *J2000* pre-processing toolbox is the *Matlab* software with mapping toolbox.

The *J2000* pre-processing toolbox can be acquired by contacting: stephan.schulz@ufz.de

B.2 OGS#SWMM

SWMM (Storm Water Management Model) is a management tool for the control of runoff volume and pollution loads in urban catchments. Storage tanks conceptualize permeable areas (greenland) and impermeable areas (streets, pavements, roofs) with a slope and width. The kinematic wave and Saint-Venant equations route channelized flows (through channels, sewer pipes, culverts, etc.). A graphical user interface (Fig. B.5), comparable to the *OGS Data Explorer* (Sec. 3.3), provides various features for urban settings, weirs, sluice gates, pumps, detention ponds, infiltration trenches and other drainage units. The users' manual contains a "quick start example" for the setup of a simple sewage network. It nicely shows the differences in the implemented Saint-Venant and kinematic wave approaches. The kinematic wave approach leads to sewage overflow (Fig. B.5), while the Saint-Venant equation captures the pressure increases in the sewage pipes. Results reveal backflow, i.e. in upstream direction, which prevent sewage overflow.

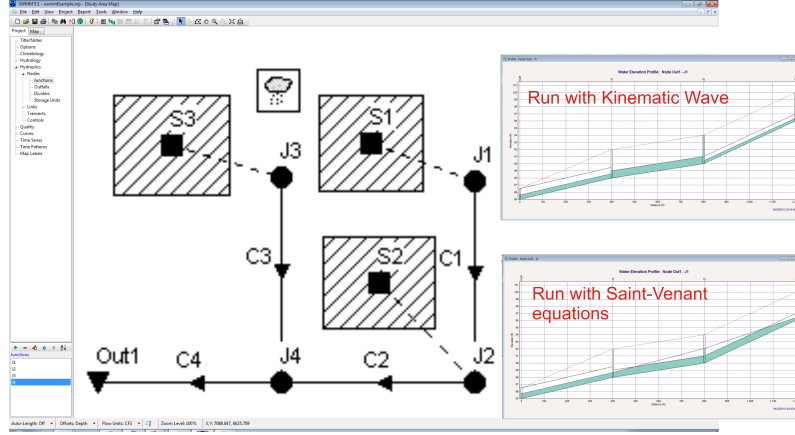


Fig. B.3: Graphical user interface of *SWMM*.

Water infiltrates from the permeable areas by sink terms, e.g. from the Green-Ampt approach (Sec. 1.5). This means that the infiltrating water is removed from the hydrological model. This water does not reappear later on the surface or the drainage system. As we know, this water recharges into aquifers below the city. There it flows towards rivers like in the Ammer aquifer model (Sec. 3.3). Thus, some modern codes close the water balance in the subsurface. The coupled model *SWMM#OGS* (Delfs et al., 2012) is an example, where feedbacks between drainage networks and aquifers are simulated.

B.3 *OGS#mHM*

Numerical modelling of interacting flow processes between different hydrological compartments, such as the atmosphere, land surface, vegetation, vadose zone, and groundwater, is essential for understanding the comprehensive processes in and between the different hydraulic compartments. The coupled surface-subsurface solutions are particularly challenging for modelling large regional scales, which is among others due to difficulties in determination and parametrization of the substantial scale-dependent coupling dynamics.

The conceptual mesoscale hydrologic model *mHM* (Samaniego et al., 2011) is currently being coupled to the *OGS* groundwater flow process module (e.g. (Kalbacher et al., 2012)). The grid based *mHM* provides a multiscale-parameter-regionalization-scheme to derive effective land surface parameters via non-linear transfer functions and has been developed to analyze the complex interaction of land-surface hydrologic processes and their spatial and temporal variability at the mesoscale (Kumar et al., 2013; Samaniego et al.,

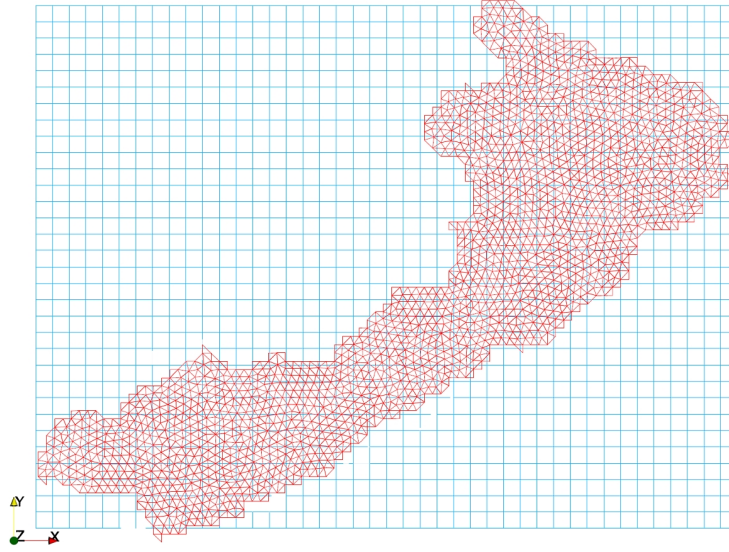


Fig. B.4: Overlying structured *mHM* grid (blue) and unstructured *OGS* mesh of the model surface (red) (Kalbacher et al., 2012)

2012). Technically, the coupling is implemented so far through a hard drive data exchange. For the output, *mHM* generates groundwater recharge data and saves the data in a cell-wise manner as a raster file format. The cell defined grid has to cover the whole study domain. The *mHM* grids have always m rows and n columns and can contain only regular and squared cells. To transform the cell-based recharge data into the finite element scheme, firstly the cell values must be projected to element nodes on the top surface of the 3D domain as a distributed Neumann boundary condition q , secondly a face integration is performed on the face elements on top surface for the domain discretization of the weak form of the groundwater flow equation. For the former, the face elements of the top surface are projected to the cell defined grid plane, and usually the projected face element do not coincide with the grid cells. Once the corresponding cell is found, we can use its neighbour cells recharge values to interpolate the flux q of the node. To this end, the cell recharge data are projected to the nodes on the top surface. The resulting recharges or discharges are saved in a binary file and passed to the right hand side of the equation system directly. The present coupling approach (Fig. B.6) has been applied and tested for a first case study of the Selke catchment (Rink et al., 2012a), located in Saxony-Anhalt and with a size of around 700 km². Current development focuses on a full coupling between both simulation tools on code level. This will ensure fast communication, thus reduced model runtime even for complex setups and acknowledge relevant exchange fluxes of surface and subsurface compartments.

Appendix C

OpenGeoSys Installation Guide

KARSTEN RINK, LARS BILKE AND THOMAS FISCHER

C.1 OGS Download and Installation

This chapter is a short guide on how to get *OpenGeoSys* running on your machine. The command line interface (CLI) is available for 64-bit *Ubuntu*- and *Mac OS X* systems as well as for 32- or 64-bit *Windows* operation systems, respectively. It is recommended to download the 64-bit version for 64-bit *Windows*.

The binary files needed to run the programme can be found at <http://www.opengeosys.org/resources/downloads>. The practical examples described in chapters 4 and 5 use basic *OGS*-functionality and as such should work with any version of the software available on the website. However, all simulations and input file configurations used in this book have been specifically tested with version 5.5.4, available at the lower part of the download site under “Older OpenGeoSys Releases”. The *Data Explorer*, the graphical user interface (GUI) for *OGS*, is available on the same website as a separate download and available for the same systems as the CLI version.

To use *OGS* or the *Data Explorer* under *Windows*, it is necessary to additionally download and install the free “Visual Studio 2013 Redistributable”-Package from *Microsoft*. It is available directly on the *OGS* download page or from <http://www.microsoft.com>. The downloaded version of this package needs to be for the same architecture (i.e. 32- or 64-bit) as the downloaded version for the *Data Explorer*. Without this additional package, DLL-related error messages will be displayed on start-up.

Both programmes need only be extracted from the downloaded zip-files to any directory and can be run instantly. For *Windows*, start `ogs.exe` for the CLI and `ogs-gui.exe` for the GUI. Using *Ubuntu* or *Mac OS X*, the programme can be run by calling `./ogs` or `./ogs-gui`, respectively.

Additional Software

For be able to use the full functionality of the *Data Explorer*, two additional utilities are needed. Both are *not* strictly required, but certain functionality used in this tutorial will not work without these additional programmes.

The first programme is the finite element mesh generator *GMSH*. It is freely available and required for creating domain discretisations (meshes) from geometry (see sections 3.4 and 5.6). The software is available for *Linux*, *Mac OS X* and *Windows* and installation files can be found at <http://geuz.org/gmsh/>. The second utility is the *OGS File Converter*. It comes with the *Data Explorer*-package, and can be either run stand-alone (`OGSFileConverter.exe` or `./OGSFileConverter`) or be called from within the *Data Explorer* by selecting **Tools** → **File Converter**....

Both programmes won't be recognised by the *Data Explorer* because it is not automatically known which path they have been installed to. Therefore, it is recommended on first start-up of the *Data Explorer* to set the location of both utility programmes. This is done by selecting **Settings** → **Data Explorer Settings**.... A new dialogue will open where the location of both programmes can be specified.

Example and Exercise Files

All files required for the *Theis*-Benchmark described in chapter 4 and the *Ammer* case study in chapter 5 are available online. They can be found at <http://tutorials.opengeosys.org>.

C.2 Source Code Availability

As mentioned before, *OpenGeoSys* is a cross-platform open-source software. If you would like to run *OGS* on an operating system where no binary files are available, it is still possible to download and compile the source code yourself.

All necessary files as well as the manual may be found on GitHub at <https://github.com/ufz/ogs>. A developer guide detailing everything necessary for compilation can be found at <http://docs.opengeosys.org>. You are also invited to join further development of the software if you are inclined to do so.

OpenGeoSys and the *Data Explorer* are available under BSD license, i.e. both are free for non-commercial use as long as the *OpenGeoSys Community* is referenced as the developer of the software. The exact conditions of use can be found in the file `LICENSE.txt` on the GitHub-repository.

References

- J. Ahrens, B. Geveci, and C. Law. ParaView: An End-User Tool for Large Data Visualization. In C.D. Hansen and C.R. Johnson, editors, *The Visualization Handbook*. Elsevier, 2005. <http://www.paraview.org>.
- C.A.J. Appelo and M. Rolle. Pht3d: A reactive multicomponent transport model for saturated porous media. *Ground Water*, 48(5):627–632, 2010.
- C.A.J. Appelo, D.L. Parkhurst, and V.E.A. Post. Equations for calculating hydrogeochemical reactions of minerals and gases such as co₂ at high pressures and temperatures. *Geochimica et Cosmochimica Acta*, 125:49–67, 2014.
- F. Aurenhammer. Voronoi Diagrams – A Survey of a Fundamental Geometric Data Structure. *ACM Comput Surv*, 23(3):345–405, 1991.
- V. Bissinger and O. Kolditz. Helmholtz interdisciplinary graduate school for environmental research (higrade). *GAIA-Ecological Perspectives for Science and Society*, 17(1):71–73, 2008.
- P. Brunner and C.T. Simmons. Hydrogeosphere: A fully integrated, physically based hydrological model. *Ground Water*, 50(2):170–176, 2012.
- M. Camporese, C. Paniconi, M. Putti, and S. Orlandini. Surface-subsurface flow modeling with path-based runoff routing, boundary condition-based coupling, and assimilation of multisource observation data. *Water Resour. Res.*, 46(W02512), 2010. doi: 10.1029/2008WR007536.
- J.-O. Delfs, F. Blumensaat, W. Wang, P. Krebs, and O. Kolditz. Coupling hydrogeological with surface runoff model in a poltva case study in western ukraine. *Env Earth Sci*, 65:1439–1457, 2012.
- H.-J.G. Diersch and O. Kolditz. Coupled groundwater flow and transport: 2. thermohaline and 3d convection systems. *Advances in Water Resources*, 21(5):401–425, 1998.
- J. M. Evans and H. Perlman. U.S. Geology Survey: The Water Cycle. <http://water.usgs.gov/edu/watercycle.html>, 2014. Accessed: 07-Jul-2014.
- B. Flemisch, M. Darcis, K. Erbertseder, et al. Dumu(x): Dune for multi-phase, component, scale, physics, ... flow and transport in porous media. *ADVANCES IN WATER RESOURCES*, 34(9):1102–1112, 2011.

- R. A. Freeze and J. A. Cherry, editors. *Groundwater*. Prentice Hall, Inc., 1979.
- C. Geuzaine and J.-F. Remacle. Gmsh: a three-dimensional finite element mesh generator with built-in pre- and post-processing facilities. *Int J Numer Meth Eng*, 79(11):1309–1331, 2009. <http://geuz.org/gmsh>.
- W. Goldstone. *Unity 3.x Game Development Essentials (2nd Edition)*. Packt Publishing, 2011. <http://unity3d.com>.
- A. Gräbe, T. Rödinger, K. Rink, et al. Numerical analysis of the groundwater regime in the western Dead Sea Escarpment, Israel + West Bank. *Environ Earth Sci*, 69(2):571–585, 2013. doi: 10.1007/s12665-012-1795-8.
- P. Grathwohl, H. Rügner, T. Wöhling, et al. Catchments as Reactors: A comprehensive approach for water fluxes and solute turn-over. *Environ Earth Sci*, 69(2):317–333, 2013.
- R. S. Gupta, editor. *Hydrology and Hydraulic Systems*. Waveland Press, Inc., Illinois, 2001.
- G.E. Hammond, P.C. Lichtner, C. Lu, and R.T. Mills. Pflotran: Reactive flow & transport code for use on laptops to leadership-class supercomputers. *Groundwater Reactive Transport Models*, pages 141–159, 2012.
- H.M. Harress. *Hydrogeologische Untersuchungen im Oberen Gäu*. PhD thesis, University of Tübingen, 1973.
- L. He, V.Y. Ivanov, G. Bohrer, K.D. Maurer, C.S. Vogel, and M. Moghaddam. Effects of fine-scale soil moisture and canopy heterogeneity on energy and water fluxes in a northern temperate mixed forest. *Agricultural and Forest Meteorology*, 184:243–256, 2014.
- B. Heinrich and C. Leibundgut. WaBoA – Wasser- und Bodenatlas Baden-Württemberg. In *Beiträge zum internationalen Workshop “GIS-gestützte hydrologische Kartenwerke in Mitteleuropa”*, pages 159–164, 2000. <http://www.hydrology.uni-freiburg.de/forsch/waboa/>, accessed 01 July 2014.
- B. Hölting. *Hydrogeologie*. Springer-Verlag Berlin Heidelberg, 8 edition, 2013.
- G. M. Hornberger, J. P. Raffensperger, P. L. Wiberg, and K. N. Eshleman. *Elements of Physical Hydrology*. The John Hopkins University Press Baltimore and London, 1998.
- J.D. Hughes, C.D. Langevin, and J.T. White. Modflow-based coupled surface water routing and groundwater-flow simulation. *Groundwater*, 2014.
- L. Jing, C.-F. Tsang, and O. Stephansson. DECOVALEX - an international cooperative research project on mathematical models of coupled THM processes for safety analysis of radioactive waste repositories. *Int J Rock Mech Min Sci*, 32:389–398, 1995.
- T. Kalbacher, J.-O. Delfs, H. Shao, W. Wang, M. Walther, L. Samaniego, C. Schneider, R. Kumar, A. Musolff, F. Centler, F. Sun, A. Hildebrandt, R. Liedl, D. Borchardt, P. Krebs, and O. Kolditz. The iwas-toolbox: Software coupling for an integrated water resources management. *Environmental Earth Sciences*, 65(5):1367–1380, 2012.

- O. Kolditz and S. Bauer. A process-orientated approach to compute multi-field problems in porous media. *Journal of Hydroinformatics*, 6:225–244, 2004.
- O. Kolditz, S. Bauer, C. Beyer, N. Boettcher, P. Dietrich, U.-J. Goerke, T. Kalbacher, C.-H. Park, U. Sauer, C. Schütze, H. Shao, A. Singh, J. Taron, W. Wang, and N. Watanabe. A systematic benchmarking approach for geologic co₂ injection and storage. *Environmental Earth Sciences*, 67(2):613–632, 2012a.
- O. Kolditz, U.-J. Goerke, H. Shao, and W. Wang, editors. *Thermo-Hydro-Mechanical-Chemical Processes in Fractured Porous Media: Benchmarks and Examples*, volume 86 of *Lecture Notes in Computational Science and Engineering*. Springer-Verlag GmbH Berlin Heidelberg, springer edition, 2012b.
- O. Kolditz, K. Rink, H. Shao, T. Kalbacher, S. Zacharias, r. Kunkel, and P. Dietrich. International viewpoint and news. *Environmental Earth Sciences*, 66(4):1279–1284, 2012c.
- P. Krause, editor. *Das hydrologische Modellsystem J2000*. Forschungszentrum Jülich: Umwelt/Environment, band 29 edition, 2001.
- P. Krause and S. Kralisch. The hydrological modeling system J2000 Ü knowledge core for JAMS. In *MODSIM 2005 International Congress on Modelling and Simulation*, pages 676Ü–682, 2005.
- N. Kresic, editor. *Hydrogeology and groundwater modeling*. CRC Press Taylor & Francis Group, 2007.
- R. Kumar, B. Livneh, L. Samaniego, and O. Kolditz. Towards computationally efficient large-scale hydrologic predictions with a multiscale regionalization scheme. *Water Resource Research*, 49:5700–5714, 2013.
- M. Kutilek and D. R. Nielsen, editors. *Soil Hydrology*. GeoEcology Publications. Catena-Verlag, Cremlingen-Destedt, 1994.
- M. Law and A. Collins. *Getting to Know ArcGIS for Desktop (3rd Edition)*. Esri Press, 2013.
- D. R. Maidment, editor. *Handbook of Hydrology*. MacGraw-Hill, Inc., New York, 1993.
- U. Maier, M. Flegr, H. Rügner, and P. Grathwohl. Long-term solute transport and geochemical equilibria in seepage water and groundwater in a catchment cross section. *Environmental Earth Sciences*, 69(2):429–441, 2013.
- R. M. Maxwell, Mario Putti, Steven Meyerhoff, Jens-Olaf Delfs, Ian M. Ferguson, Valeriy Ivanov, Jongho Kim, Olaf Kolditz, Stefan J. Kollet, Mukesh Kumar, Sonya Lopez, Jie Niu, Claudio Paniconi, Young-Jin Park, Mantha S. Phanikumar, Chaopeng Shen, Edward A. Sudicky, and Mauro Sulis. Surface-subsurface model intercomparison: A first set of benchmark results to diagnose integrated hydrology and feedbacks. *Water Res. Research*, 50(2):1531–1549, 2014a.

- R.M. Maxwell. A terrain-following grid transform and preconditioner for parallel, large-scale, integrated hydrologic modeling. *Advances in Water Resources*, 53:109–117, 2013.
- R.M. Maxwell, M. Putti, S. Meyerhoff, J.-O. Delfs, I.M. Ferguson, V. Ivanov, J. Kim, O. Kolditz, S.J. Kollet, M. Kumar, S. Lopez, J. Niu, C. Paniconi, Y.-J. Park, M.S. Phanikumar, C. Shen, E.A. Sudicky, and M. Sulis. Surface-subsurface model intercomparison: A first set of benchmark results to diagnose integrated hydrology and feedbacks. *Water Resources Research*, 50(2):1531–1549, 2014b.
- J.C.L. Meeussen. Orchestra: An object-oriented framework for implementing chemical equilibrium models. *Environmental Science and Technology*, 37(6):1175–1182, 2003.
- A. Musy, editor. *e-drologie*. Ecole Polytechnique Fédérale, Lausanne, Suisse, 2001.
- A. Musy and C. Highy, editors. *Hydrologie appliquée. Cours polycopié d’hydrologie générale*. Bucarest, editions hga edition, 1998.
- M. Nakhaei and J. Šimuněk. Parameter estimation of soil hydraulic and thermal property functions for unsaturated porous media using the hydrus-2d code. *Journal of Hydrology and Hydromechanics*, 62(1):7–15, 2014.
- M. Neteler and H. Mitasova. *Open Source GIS: A GRASS GIS Approach*. Springer, New York, 3rd edition, 2008. ISBN 978-0387357676. <http://grass.osgeo.org>.
- I. Pavlovskiy and B. Selle. Integrating Hydrogeochemical, Hydrogeological and Environmental Tracer Data to Understand Groundwater Flow for a Karstified Aquifer System. *GROUNDWATER*, 2014.
- J. P. Peixoto and M. Kettani. The control of the water cycle. *Sci. Amer*, 228(4):46–61, 1973.
- J. Plümacher. *Kalibrierung eines regionalen Grundwasserströmungsmodells mit Hilfe von Umweltisotopeninformation*. PhD thesis, ETH Zürich, 1999.
- P. Rekacewicz. Global waterstress and scarcity. <http://www.grida.no/publications/vg/water2/page/3239.aspx>, 2009. Accessed: 31-Jul-2014.
- P. Rekacewicz and E. Bournay. Proportion of population with improved drinking water supply in 2002. <http://www.millenniumassessment.org/en/GraphicResources.aspx>, 2007. Accessed: 31-Jul-2014.
- C. D. Reuther. Zur Schichtlagerung und Tektonik im Oberen Gäu. Master’s thesis, University of Tübingen, Tübingen, 1973.
- K. Rink. The OpenGeoSys Data Explorer Manual. Technical report, Department of Environmental Informatics, Helmholtz Centre for Environmental Research - UFZ, Leipzig, Germany, 2013. https://github.com/ufz/data_explorer_manual.
- K. Rink, T. Fischer, and O. Kolditz. Data Visualisation and Validation for Hydrological Models. In *Proc of Int Conf on Computer Graphics, Visualization, Computer Vision and Image Processing*, pages 169–176, 2011. ISBN:978-989-8533-00-5.

- K. Rink, T. Kalbacher, and O. Kolditz. Visual data exploration for hydrological analysis. *Env Earth Sci*, 65:1395–1403, 2012a.
- K. Rink, T. Kalbacher, and O. Kolditz. Visual Data Exploration for Hydrological Analysis. *Environ Earth Sci*, 65(5):1395–1403, 2012b. doi: 10.1007/s12665-011-1230-6.
- K. Rink, T. Fischer, B. Selle, and O. Kolditz. A Data Exploration Framework for Validation and Setup of Hydrological Models. *Env Earth Sci*, 69(2): 469–477, 2013.
- K. Rink, L. Bilke, and O. Kolditz. Visualisation Strategies for Environmental Modelling Data. *Env Earth Sci*, 2014. DOI:10.1007/s12665-013-2970-2.
- L. Samaniego, R. Kumar, and C. Jackisch. Predictions in a data-sparse region using a regionalized grid-based hydrologic model driven by remotely sensed data. *Hydrol. Res.*, 42:338–355, 2011.
- L. Samaniego, R. Kumar, and M. Zink. Implications of parameter uncertainty on soil moisture drought analysis in germany. *J. Hydrometeor.*, 14:47–68, 2012.
- W. Schroeder, K. Martin, and B. Lorensen. *Visualization Toolkit: An Object-Oriented Approach to 3D Graphics*. Kitware, Inc., 4th edition, 2006. <http://www.vtk.org>.
- S. Schulz, C. Siebert, T. Rödiger, M. M. Al-Raggad, and R. Merz. Application of the water balance model j2000 to estimate groundwater recharge in a semi-arid environment: a case study in the zarqa river catchment, nw-jordan. *Env Earth Sci*, 69:605–615, 2013.
- M. Schwientek, H. Rügner, B. Beckingham, B. Kuch, and P. Grathwohl. Integrated monitoring of particle associated transport of PAHs in contrasting catchments. *Environmental Pollution*, 172:155–162, 2013.
- B. Selle, K. Rink, and O. Kolditz. Recharge and discharge controls on groundwater travel times and flow paths to production wells for the Ammer catchment in SW Germany. *Environ Earth Sci*, 69(2):443–452, 2013a.
- B. Selle, M. Schwientek, and G. Lischeid. Understanding processes governing water quality in catchments using principal component scores. *Journal of Hydrology*, 486:31–38, 2013b.
- E. M. Shaw, K. J. Beven, N. A. Chappell, and R. Lamb, editors. *Hydrology in Practise*. Spon Press, 4th edition, 2011.
- C. Shen and M.S. Phanikumar. A process-based, distributed hydrologic model based on a large-scale method for surface-subsurface coupling. *Advances in Water Resources*, 33(12):1524–1541, 2010.
- C. Shen, J. Niu, and M.S. Phanikumar. Evaluating controls on coupled hydrologic and vegetation dynamics in a humid continental climate watershed using a subsurface-land surface processes model. *Water Resources Research*, 49(5):2552–2572, 2013.
- H. Si. TetGen – A Quality Tetrahedral Mesh Generator and Three-Dimensional Delaunay Triangulator. Technical Report WIAS Technical Report No. 13, Weierstrass Institute for Applied Analysis and Stochastics, 2013. <http://www.tetgen.org>.

- R. Srivastava and A. Guzman-Guzman. Practical approximations of the well function. *Ground water*, 36(5):844–848, 1998.
- C.I. Steefel and A.C. Lasaga. A coupled model for transport of multiple chemical species and kinetic precipitation/dissolution reactions with application to reactive flow in single phase hydrothermal systems. *American Journal of Science*, 294:529–592, 1994.
- C.I. Steefel, B. Arora, C.A.J. Appelo, et al. Reactive transport codes for subsurface environmental simulation. *Computational Geosciences*, submitted, 2014.
- F. Sun, H. Shao, W. Wang, et al. Groundwater deterioration in Nankou – a suburban area of Beijing: data assessment and remediation scenarios. *Environ Earth Sci*, 67(6):1573–1586, 2012.
- C.-F. Tsang, O. Stephansson, L. Jing, and F. Kautsky. Decovalex project: from 1992 to 2007. *Environmental Geology*, 57:1221–1237, 2009.
- United Nations Environment Programme UNEP, editor. *Vital Water Graphics - An Overview of the State of the World's Fresh and Marine Waters*. UNEP, Nairobi, Kenya, 2nd edition edition, 2008.
- VICAIRE. Virtual campus in hydrology and water resources. <http://http://echo2.epfl.ch/VICAIRE/>, 2006. Accessed: 31-Jul-2014.
- E. Villinger. Grundwasserbilanzen im Karstaquifer des Oberen Muschelkalks im Oberen Gäu (Baden-Württemberg). *Geologisches Jahrbuch*, Reihe C (32):43–61, 1982.
- M Walther, L Bilke, J-O Delfs, T Graf, J Grundmann, O Kolditz, and R Liedl. Assessing the saltwater remediation potential of a three-dimensional, heterogeneous, coastal aquifer system. model verification, application and visualization for transient density-driven seawater intrusion. *Environ Earth Sci*, 2014. DOI: 10.1007/s12665-014-3253-2.
- W. Wang, J. Rutqvist, U.-J. Gorke, et al. Non-isothermal flow in low permeable porous media: a comparison of Richards' and two-phase flow approaches. *Environ. Earth Sci.*, 62(6):1197–1207, 2011.
- J. Westervelt. *Simulation modeling for watershed management*. Springer-Verlag New York, 2001.
- L. De Windt, F. Marsal, J. Corvisier, and D. Pellegrini. Modeling of oxygen gas diffusion and consumption during the oxic transient in a disposal cell of radioactive waste. *Applied Geochemistry*, 41:115–127, 2014.
- T. Xu, E. Sonnenthal, N. Spycher, G. Zhang, L. Zheng, and K. Pruess. Toughreact: A simulation program for subsurface reactive chemical transport under non-isothermal multiphase flow conditions. *Groundwater Reactive Transport Models*, pages 74–95, 2012.
- S.B. Yabusaki, Y. Fang, K.H. Williams, C.J. Murray, A.L. Ward, R.D. Dayvault, S.R. Waichler, D.R. Newcomer, F.A. Spaine, and P.E. Long. Variably saturated flow and multicomponent biogeochemical reactive transport modeling of a uranium bioremediation field experiment. *Journal of Contaminant Hydrology*, 126(3-4):271–290, 2011.

- G.T. Yeh, V.S. Tripathi, J.P. Gwo, H.P. Cheng, J.R.C. Cheng, K.M. Salvage, M.H. Li, Y. Fang, Y. Li, J.T. Sun, F. Zhang, and M.D. Siegel. Hydro-geochem: A coupled model of variably saturated flow, thermal transport, and reactive biogeochemical transport. *Groundwater Reactive Transport Models*, pages 3–41, 2012.